Academic Science

International Journal of Electronics, Electrical and Computational System
IJEECS
ISSN 2348-117X
Volume 4, Issue 4
April 2015

A Neural Network based Approach for Pattern Recognition

Ruchi Varshney
Assistant Professor, Department of Electronics & Communication Engineering
MIT, Moradabad, UP, India

Abstract— In this paper an attempt is made to recognize the noise corrupted patterns. Eight numerals namely 0, 1, 2, 3, 4, 6, 9 and block are considered. For recognition both Hopfield neural network and centroid method techniques are adopted. Both approaches are implemented and tested on patterns consisting of digit and block. On the basis of simulation a comparative study for recognition rate has been carried out that proclaiming Hopfield neural network (HNN) is more efficient to recognize the noise corrupted patterns.
Keywords- Hopfield neural network, Pattern recognition

I. INTRODUCTION

An interesting model studied by Amari and formally introduced by Hopfield in 1982, has a wide range of applications, this model is sometimes referred to as Amari-Hopfield model. Hopfield neural network is a single-layer, non-linear, auto associative, discrete or continuous-time network that is easier to implement in hardware [4]. In 1982, John Hopfield published the famous paper "Neural networks and physical systems with emergent collective computational abilities". Hopfield networks [7] are typically used for classification problems with binary pattern vectors.

Artificial intelligence (AI), neural computing, and character recognition share a common knowledge base comprising of multiple disciplines. Contemporary neuro computing takes its models from the biological system [12].The neural approach applies biological concepts to machines to recognize patterns [15],[10],[11]. Our brain has been the basic motivation in the endeavor to building intelligent machine in the field of artificial intelligence [14]. Fault-tolerance [13] is a significant feature where the neural networks come in, trying to overcome the mismatch between conventional computer processing and the working of human brain. Neural network research has faced many ups and downs in its history. The idea of creating a network of neurons got a boost when McCulloch and Pitts presented their model of the artificial neuron laying the foundations. Hebb was responsible for presenting the concept of learning. Much work was done in the field to a point where simulations of the net could be performed on computers. This situation changed drastically when the Minsky and Papert book cast a shadow on the computation ability of neural networks. In 1982, John J. Hopfield presented a neural network model that he proposed as a theory of associative memory, thus changing the status resulting in a sudden surge of research activities that is ongoing. A HNN network has the following interesting features [12], distributed representation, and distributed asynchronous control, content addressable memory, and fault tolerance. Hopfield's work is of particular importance as he established the isomorphism between Lyapunov energy function or Ising spin-glass and recurrent networks and was able to excite a large number of researchers to these powerful yet simple content-addressable associative memories. Studies of HNN have been focused on network dynamics, memory capacity [4],[1] higher-ordered networks, error correction. Hopfield [5] proposed a method for improving the storage capacity through the use of "unlearning" of information. HNN strengths include total recall from partial or incomplete data, its stability under asynchronous conditions, and fault-tolerance. In [16], a variant of HNN is discussed, that is, the multi-layer HNN model

Academic Science
International Journal of Electronics, Electrical and Computational System
IJEECS
ISSN 2348-117X
Volume 4, Issue 4
April 2015

for pattern or object recognition, which converges to the single-layer model.

The remaining paper is organized as follows. In section 2 the basic concept of HNN, weight matrix and centroid method are introduced. Simulations and results are discussed in section 3 and finally in section 4 conclusions are made.

II. HOPEFIELD NEURAL NETWORK

Hopfield added feedback connections (the outputs are fed back into the inputs) to the feed forward network, and showed that with these connections the networks are capable of interesting behaviors; in particular they can hold memories. Feedforward network with feedback connections is shown in Figure 1[3].

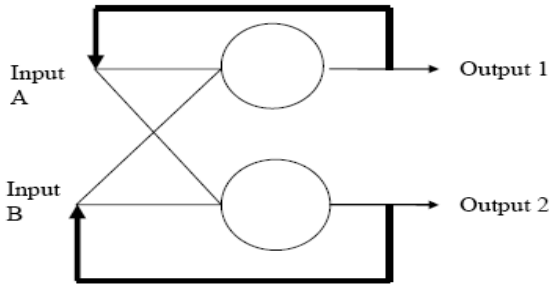

Fig. 1 Feed Forward network with feedback connections

Networks with such connections are called "feedback" or "recurrent" networks. The network operates in a similar way as a feed forward network and the neurons perform the same function. Inputs are applied to A and B and the outputs are calculated as in feed forward network. The difference is that once the output is obtained, fed it back into the inputs again means output 1 is fed back into input A and likewise output 2 into input B. This gives two new inputs (the previous outputs) and the process is repeated. This process continues until the outputs don't change any more (they remain constant). At this point the network is said to have relaxed. A Hopfield network can reconstruct a pattern from a corrupted original. This means that the network is able to store the correct (uncorrupted) pattern, in other words it has a memory. Because of this these networks are sometimes called Associative Memories or Hopfield Memories [7].In this case, the weights of the connections between the neurons have to be thus set that the states of the system corresponding with the patterns which are to be stored in the network are stable. These states can be seen as 'dips' in energy space [9]. When the network is cued with a noisy or incomplete test pattern, it will render the incorrect or missing data by iterating to a stable state which is in some sense 'near' to the cued pattern.

A. Deriving the Weight Matrix

In present work HNN is used to recognize eight (08) patterns. Each pattern is represented by 12 X 10 bits. In HNN every neuron can potentially be connected to every other neuron, so a two dimensional array will be used. The connection weights putted into this array is called weight matrix which allows the HNN to recall patterns. As in HNN every neuron is not connected to itself so the connection between N_i to N_i neuron is not applicable. First one may start with a blank connection weight matrix of 120 X 120. Now train this neural network to accept the pattern P, where P is a column vector of 120 X 1. To do this P's contribution matrix is required. The contribution matrix will then be added to the actual connection weight matrix. As additional contribution matrices are added to the connection weight matrix, the connection weight is said to learn each of the new patterns. For calculation of the contribution matrix of P three steps are involved. In first step the bipolar values of P have been calculated. Bipolar simply mean that representing a binary string with –1's and 1's rather than 0's and 1's. In next step a multiplication of the transpose of the bipolar equivalent of P with P itself has been performed and finally in last step all the elements of north-west diagonal have been set to zero, because neurons do not connect to themselves in a HNN. If diagonal elements were not zero, the network would tend to reproduce the input vector rather than a stored vector. This contribution matrix can now be added to whatever connection weight matrix we already had. If one may want this network to recognize P pattern, then this contribution matrix becomes connection weight matrix. If one may also want to recognize P1

Academic Science
International Journal of Electronics, Electrical and Computational System
IJEECS
ISSN 2348-117X
Volume 4, Issue 4
April 2015

pattern, then calculate both contribution matrices and add each value in their contribution matrices to result in a combined matrix, which would be the final connection weight matrix [9].

B. Recalling patterns

To recall the patterns, pattern P has been presented to each input neuron. Each neuron will activate based upon the input pattern. When neuron is presented with pattern P its activation will be the sum of all weights that have a 1 in input pattern. Only the values that contain a 1 in the input pattern is summed. Likewise the activation of 120 neurons can be calculated. The output neurons, which are also the input neurons, will report the above activations. These values are meaningless without a threshold method. A threshold method determines what range of values will cause the neuron, in this case the output neuron, to fire. The threshold usually used for a HNN, is any value greater than zero [6],[8]. All neurons that fired are assigned with binary 1, and a binary 0 to all neurons that did not fire [2]. The final binary output from the Hopfield network would be P. This is the same as the input pattern. An auto associative neural network, such as a Hopfield network, will echo a pattern back if the pattern is recognized. Any time a HNN is created that recognizes a binary pattern, the network also recognizes the inverse of that bit pattern.

C. Centroid (center of mass) Method

By determination of average values of coordinates of pattern, centroid can be calculated. Centroid method involves three steps. In first step centroid of corrupted pattern has been calculated. In second step the distance between the centroid of noise corrupted pattern and centroid of original eight (08) patterns has been calculated. Finally in third step declaration has being done on the basis of minimum Euclidean distance which is corresponding to original pattern [17].

III. Simulation Results And Discussion

The generalized Hebb Rule is implemented to train the network. To retrieve the patterns Hopfield neural network with 120 neurons is used. Numbers of stored pattern are eight (08). The stored patterns are ‘zero’, ‘one’, ‘two’, ‘three’, ‘four’, ‘six’, ‘nine’, and ‘block’. The weight matrix (120X120) of Hopfield network has been calculated and stored. Here learning phase of Hopfield network is performed. User is free to introduce noise level (0-100%) in selected input pattern, which means that bits of chosen pattern can be randomly flipped between 0 to 100%. Each pattern is of order 12 X 10. Suppose noise introduced is of the order of 10% meaning thereby 12 bits are randomly flipped. Simulation study has been carried out for two cases. All the patterns are displayed in Fig 2. In Fig 3 chosen input pattern is displayed. In first case pattern no. 5 or numeral ‘four’ is considered

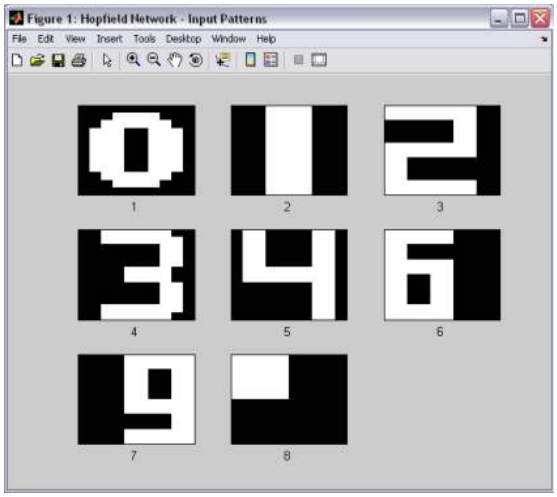

Fig. 2 Input patterns

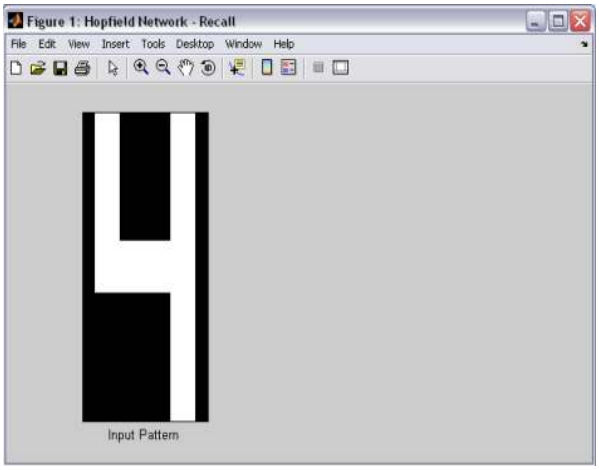

Fig. 3 Selected pattern number 5

International Journal of Electronics, Electrical and Computational System
IJEECS
ISSN 2348-117X
Volume 4, Issue 4
April 2015

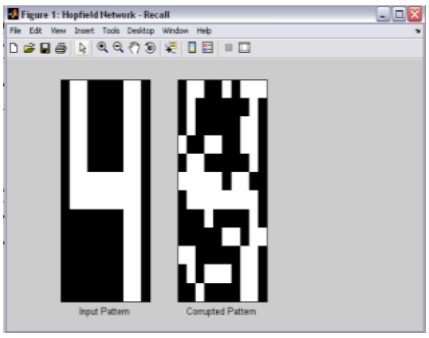

Fig. 4 Pattern with 30 % noise probability

Noise introduced in pattern is 30%, 36 bits are randomly flipped and corrupted pattern is observed in Fig 4. Progress of algorithm is examined at every 6th iteration. In Fig. 5, 6, 7, 8 current states of 6th, 12th, 18th, 24th iterations respectively are observed. Training is stopped after 28th iteration and original pattern is recognized (Fig. 9)

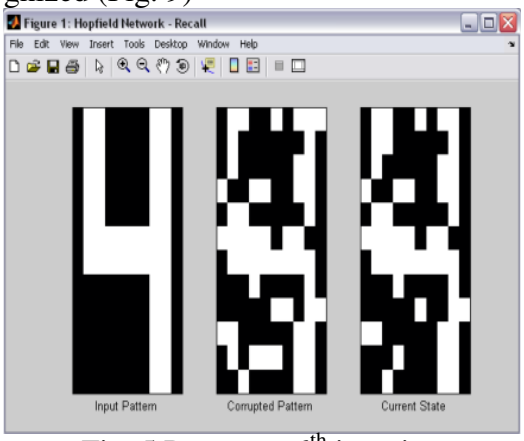

Fig. 5 Pattern at 6th iteration

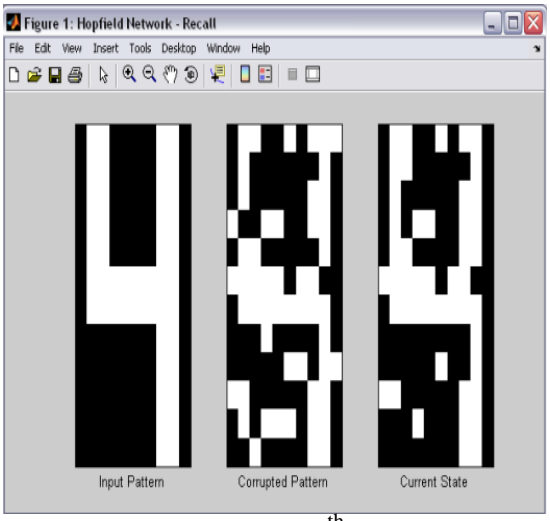

Fig.6 Pattern at 12th iteration

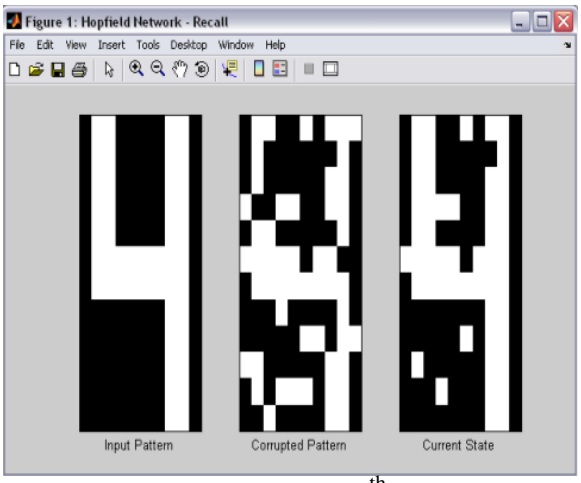

Fig.7 Pattern at 18th iteration

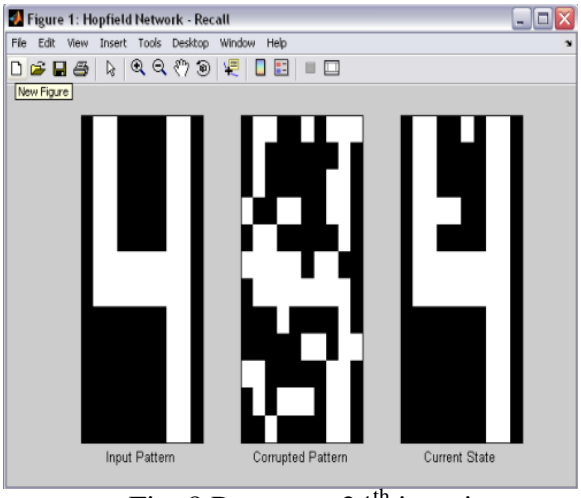

Fig. 8 Pattern at 24th iteration

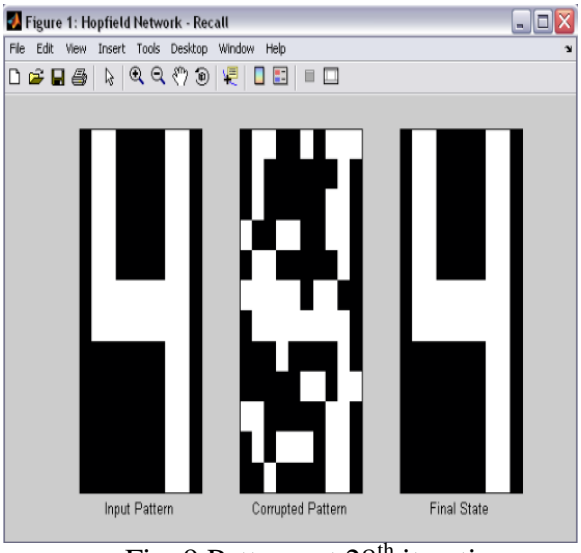

Fig. 9 Pattern at 28th iteration

Academic Science

International Journal of Electronics, Electrical and Computational System
IJEECS
ISSN 2348-117X
Volume 4, Issue 4
April 2015

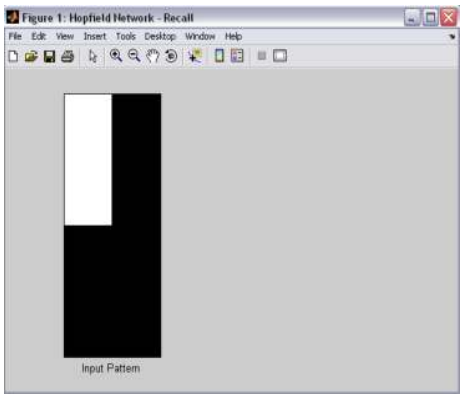

Fig. 10 Selected Pattern number 8

In second case, input pattern no. 8 or 'block' is of interest, shown in Fig.10 which is flipped 80%. Corrupted pattern along with input pattern is shown in Fig. 11. Current state of pattern has been observed at every 9th iteration (Fig. 12, 13). Noise free pattern is recalled at 22nd iteration which is shown in Fig. 14. By observation from Fig. 14 It is clear that recalled pattern is inverse of chosen input pattern.

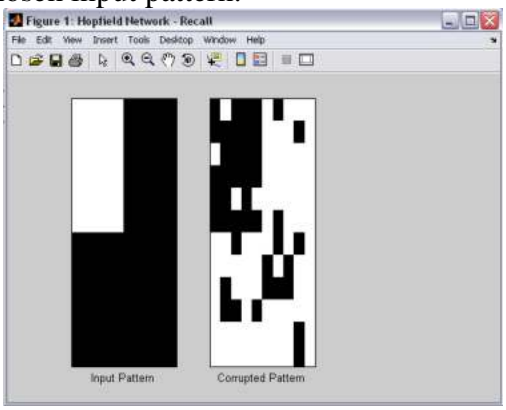

Fig. 11 Pattern with 80 % noise probability

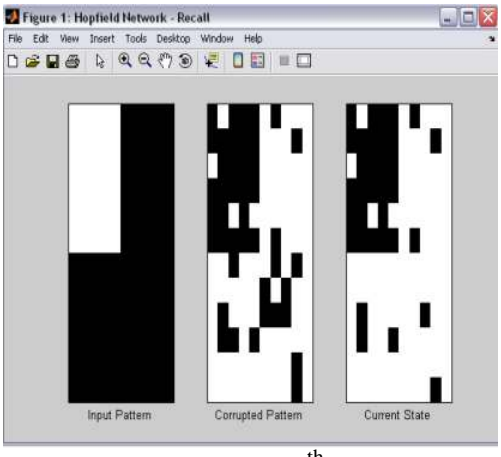

Fig. 12 Pattern at 9th iteration

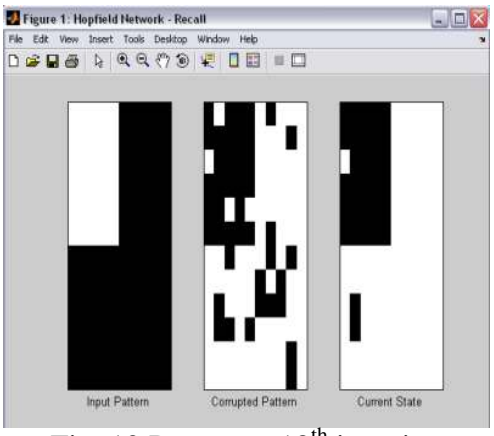

Fig. 13 Pattern at 18th iteration

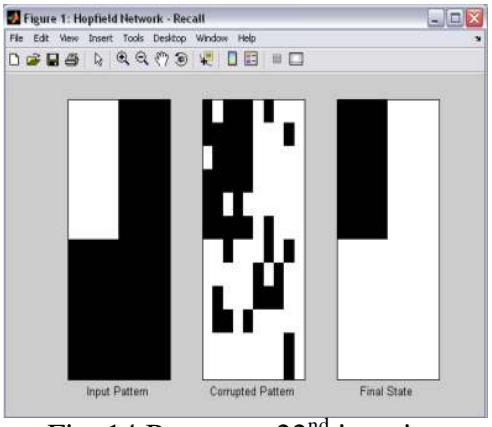

Fig. 14 Pattern at 22nd iteration

From above two cases it has been observed that Hopfield neural network is capable of extracting original pattern s from noise corrupted patterns and can also recall inverse of these patterns. A comparison for recognition rate also has been made on the basis of simulations by recalling the patterns from HNN and centroid method. A hundred observations are taken for each pattern. The probability of flipping the bits of pattern is chosen 25%. A comparative study is carried out and has been shown in the tabular form (Table 1). The first sub column shows the recognition rate by using HNN and the second sub column represents the recognition rate by centroid method. Recognition rate is 100 % for pattern no 1, 4, 6, 8 and it is between 90- 100 % for pattern no 2, 3, 5, 7 by HNN while centroid method have 100 % recognition rate for only pattern no 1. It is clear from the table that centroid method is not efficient to recognize the pattern except pattern no 1. The table proves

that the efficiency of recognition by using HNN is more than by centroid method.

IV. CONCLUSIONS

By using HNN and centroid method, noise corrupted patterns are recognized. Noisy patterns are recognized at 25 % probability of flipping the bits. Recognition rates for both methods are compared. On the basis of simulation it is concluded that HNN have higher recognition rate than centroid method which means it can recall noise corrupted patterns more efficiently.

REFERENCES

[1] Abu Mustafa Y. S. and Jacques, J. M.: Information Capacity of the Hopfield Model. IEEE Transactions on Information Technology, Vol. IT-31, No. 4, pp. 461-464 (1985)

[2] Bhartikar S. and Mendel J. M. : The Hysteretic Hopfield Neural Network. IEEE Transactions on Neural Networks, Vol. 11, No. 4, pp. 879-888 (2000)

[3] Haykin S.: Neural Networks—A Comprehensive Foundation, 2nd edition. Pearson Education, Singapore (1999)

[4] Hopfield J. J.: Neural networks and physical systems with emergent collective computational abilities. Proceedings of the National Academy of Sciences, Vol. 79, pp. 2554-2558 (1982)

[5] Hopfield J. J. and Feinstein D. I. and Palmer R. G.: Unlearning' has a stabilizing effect in collective memories. Nature, Vol. 304 (1983)

[6] Humayun K. S. and Zhang Ye: Hopfield Neural Networks—A Survey. Proceedings of the 6th WSEAS Int. Conf. on Artificial Intelligence, knowledge Engineering and Data Bases, Corfu Island, Greece, pp 125-130 (2007)

[7] Jessye B. : Hopfield Networks. IEEE IJCNN '99 ,Volume 6, 1999, pp 4435- 4437.

[8] Kamel M.S. : Neural networks: the state of the art. IEEE International Conference on Microelectronics, ICM, pp 5 – 9 (1999)

[9] Kussay N.M. and Imad I.A.K. : Gray image recognition using hopfield neural network with multi bit plane and multi connect architecture. ICCGIV (2006.)

[10] D. Le and . Makoto M: A Pattern Recognition Neural Network Using Many Sets of Weights and Biases. Proceedings of the IEEE International Symposium on Computational Intelligence in Robotics and Automation, Jacksonville, FL, USA, pp 285-290 (2007)

[11] Osowski S. and Nghia D.D.: Neural networks for classification of 2-D patterns. Proceeding of ICSP pp 1568-1571 (2000)

[12] Pao Y. H.: Adaptive Pattern Recognition and Neural Networks. Addison-Wesley Publishing Company Inc. New York, (1989)

[13] Patavardhan P. P. and Rao D. H. and Anita Deshpande G.,: Fault Tolerance Analysis of Neural Networks for Pattern Recognition. International Conference on Computational Intelligence and Multimedia Applications , pp 222- 226. (2007)

[14] Rich and Knight K : Artificial Intelligence. McGraw-Hill, New York (1991).

[15] Yoshida T. and Omatu S. : Pattern Recognition with Neural Network. IEEE, Geoscience and Remote Sensing Symposium, Proceedings. IGARSS ,Volume 2, pp 699 -701 (2000)

[16] Young S. S. and Scott P. D. and Nasrabad N.M. i: Object Recognition using Multi-layer Hopfield Neural Network. IEEE Transactions on Image Processing, Vol. 6, No. 3, pp. 357-372 (1997)

[17] Luciano da fontoura costa, Roberto Marcoandes cesar: Shape analysis and classification theory and practice. CRC press, pp- 425- 430 (2000)

International Journal of Electronics, Electrical and Computational System
IJEECS
ISSN 2348-117X
Volume 4, Issue 4
April 2015

TABLE I. RECOGNITION RATE

Pattern No.	1		2		3		4		5		6		7		8	
	HNN	Cent.	HNN	Cent.	HNN	Cent.	HNN	Cent.	HNN	Cent.	HNN	Cent.	HNN	Cent.	HNN	Cent.
1	100	100														
2	1		95	89		5	1	3		3	3					
3		44			92	56					8					
4		64					100	16		20						
5		48	1				3	8	93	44	3					
6		4				96					100	0				
7		4					4	80		12			96	4		
8		16								12					100	72

MIT International Journal of Computer Science and Information Technology, *Vol. 4, No. 2, August 2014, pp. 60-64* 60
ISSN 2230-7621©MIT Publications

A Survey on Techniques for Privacy Preserving Data Publishing (PPDP)

Amita Sharma
B.Tech Student
Moradabad Institute of Technology
Moradabad, U.P., INDIA

Ranjan Baghel
CSE Department
Moradabad Institute of Technology
Moradabad, U.P., INDIA

Puneeta Panday
B.Tech Student
Moradabad Institute of Technology
Moradabad, U.P., INDIA

Praveen Saini
CSE Department
Moradabad Institute of Technology
Moradabad, U.P., INDIA

ABSTRACT

Microdata information is collected by many governments, corporates and individuals. This data is used for knowledge and information based decision- making. For this data is published. So, there is a need of preserving privacy of published data. This paper focuses on various Privacy Preserving Data Publishing (PPDP) techniques.
Key words: *Privacy Preservation, PPDP, privacy threats, anonymization, PPDM.*

1. INTRODUCTION

Microdata contain information about an individual entity such as a person, a household or an organization. Privacy of database containing microdata becomes important because personal data may be misused for various purpose. So, various privacy preserving methods have been developed in recent years to preserve the privacy of microdata. A stringent definition of privacy preservation is given by Dalenius in 1977 which states that "access to the published data should not enable the adversary to learn anything extra about any target victim compared to no access to the database, even with the presence of any adversary's background knowledge obtained from other sources".

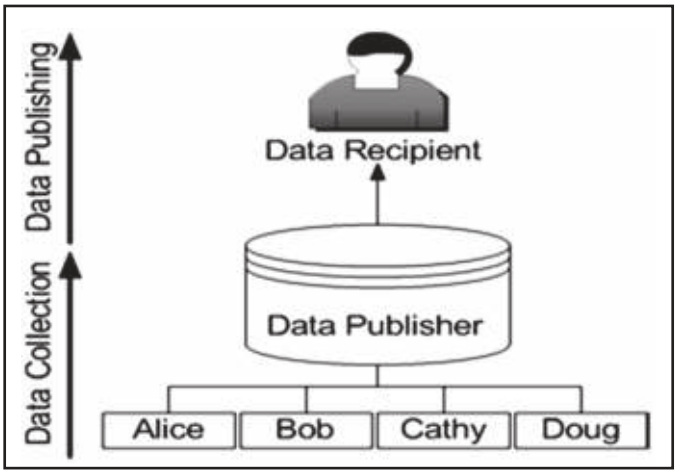

Fig. 1: Data collection and data publishing

In the data collection phase, the data holder collects data from record owners (e.g., Alice and Bob). In the data publishing phase, the data holder releases the collected data to a data miner or the public, called the data recipient, who will then conduct data mining on the published data.

Privacy Preserving methods are Privacy Preservation Data Mining (PPDM) and Privacy Preservation Data Publishing (PPDP) [12]. PPDM maintains privacy by using data mining tools. PPDP provides methods and tools for publishing useful information while preserving data publishing. In the basic form of PPDP, data holder has a table of the form:

D (Explicit Identifier, Quasi Identifiers, Sensitive Attributes, Non-Sensitive Attributes) where Explicit Identifier is a set of attributes, such as name and social security number (SSN), containing information that explicitly identifies record owners; Quasi Identifier (QI) is a set of attributes that could potentially identify record owners; Sensitive Attributes (SA) consist of sensitive person-specific information such as disease, salary, and disability status; and Non-Sensitive Attributes contains all attributes that do not fall into the previous three categories. Various techniques for Privacy Preserving Data Publishing (PPDP) include Generalization [7], [9], Bucketization [3], [6], [10], Slicing [1], and Overlapping Slicing [11].

2. RELATED AREAS

2.1 Privacy Preserving Data Mining (PPDM)

PPDM method of privacy preserving emerges in 2000. The idea of PPDM was to extend traditional data mining tools and

techniques to work with modified data to mask the sensitive information. In PPDM sometimes data mining task is unknown at the time of data publishing.

Limitations of PPDM are as follows:

- It focuses on the techniques of publishing data, not on the techniques for data mining.
- It seeks to directly hide the sensitive data.
- It does not prevent the truthfulness at the record level.

2.2 Attack Models and Privacy Models

Privacy models are classified into two categories based on their attack principles.

First category includes a privacy threat that occurs when an adversary is able to link a record owner to a record in a published data table, to a sensitive attribute in a published data table, or to the published data table itself. There exist three types of linkages.

- record linkage
- attribute linkage
- table linkage

Second category includes a privacy threat that occurs when a published table should provide the adversary with little additional information beyond the background knowledge. This type of model is known as probabilistic attack model.

Table summarizes the attack models addressed by the privacy models.

Table 1: Privacy Models

Privacy Model	Attack Model			
	Record linkage	Attribute linkage	Table linkage	Probabilistic attack
k-Anonymity [201, 217]	✓			
MultiR k-Anonymity [178]	✓			
ℓ-Diversity [162]	✓	✓		
Confidence Bounding [237]		✓		
(α, k)-Anonymity [246]	✓	✓		
(X, Y)-Privacy [236]	✓	✓		
(k, e)-Anonymity [269]		✓		
(ϵ, m)-Anonymity [152]		✓		
Personalized Privacy [250]		✓		
t-Closeness [153]		✓		✓
δ-Presence [176]			✓	
(c, t)-Isolation [46]	✓			✓
ϵ-Differential Privacy [74]			✓	✓
(d, γ)-Privacy [193]			✓	✓
Distributional Privacy [33]			✓	✓

2.3 Privacy Models used in Privacy Preserving Data Publishing

k-Anonymity

k-Anonymity [4], [8], [9] is one of the record linkage models. Samarati and Sweeney propose the notion of k-anonymity as: If one record in the table has some value QI, at least k − 1 other records also have the value QI. In other words, the minimum equivalence group size on QI is at least k. A table satisfying this requirement is called k-anonymous.

l-Diversity

l-Diversity [5] is one of the attribute linkage models. Machanavajjhala et al. propose the diversity principle, called l-diversity, to prevent attribute linkage. The l-diversity requires every QI group to contain at least l "well-represented" sensitive values.

2.4 Privacy Threats

In publishing microdata, there are three types of information disclosure threats.

2.4.1 Membership Disclosure

Membership disclosure occurs when the data to be published is selected from a larger population and the selection criteria are sensitive (e.g., when publishing datasets about diabetes patients for research purposes), it is important to prevent an adversary from learning whether an individual's record is in the data or not.

2.4.2 Identity Disclosure

Identity Disclosure occurs when an individual is linked to a particular record in the released table. In some situations, one wants to protect against identity disclosure when the adversary is uncertain of membership. In this case, protection against membership disclosure helps protect against identity disclosure. In other situations, some adversary may already know that an individual's record is in the published dataset, in which case, membership disclosure protection either does not apply or is insufficient.

2.4.3 Attribute Disclosure

Attribute disclosure, occurs when new information about some individuals is revealed, i.e., the released data makes it possible to infer the attributes of an individual more accurately than it would be possible before the release. Similar to the case of identity disclosure, we need to consider adversaries who already know the membership information. Identity disclosure leads to attribute disclosure. Once there is identity disclosure, an individual is re-identified and the corresponding sensitive value is revealed. Attribute disclosure can occur with or without identity disclosure, e.g., when the sensitive values of all matching tuples are the same.

3. TECHNIQUES OF PRIVACY PRESERVING DATA PUBLISHING (PPDP)

Consider table as an example of microdata.

Table 1: The Original Table

Age	Sex	Zipcode	Disease
22	M	47906	dyspepsia
22	F	47906	flu
33	F	47905	flu
52	F	47905	bronchitis
54	M	47302	flu
60	M	47302	dyspepsia
60	M	47304	dyspepsia
64	F	47304	gastritis

3.1 Generalization

Generalization [7], [9] is the commonly used anonymized approach, in which quasi-identifier values are replaced with less-specific but semantically consistent values. Then, all quasi-identifier values in a group would be generalized to the entire group. It uses the k-anonymity [4], [8], [9] model of privacy.

Steps

1. Removes identifiers from the data.
2. Partition tuples into buckets.
3. Transform QI values in each bucket with less-specific but semantically consistent values.

Table 2: The Generalized Table

Age	Sex	Zipcode	Disease
[20-52]	*	4790*	dyspepsia
[20-52]	*	4790*	flu
[20-52]	*	4790*	flu
[20-52]	*	4790*	bronchitis
[54-64]	*	4730*	flu
[54-64]	*	4730*	dyspepsia
[54-64]	*	4730*	dyspepsia
[54-64]	*	4730*	gastritis

Limitations

- k-Anonymity suffers from the curse of dimensionality [2].
- The data analyst has to make the uniform distribution assumption that every value in each generalized set is equally possible.
- Correlations between different attributes are lost.

Generalization suffers with two types of attacks:-

- Background Knowledge Attack.
- Homogeneity Attack.

3.2 Bucketization

Bucketization [6], [3], [10] firstly, Partitions tuples into buckets, and then separate the sensitive attribute from the non-sensitive by randomly permuting the sensitive attribute values within each bucket. It uses l-diversity [5] model of privacy.

Steps

1. Removes identifiers from the data.
2. Partition tuples into buckets.
3. Separate the SAs from the QIs by randomly permuting the SA values in each bucket.

Limitations

- Does not prevent membership disclosure.
- Requires a clear separation between QIs and SAs.
- Breaks the attribute correlations between the QIs and the SAs.

Bucketization suffers with two types of attacks:

- Skewness attack.
- Similarity attack.

Skewness attack is defined as overall distribution is skewed by satisfying the l-diversity and does not prevent membership disclosure. Similarity Attack is defined as sensitive attributes in a column are distinct but semantically similar.

Table 3: The Bucketized Table

Age	Sex	Zipcode	Disease
22	M	47906	dyspepsia
22	F	47906	flu
33	F	47905	flu
52	F	47905	bronchitis
54	M	47302	flu
60	M	47302	dyspepsia
60	M	47304	dyspepsia
64	F	47304	gastritis

3.3 Anatomy

Table 4: The Anonymized Tables

Age	Sex	Zipcode	Group-ID
22	M	47906	1
22	F	47906	1
33	F	47905	1
52	F	47905	1
54	M	47302	2
60	M	47302	2
60	M	47304	2
64	F	47304	2

(a) The quasi-identifier table (QIT)

Group-ID	Disease	Count
1	flu	2
1	dyspepsia	1
1	bronchitis	1
2	gastritis	1
2	flu	1
2	dyspepsia	2

(b) The sensitive table (ST)

Anatomy [10] uses the l-diversity [5] model of privacy. It releases the values of QIs and SAs into two separate tables. The inherent problem in Generalization is that it prevents an analyst from correctly understanding the data distribution inside each QI-group. Anatomy removes this problem by capturing the exact QI-distribution. In this the correlation between the different attribute remain preserve. It uses grouping mechanism.

Steps

1. Partition tuples of microdata into several QI-groups.

2. Create QI Table.
3. Create ST (SA table) which contains SA statistics for each QI group.

3.4 Slicing

A novel data anonymization technique called slicing [1] introduced partitions the data set both vertically and horizontally. Vertical partitioning is done by grouping attributes into columns based on the correlations among the attributes. Each column contains a subset of attributes that are highly correlated. Horizontal partitioning is done by grouping tuples into buckets. Finally, in each bucket, values in each column are randomly permutated to break the linking between different columns. Slicing preserves membership disclosure and it is suitable for high dimensional data. The basic idea behind slicing is to break association cross columns, but to preserve the association within each columns. It uses k-anonymity [4], [8], [9] and l-diversity [5] model of privacy.

Steps

1. Attribute Partitioning.
2. Column generalization.
3. Tuple partitioning.

Limitation

- It cannot provide better data utility for an analyst.

Table 5: The Sliced Table

(Age, Sex)	(Zipcode, Disease)
(22,M)	(47905,flu)
(22,F)	(47906,dyspepsia)
(33,F)	(47905,bronchitis)
(52,F)	(47906,flu)
(54,M)	(47304,gastritis)
(60,M)	(47302,flu)
(60,M)	(47302,dyspepsia)
(64,F)	(47304,dyspepsia)

3.5 Overlapping Slicing

Overlapping slicing [11] is an enhance version slicing [1]. It partitions attributes both horizontally and vertically like slicing. In horizontal partitioning, tuples are grouped together and in vertical partitioning, highly correlated attributes are grouped together. Sensitive attribute in the relational table should be placed in the each column of a table.

Steps

1. Attribute Partitioning.
2. Column generalization.
3. Tuple partitioning.

Table 6: The Overlapping Slicing Table

(Age, Sex, Disease)	(Zipcode, Disease)
(22,M,flu)	(47905,flu)
(22,F,dyspepsia)	(47906,dyspepsia)
(33,F,bronchitis)	(47905,bronchitis)
(52,F,flu)	(47906,flu)
(54,M,gastritis)	(47304,gastritis)
(60,M,flu)	(47302,flu)
(60,M,dyspepsia)	(47302,dyspepsia)
(64,F,dyspepsia)	(47304,dyspepsia)

4. CONCLUSION

With the development of data analysis and processing technique, the privacy disclosure problem about individual or company is important when releasing or sharing data to publish, this give the birth to the research field called privacy preserving data publishing (PPDP). In this paper, we presented different native privacy preserving methods for publishing microdata. While all the purposed methods are only approximate to our goal of privacy preservation, we need to further perfect those approaches or develop some efficient methods. To address these issues, following problem should be widely studied.

- Privacy and accuracy is a pair of contradiction; improving one usually incurs a cost in the other. How to apply various optimizations to achieve a trade-off should be deeply researched.
- Side-effects are unavoidable in data sanitization process. How to reduce their negative impact on privacy preserving needs to be considered carefully. We also need to define some metrics for measuring the side-effects resulted from data processing.

REFERENCES

1. Tianchen Li, Ninghui Li, Jian Zhang, Lan Molloy. Slicing: A new approach for privacy preserving data publishing. *Proc. IEEE transactions on knowledge and data engineering,* Vol. 24, No. 3, pp. 561-574, March 2012.
2. C. Aggarwal, "On k-Anonymity and the Curse of Dimensionality," *Proc. Int'l Conf. Very Large Data Bases* (VLDB), pp. 901-909, 2005.
3. N. Koudas, D. Srivastava, T. Yu, and Q. Zhang, "Aggregate Query Answering on Anonymized Tables," *Proc. IEEE 23rd Int'l Conf. Data Eng.* (ICDE), pp. 116-125, 2007.
4. K. LeFevre, D. DeWitt, and R. Ramakrishnan, "Incognito: Efficient Full-Domain k-Anonymity," *Proc. ACM SIGMOD Int'l Conf. Management of Data* (SIGMOD), pp. 49-60, 2005.
5. L. Sweeney, "Achieving k-Anonymity Privacy Protection Using Generalization and Suppression," *Int'l J. Uncertainty Fuzziness and Knowledge-Based Systems,* Vol. 10, No. 6, pp. 571-588, 2002.
6. L. Sweeney, "k-Anonymity: A Model for Protecting Privacy," *Int'l J. Uncertainty Fuzziness and Knowledge-Based Systems,* Vol. 10, No. 5, pp. 557-570, 2002.

7. A. Machanavajjhala, J. Gehrke, D. Kifer, and M. Venkitasubramaniam, "l-Diversity: Privacy Beyond k-Anonymity," *Proc. Int'l Conf. Data Eng.* (ICDE), p. 24, 2006.
8. X. Xiao and Y. Tao, "Anatomy: Simple and Effective Privacy Preservation," *Proc. Int'l Conf. Very Large Data Bases* (VLDB), pp. 139-150, 2006.
9. P. Samarati, "Protecting Respondent's Privacy in Microdata Release," *IEEE Trans. Knowledge and Data Eng., vol*. 13, no. 6, pp. 1010-1027, Nov./Dec. 2001.
10. D.J. Martin, D. Kifer, A. Machanavajjhala, J. Gehrke, and J.Y. Halpern, "Worst-Case Background Knowledge for Privacy-Preserving Data Publishing," *Proc. IEEE 23rd Int'l Conf. Data Eng.* (ICDE), pp. 126-135, 2007.
11. V.Poovarasi, D.Vijay Anand "Overlapping Slicing: A narrative approach to privacy preserving data publishing," *Proc. Research Journal of Computer Systems Engineering,* vol. 04, Special Issue, June 2013.
12. Benjamin C. M. Fung, Ke Wang, Rui Chen, and Philip S. Yu, "privacy-preserving data publishing: a survey of recent developments," proc. ACM computing surveys, vol. 42, no. 4, article 14, June 2010.

Volume 2, Issue 3 (2014) 618-622 ISSN 2347 - 3258
International Journal of Advance Research and Innovation

High Speed Data Collection in Wireless Sensor Network

Kamal Kr. Gola [a, *], Bhumika Gupta [b], Zubair Iqbal [c]
[a] Department of Computer Science & Engineering, Uttarakhand Technical University, Uttarakhand, India
[b] Department of Computer Science & Engineering, GB Pant Engineering College, Pauri Garhwal, Uttarakhand, India
[c] Department of Computer Science & Engineering, M.I.T, Moradabad, Uttar Pradesh, India

Article Info
Article history:
Received 20 July 2014
Received in revised form
30 July 2014
Accepted 20 August 2014
Available online 15 September 2014

Keywords
Wireless Sensor Network,
Energy Efficient,
Cluster Head,
Sub Cluster Head,
Data Aggregation,
Shortest Path Algorithm,
Base Station

Abstract
A Wireless Sensor Network (WSN) is composed of sensor nodes spread over the field to sense the data. The sensed data must be gathered & transmitted to Base Station (BS) for end user queries. Sensor nodes can be deployed in the harsh environment. As we know that Energy efficient routing is one of the key issues in wireless sensor network because all the nodes are battery powered, so failure of one node affects the entire network that's why Energy saving is always crucial to the lifetime of a wireless sensor network. Many routing protocols have been proposed to maximize the network lifetime and decrease the energy consumption. But these algorithms do not define how to collect data quickly in efficient way. We proposed an algorithm to provide this service. The main purpose of the proposed algorithm is to reducing the time in the collection process of data in the wireless sensor networks.

1. Introduction

Wireless sensor network (WSN) is widely considered as one of the most important technologies for the twenty-first century. [1] A simplest wireless sensor network (WSN) is a network possibly having low-size and minimum complexity or someone can define a sensor network as a composition of a large number of sensor nodes that are densely deployed. A wireless sensor network mainly consists of spatially distributed autonomous sensors those monitor the physical or environmental conditions cooperatively like temperature, sound, vibration, motion, pressure, pollutants etc. A single WSN can contain a few or several hundreds or even thousands sensors, generally called as nodes, where each node is connected to one or many sensors. Nodes sense the environment and then communicate the information which is collected from the monitored field. The data is forwarded through wireless links, possibly via multiple hops, to a sink that can use it locally, or is connected to other networks (e.g. the Internet) through a gateway. The sink node is a kind of destination node, where the entire messages originated by sensor nodes are collected. Or in other words it represents the end point of data collection in wireless sensor network.

When the environment is needed to be monitored remotely then a sensor network is designed in such a way that the data from the individual sensor node is sent to a central base station that is located far from the network, through which the end-user can access the data. The main characteristics of WSNs include,

1. Ease of use
2. Ability to cope with failures of nodes and communication
3. Scalability to large scale deployment
4. Power consumption constrains for nodes that use batteries or Energy harvesting
5. Ability to cooperate with harsh environmental conditions

In the past decades, it has received tremendous attention from both academia and industry all over the world. A WSN typically consists of a large number of low-cost, low-power, and multifunctional wireless sensor nodes, with sensing, wireless communications and computation capabilities. [2][3] These sensor nodes communicate over short distance via a wireless medium and collaborate to accomplish a common task, for example, environment monitoring, military surveillance, and industrial process control. [4]

2. Energy Efficient Routing Protocols in WSN

2.1 Low-energy adaptive clustering hierarchy (LEACH)

LEACH [5] is a cluster-based, distributed, autonomous protocol. The algorithm randomly chooses a portion of the sensor nodes as cluster heads, and lets the remaining sensor nodes choose their nearest heads to join. The cluster member's data is transmitted to the head, where the data is aggregated and further forwarded to the base station. The LEACH algorithm reduces the number of nodes that directly communicate with the base station. It also reduces the size of data being transmitted to the base station. Thus, LEACH greatly saves communication energy.

2.2 Power-Efficient Gathering in Sensor Information Systems (PEGASIS)

In the PEGASIS protocol [6], a cluster is a chain based on geographical location. The PEGASIS protocol constructs all sensor nodes into a chain with the shortest length. Sensor nodes only communicate with their adjacent nodes so that they can send data at the lowest power level. In each round, the system randomly chooses a sensor node as the cluster

Corresponding Author,
E-mail address: kkgolaa1503@gmail.com

head to communicate with the base station. Therefore, communication traffic is reduced.

2.3 Hybrid Energy-Efficient Distributed Clustering (HEED)

HEED [7] extends the basic scheme of LEACH by using residual energy and node degree or density as a metric for cluster selection to achieve power balancing. It operates in multi-hop networks, using an adaptive transmission power in the inter-clustering communication. HEED was proposed with four primary goals namely

i. Prolonging network lifetime by distributing energy consumption,
ii. Terminating the clustering process within a constant number of iterations,
iii. Minimizing control overhead
iv. Producing well-distributed CHs and compact clusters.

In HEED, the proposed algorithm periodically selects CHs according to a combination of two clustering parameters. The primary parameter is their residual energy of each sensor node (used in calculating probability of becoming a CH) and the secondary parameter is the intra-cluster communication cost as a function of cluster density or node degree (i.e. number of neighbors).

2.4 Power Efficient Data Gathering and Aggregation Protocol

The PEDAP protocol [8] further extended the PEGASIS protocol. In the PEDAP protocol, all sensor nodes are constructed into a minimum spanning tree. PEDAP assumes that the base station knows the location information of all sensor nodes, and the base station can predict the remaining energy of any node based on some energy dissipation model. After certain rounds, the base station removes dead sensor nodes and re-computes routing information for the network. In the setup stage, all sensor nodes only need to receive the routing information broadcasted by the base station. Thus, the PEDAP consumes less energy than the LEACH and PEGASIS protocols in the setup stage.

2.5 Top Down Approach

A Delay-aware data collection was done by Cheng et al. 2011 [9]. In their work they gave two approaches for data collection, one is Top-down and another one is bottom up approach. In bottom up approach the network structure is not that much energy efficient while transmitting the data to base station because in their network structure large numbers of nodes are involve in transmit their data to a longer distance so large amount of energy is consumed.

3. Routing Challenges and Design issues in WSN

i. **Node deployment:** Node deployment in WSNs is application dependent and affects the performance of the routing protocol. The deployment can be either deterministic or randomized.
ii. **Energy consumption without losing accuracy:** sensor nodes can use up their limited supply of energy performing computations and transmitting information in a wireless environment.
iii. **Data Reporting Model:** Data reporting can be categorized as either time-driven (continuous), event-driven, query-driven, and hybrid.[10]
iv. **Node/Link Heterogeneity:** In many studies, all sensor nodes were assumed to be homogeneous, i.e. having equal capacity in terms of computation, communication, and power. However, depending on the application a sensor node can have different role or capability.
v. **Fault Tolerance:** Some sensor nodes may fail or be blocked due to lack of power, physical damage, or environmental interference. The failure of sensor nodes should not affect the overall task of the sensor network.
vi. **Scalability:** The number of sensor nodes deployed in the sensing area may be in the order of hundreds or thousands, or more. Any routing scheme must be able to work with this huge number of sensor nodes.
vii. **Network Dynamics:** Most of the network architectures assume that sensor nodes are stationary. However mobility of BS's and sensor nodes is sometimes necessary in many applications.[6]
viii. **Transmission Media:** In a multi-hop sensor network, communicating nodes are linked by a wireless medium.
ix. **Connectivity:** High node density in sensor networks precludes them from being completely isolated from each other.
x. **Coverage:** In WSNs, each sensor node obtains a certain view of the environment. A given sensor's view of the environment is limited both in range and in accuracy.
xi. **Data Aggregation:** Since sensor nodes may generate significant redundant data, similar packets from multiple nodes can be aggregated so that the number of transmissions is reduced.
xii. **Quality of Service:** In some applications, data should be delivered within a certain period of time from the moment it is sensed; otherwise the data will be useless.

4. Network Model

The protocol assumes that 100 sensor nodes are distributed randomly in the network area of diameter 100m. In addition to data aggregation, each node of the network has the capability to transmit data to other sensor nodes as well as to BS. The aim is to transmit the aggregated data to base station with minimum loss of energy which in fact increase system life time in terms of rounds. In this work we consider sensor network environment where:

- Each node periodically senses its nearby environment & likes to send this data to BS.
- Base Station is placed at a fix location.
- Sensor nodes are homogeneous & energy constrained.
- Sensor nodes are dynamic & are uniquely identified time to time.

- Data fusion & aggregation is used to reduce the size of message in the network. We assume that combining n packets of size k results in one packet of size k instead of size nk.

5. Energy Consumption Model

Here in this model, the first component reflects the energy consumed by the radio. The second component presents the energy consumed by the amplifier and depends on the distance between the transmitter and the receiver.

Etransmit = C1 (size) + C2 (size; d) = C1 size + C2 size d

= size (C1 + C2 d)……...…….. (1)

Where: C1: Energy consumed by the radio of the transmitter to transmit a bit,

C2: Energy consumed by the amplifier to send a bit at a distance of 1 meter, size: Packet size,

d: Distance between the transmitter and the receiver,

And $0 < \alpha < 6$ values of 2 or 4 are the most frequently used.

Many works about topology control focus on the component proportional to the distance. Equation 1 becomes, when uniformed by the size of the transmitted packet: Etransmit = C1 + C2. dα This formula points out the relation between energy consumption and distance. This relation is used in topology control to optimize energy consumption by tuning the transmission power taking in to account the distance between the transmitter and the receiver. Many other works suppose that the transmissions are done at the maximum power. In other words, the transmitter uses the transmission power such that any receiver at a distance equal to the transmission rage correctly receives the message. Consequently, we can consider the quantity (C1 + C2.dα) as a constant named C. Hence, the energy dissipated in a transmission by a transmitter is: Etransmit =Csize where size denotes the packet size in bits. In our work, we will assume accordingly.

Sensor Node Information

X	Y	C_id	SCH_id	N_id	Energy	TH	Distance	TE	LOC_T	RCT

Where x and y are coordinates that represents the location of the node in the network.

C_id=Cluster _id, SCH_id=Sub Cluster _id, N_id=Node_id, TH=Threshold Value, TE=Transmission Energy, LOC_T= Locatio Table =Location of the nearest node to which data will be transmitted, RCT=Route Cache Table.

6. Proposed Algorithm

1. All nodes will broadcast a message which contains node_id, transmission range, location and energy status in the network. With the help of this message each node must know about the node _id, transmission range and energy status of all other node in the network. Threshold will be defined by base station.
2. With the help of transmission range, location and energy status cluster will be formed and cluster head will be announced.
3. For every cluster there may be any number of sub cluster head but the number of Sub cluster head is depended upon the number of node in the cluster. For example if number of node in a cluster is N then including cluster head then number of sub cluster head =>N/2.
4. Number of node in a cluster will be calculated with the help of degree of node which define how much message received by node at the time of cluster form.
5. Each node will transmit their data to nearest node. And one of them will be selected as a Sub cluster head according to their energy status.
6. Data aggregation function will be implemented at each level by each node, sub cluster head and cluster head
7. Each node in a cluster maintains their respective RCT that is route cache table after every transmission.
8. The nodes that already sent their data will be kept in sleep mode so that their energy level does not decrease.
9. After this Sub cluster Head transmit their data to the nearest Sub Cluster Head in parallel way. This process will continue until all the data has to be transmitted to the Sub Cluster Head.
10. After this each Cluster Head received all the data from their Sub Cluster Head in their respective cluster.
11. Finally transmit the data to the nearest cluster head in parallel way. If the distance between cluster head and base station is less as compare to another cluster head then this cluster head transmit their data to base station directly.
12. If the threshold value is greater than energy status then new threshold with less value will be defined by the base station and the same process will be apply again until the node in WSN are died.

7. Protocol Description

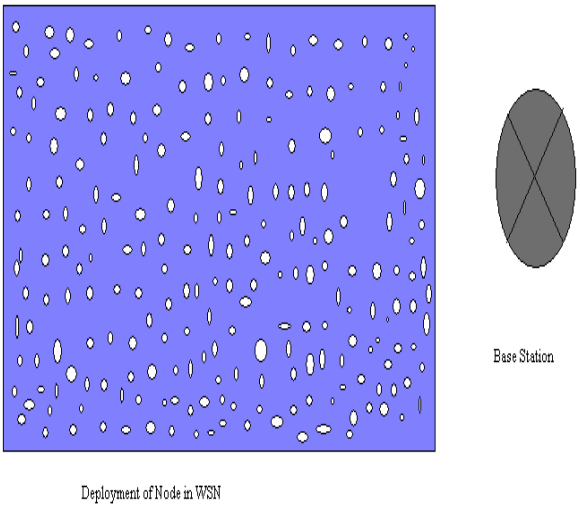

Fig: 1. Deployment of Node in WSN

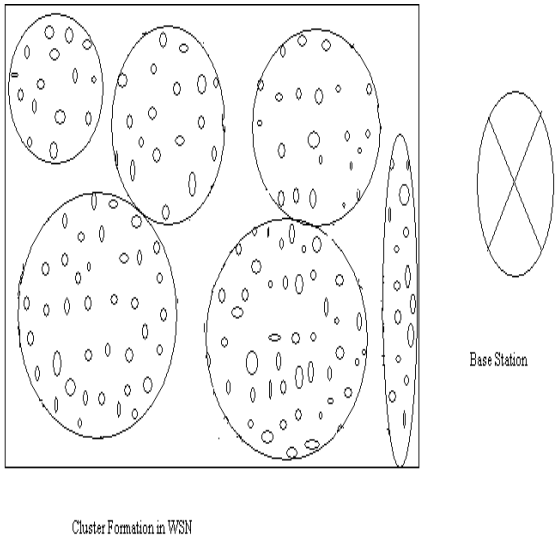

Fig: 2. Cluster Formation

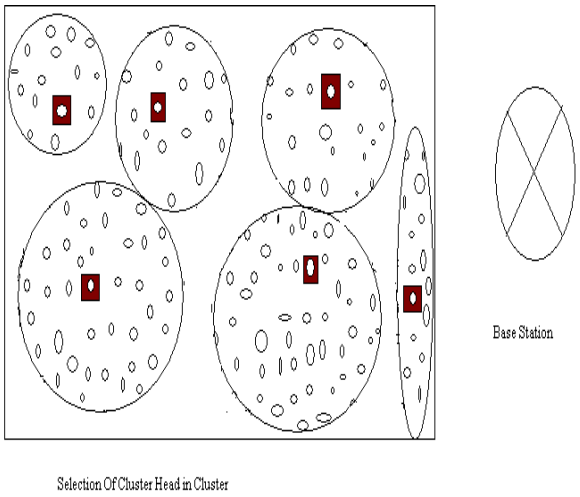

Fig: 3. Selection of Cluster Head

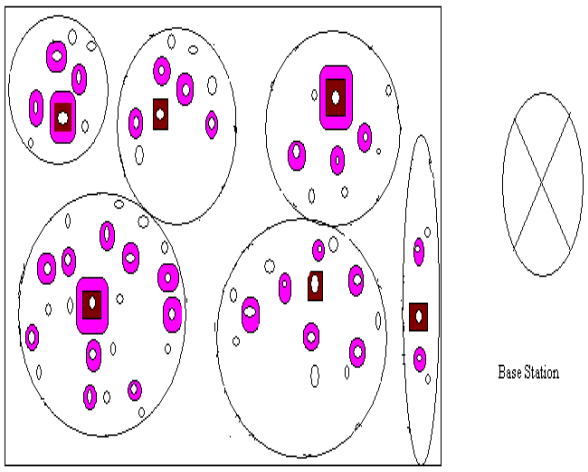

Fig: 4. Selection of sub Cluster Head

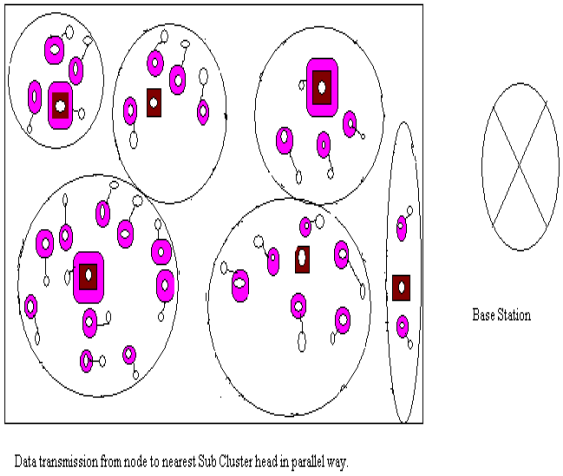

Fig: 5. Data Transmission from Node to Nearest sub Cluster Head in Parallel Way

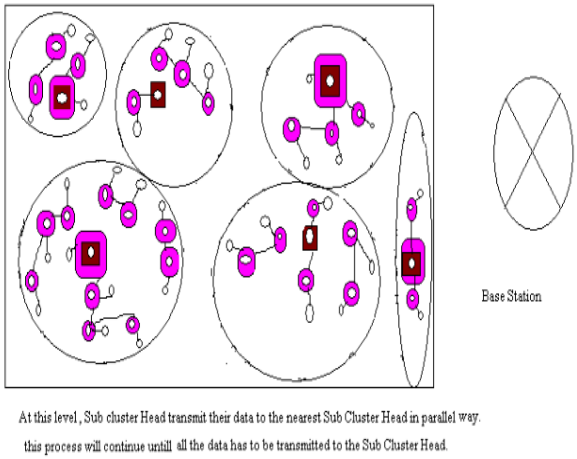

Fig: 6. Data Transmission from Sub Cluster Head to Nearest sub Cluster Head

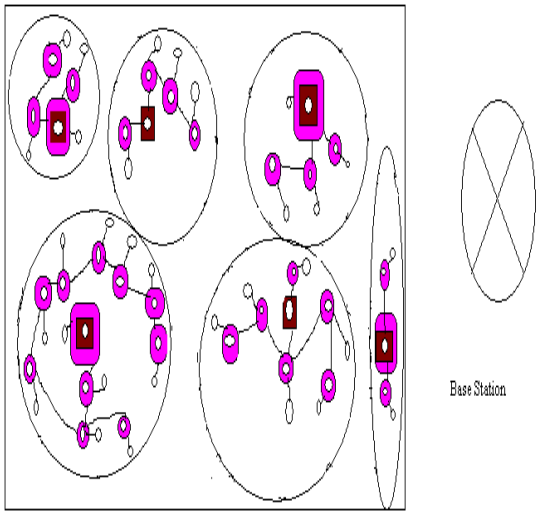

Fig: 7. Data Collection at Cluster Head

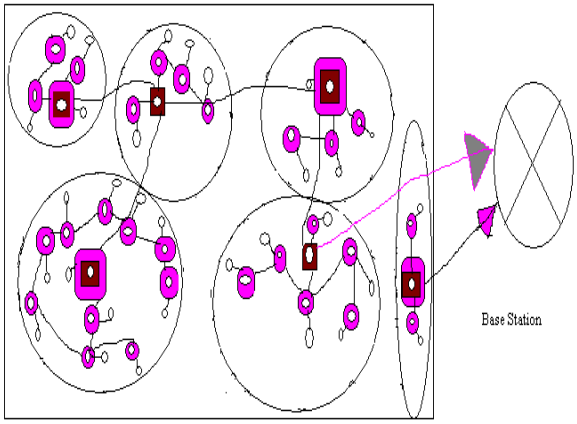

Fig: 8. Data Transmission between Cluster Head to Cluster Head and Between Cluster Head to Base Station

8. Result and Conclusion

In this paper a strategy for high speed data transmission is used with some advancement to securely transfer the data. In the presented work we have taken dynamically arranged WSN which is randomly deployed and arranged. In dynamically arranged WSN, each time data is transferred, so we use the concept of dynamic source routing protocol for energy saving in which new route cache Table is formed. By this arrangement data travel at less nodes. Also using the node activity scheduling scheme node energy is also saved when nodes have no data to transfer or node already sent the data then it is in sleep mode. Using this algorithm we can reduce the time in the collection process of data in the wireless sensor networks and at the time of transmission (among the node and node to base station). Using proposed algorithm we can maximize the network lifetime and decrease the energy consumption. We will implement in C++ to show the performance of our scheme In future we will try to make secure and more energy efficient technique for high speed transmission and collection of data.

References

[1] "21 ideas for the 21st century", Business Week, Aug. 30 1999, 78-167

[2] S. K. Singh, M. P. Singh, D. K. Singh, A survey of Energy-Efficient Hierarchical Cluster-based Routing in Wireless Sensor Networks, International Journal of Advanced Networking and Application, 2010, 02(02), 570–580

[3] S. K. Singh, M. P. Singh, D. K. Singh, Energy-efficient Homogeneous Clustering Algorithm for Wireless Sensor Network, International Journal of Wireless & Mobile Networks, 2010, 2(3), 49-61

[4] Jun Zheng, Abbas Jamalipour, Wireless Sensor Networks: A Networking Perspective, a book published by A John & Sons, Inc, and IEEEE, 2009

[5] W. R. Heinzelman, A. Chandrakasan, H. Balakrishnan, Energyefficient communication protocol for wireless microsensor networks, 33rd Annual Hawaii International Conference on System Sciences, 2000, 3005 – 3014

[6] S. Lindsey, C. S. Raghavendra, Pegasis: Power-efficient gathering in sensor information systems, IEEE Aerospace Conference, 2002, 924-955

[7] Ossama Younis, Sonia Fahmy, Heed: A hybrid, Energy-efficient, Distributed Clustering Approach for Ad-hoc Networks, IEEE Transactions on Mobile Computing, 3(4), 2004, 366-369

[8] HO. Tan, Power efficient data gathering and aggregation in wireless sensor networks, SIGMOD Record, 2003, 32(4): 66 -71

[9] Chi-Tsun Cheng, Chi K Tse, Francis CM Lau. A delay-aware data collection network structure for wireless sensor networks. Sensors Journal, IEEE, 11(3):699–710, 2011.

[10] Y. Yao, J. Gehrke, The cougar approach to in-network query processing in sensor networks, SIGMOD Record, 2002

MIT International Journal of Computer Science and Information Technology, *Vol. 4, No. 2, August 2014, pp. 70-72* 70
ISSN 2230-7621©MIT Publications

Solving TSP by using IWD Algorithm

Vikas Kumar Mittal
Moradabad Institute of Technology
Moradabad, U.P., INDIA
E-mail: vikas_mittal_in@rediffmail.com

Komal Verma
Moradabad Institute of Technology
Moradabad, U.P., INDIA
E-mail: komalverma0292@gmail.com

Anshika Goyal
Moradabad Institute of Technology
Moradabad, U.P., INDIA
E-mail: anshikagoyalag@gmail.com

ABSTRACT

In this paper, we have given an overview on algorithm called "intelligent water drops" or IWD algorithm which is based on the processes that happen in the natural river systems and the actions and reactions that take place between water drops in the river and the changes that happen in the environment that river is flowing. It is always observed that a river often chooses an optimum path regarding the conditions of its surroundings to get to its ultimate goal which is often a lake or sea. And this paper also show how this IWD algorithm is used solve the traveling salesman problem or the TSP.
Index Terms: *Swarm intelligence, Intelligent Water Drop Algorithm (IWD), Travelling Salesman Problem (TSP).*

1. INTRODUCTION

The natural systems that have developed for so long are one of the rich sources of inspiration for inventing new intelligent systems. Swarm intelligence is a field that is closely related to natural swarms existing in nature. Swarm Intelligence (SI) is the collective behavior of decentralized, self-organized systems, natural or artificial. In particular, the Swarm Intelligence system focuses on the collective behaviors from the result of the local interactions of the individuals with each other and with their environment. Some Examples of systems studied by swarm intelligence are colonies of ants, schools of fish, flocks of birds and herds of land animals.

Among the most recent nature-inspired swarm-based optimization algorithms is the Intelligent Water Drops (IWD) algorithm. Intelligent Water drops Algorithm was introduced by Shah Hosseini, H. in 2007.

2. NATURAL WATER DROPS

Water is the indispensible and the sole reason of existence of living being. We see water drop almost everywhere, on the leaves of a tree, moving in rivers, ponds and seas. The movement of water changes the environment where it flows, and so is the effect of the environment on the path of the water drops that flow. There are various twists and turns that changes the course of the water drops from its ideal path from its ideal and shortest path which is straight. And moreover the water drops always try to change the real path to make it a better path and to approach the ideal path.

3. INTELLIGENT WATER DROPS

As discussed in the previous section, on the basis of the properties of the water drops an Intelligent Water Drop (IWD) is discussed which possess few properties of natural water drop. This intelligent water drop has the following properties:

1. The soil it carries, denoted by (IWD).
2. The velocity that it possess, denoted by velocity (IWD).

For each IWD, the values of both properties, soil (IWD) and velocity (IWD) may change as the IWD flows in its environment. From the point of view of engineering, an environment represents a problem that is desired to be solved. How the IWD will move from location i to j is decided by the probability which is inversely proportional to the amount of soil on the available path that is:

$$p(i, j; IWD)\alpha^{L} \frac{1}{soil(i, j)} \quad \ldots(1)$$

Here *soil* (*i, j*) is the amount of soil of the path between location *i* and *j*.

The lower the soil of the path, more the chances to choose that path.

When an IWD moves from its current location i to its next location j, the velocity of the IWD denoted by is update by the amount of soil that is given as:

$$\Delta velocity\,(IWD)\,\alpha^{NL} \frac{1}{soil(i, j)} \quad \ldots(2)$$

Moreover, soil (IWD) is increased by removing some soil of the path (i, j).which is given as:

$$\Delta\, soil\,(IWD) = \Delta soil(i, j)\,\alpha^{NL} \frac{1}{time(i, j, IWD)} \quad \ldots(3)$$

Where *time* (*i, j; IWD*) represent the time taken by the IWD to move from location *i* to *j*.

The time taken for the IWD to travel from location i to j with velocity (IWD) is given as:

$$time(i, j; IWD)\ \alpha^{L} \frac{1}{velocity\,(IWD)} \quad \ldots(4)$$

When IWD moves from location i to j some soil is remove from the path that is $\Delta soil(i, j)$ which is equals to $\Delta soil\ (IWD)$ and updated soil of the path denoted by $soil(i, j)$.

$$\Delta\, soil\ (i, j)\ \alpha^{L}\ \Delta soil(i, j) \quad \ldots(5)$$

4. INTELLIGENT WATER DROP ALGORITHM

Almost every IWD algorithm is composed of two parts: a graph that plays the role of distributed memory on which soils of different edges are preserved, and the moving part of the IWD algorithm, which is a few number of intelligent water drops. These Intelligent Water Drops (IWDs) both compete and cooperate to find better solutions and by changing soils of the graph, the paths to better solutions become more reachable. It is mentioned that the IWD-based algorithms need at least two IWDs to work.

The IWD algorithm is specified in the following steps:

1. Initialization of static parameters:
   - The graph is given to the algorithm, which contains nodes.
   - Velocity updating parameters are and. Here and
   - Soil updating parameters are and. Here and
   - The local soil updating parameter is. Here
2. Spread the IWDs randomly on the nodes of the graph.
3. Update the visited node list of each IWD.
4. Repeat Steps 5.1 to 5.4 for those IWDs with partial solutions.

   i. For the IWD residing in node i, choose the next node j, which does not violate any constraints of the problem and is not in the visited node list of the IWD.

$$p_i^{IWD}(j) = \frac{f(soil(i,j))}{\sum k \notin vc(IWD) f(soil(i,k))} \quad \ldots(6)$$

   Such that

$$f(\text{soil}(i,j)) = p_i^{IWD}(j) = \frac{1}{\varepsilon_s + g(soil(i,j))} \quad \ldots(7)$$

   Where ε_s is a small positive number to prevent possible division by zero and the set *vc* (*IWD*) denotes the node that the IWD should not visit to keep satisfied the constraints of the problem.

   The function *g*(soil (*i, j*) is used to shift the of the path joining nodes *i* and *j* toward positive values and is computed as:

$$\begin{cases} soil(i,j) \ \ if \ \ \min_{l \notin vc(IWD)}(soil(i,l) \geq 0 \\ soil(i,j) - \ \min_{l \notin vc(IWD)}(soil(i,l) \ \ \text{else} \end{cases} \quad \ldots(8)$$

   ii For each IWD moving from node i to node j, update its velocity vel^{IWD} (*t*) by:

$$vel^{IWD}(t+1) = vel^{IWD}(t) + \frac{a_v}{b_v + c_v soil^2(i,j)} \quad \ldots(9)$$

   iii **Compute the soil**

$$\Delta soil(i,j) = \frac{a_s}{b_s + c_s . time^2(i,j; vel^{IWD}(t+1)} \quad \ldots(10)$$

   iv **Update the soil**

$$soil\ (i,j) = (1 - \rho_n).soil(i,j) - \rho_n . \Delta\ soil(i,j) \quad \ldots(11)$$

$$soil^{IWD} = soil^{IWD} + \Delta\ soil(i,j) \quad \ldots(12)$$

   v. Find the iteration-best solution T^{IB} from all the solutions T^{IWD} found by the IWDs.

$$T^{IB} = \max_{\forall T^{IWD}} q(T^{IWD}) \quad \ldots(13)$$

   vi. Update the soils on the paths that form the current iteration best solution.

$$soil\ (i,j) = (1 + \rho_{IWD}).soil(i,j) \quad \ldots(14)$$

$$-\rho_{IWD} \cdot \frac{1}{(N_{IR} - 1)} \cdot soil_{IB}^{IWD} \quad \forall (i,j) \in T^{IB} \quad \ldots(15)$$

   vii. Update the total best solution by the current iteration best solution as follows:

$$T^{TB} = \begin{cases} T^{TB} \ \text{if} \ q(T^{TB}) \geq q(T^{TB}) \\ T^{TB} \qquad \text{otherwise} \end{cases} \quad \ldots(16)$$

   viii. Stops with the total best solution.

5. EXPERIMENTAL RESULTS

Every IWD in the IWD algorithm searches and changes its environment at the same time. A solution is constructed incrementally during the search. The problem of the IWD algorithm is in the form of a graph and IWDs visit nodes of the graph by travelling on the edges of the graph. A swarm of IWDs flows in the graph to find the optimal and near optimal solution with the guidance of a local heuristic. In the following, the IWD algorithm is used to find the best optimal solution for the well-known Travelling Salesman Problem (TSP).

6. TRAVELLING SALESMAN PROBLEM

In the TSP (travelling salesman problem), a map of cities is given to the salesman and he is required to visit every city only once one after the other to complete his tour and return to its first city. The goal in the TSP is to find the tour with the minimum total length among all such possible tours for the given map.

TSP can be modeled as an undirected weighted graph, such that cities are the graph's vertices, paths are the graph's edges, and a path's distance is the edge's length. It is a minimization problem starting and finishing at a specified vertex after having visited each other vertex exactly once. Often, the model is a complete graph (i.e. each pair of vertices is connected by an edge). If no path exists between two cities, adding an arbitrarily long edge will complete the graph without affecting the optimal tour.

A TSP solution for an n-city problem may be represented by the tour T = (c_1,. c_2, c_3,…, c_n). The salesman travels from city c_1 to c_2 then from c_2 to c_3, and he continues this way till he gets to city then he returns back to where he started to city c_1. The tour length is defined by:

$$TL\ (c_1,.\ c_2,\ c_3,\ldots,\ c_n) = \sum_{i=1}^{n} d(c_i, c_{i+1}) \quad (17)$$

In order to use the IWD algorithm for the TSP, the TSP problem is represented as a complete undirected graph N, E . Each link of the edge set E has an amount (cost).of soil. An IWD visits nodes of the graph through the links. The IWD is able to change the amount of the soils on the links. Moreover, cities of the TSP are denoted by nodes of the graph, which hold the physical positions of cities. An IWD starts its tour from a random node and it visits other nodes using the links of the graph until it returns to the first node. The IWD changes the soil of each link that it flows on while completing its tour.

For the TSP, the constraint that each IWD never visits a city twice in its tour must be kept satisfied. Therefore, for the IWD, a visited city list V_c (*IWD*) is employed. This list includes the cities visited so far by the IWD. So, the next possible cities for an IWD are selected from those cities that are not in the visited list V_c (*IWD*) of the IWD.

One possible local heuristic for the TSP, denoted by HUD_{TSP} (i, j) is as follows:

$$HUD_{TSP}(i, j) = ||c(i) - c(j)|| \quad \ldots(18)$$

Where c(k) represents a two dimensional positional vector for the city k. The function $|.|$ is the Euclidian norm. The local heuristic HUD_{TSP} (i, j) measures the undesirability of an IWD to move from city i to j. The heuristic measure becomes small for near cities and large for the cities that are far.

It is reminded that paths with high levels of undesirability are chosen fewer times than paths with low levels of undesirability. In the IWD algorithm, the time taken for the IWD to pass from city i to city j, is proportional to the heuristic HUD_{TSP} (i, j).

This algorithm IWD finds better tours and hopefully escapes local optimums. After a few number of iterations. The soils of all paths (i, j) of the graph of the given TSP are reinitialized again with the initial soil *InitSoil* except the paths of the total-best solution T^{TB}, which are given less soil than *initsoil*.

IWDs prefer to choose paths of TB because less soil on its paths is deposited.

We may refer to the IWD algorithm for the TSP as the "IWD-TSP" algorithm.

7. CONCLUSION

IWD algorithm is closely related to the way the water drops flow in the natural environment. The IWD algorithm is used to solve the well-known Travelling Salesman Problem. This algorithm is capable to find optimal or near optimal solutions. However, there is an open space for modifications in the standard IWD algorithm, using other mechanisms that exist in natural rivers, inventing better local heuristics that fits better and making graphs that are closely related with the problem.

REFERENCES

1. Hamed Shah-Hosseini (2009). Optimization with the Nature-Inspired Intelligent Water Drops Algorithm, Evolutionary Computation, Wellington Pinheiro dos Santos (Ed.), ISBN: 978-953-307-008-7.
2. Hamed Shah-Hosseini (2009), The intelligent water drops algorithm: a nature-inspired swarm-based optimization algorithm, International Journal of Bio-Inspired Computation Volume 1, No.1/2, pp.71–79.

MIT International Journal of Computer Science and Information Technology, *Vol. 5, No. 2, August 2015, pp. 76-78* 76
ISSN 2230-7621©MIT Publications

Regression Test Cases : Selection and Prioritization using Statement Coverage

Praveen Saini
Assistant Professor, CSE Department
Moradabad Institute of Technology
Moradabad, U.P., India
praveensaini5@gmail.com

Puneet Kumar
Assistant Professor, CSE Department
Moradabad Institute of Technology
Moradabad, U.P., India
praveensaini5@gmail.com

Manoj Kumar Singh
Assistant Professor, CSE Department
Moradabad Institute of Technology
Moradabad, U.P., India
praveensaini5@gmail.com

Anurag Panday
Assistant Professor, CSE Department
Moradabad Institute of Technology
Moradabad, U.P., India
praveensaini5@gmail.com

ABSTRACT

Software Testing is integral part of Software development cycle, and having largest proportion in the cost of software development. Cost of testing is directly proportion to numbers of Test cases used in Testing. In Regression Testing, no of test cases keep on increasing as after the changes or in new version, we need to retest the previous test cases to ensure the functionality of previous code before adding new functionality remains working and intact. So Test case selection is very important and optimize the cost of software Testing. After that we need to prioritize them under some criteria or preferences as code coverage, path coverage and dependencies among them.

Keywords: *Software Testing; Regression Testing; Test cases; Test case selection; Execution Trace; Code Changes; Versions; Prioritization.*

I. INTRODUCTION

Software Testing is very important part of software development and the goal of software testing is to ensure the error free of execution of software [1]. As in software development, we identify the software requirements and use the modular approach for the development for verification and validation of requirements and better utilization, that is why Regression Testing is required for ensuring that all previous functionalities works as specified after adding of new functionalities or on integration of two functionalities/modules or to ensure that any new change is code does not affect the old working functionalities [1].

Version 1.

- Develop P
- Test P with Test suite T
- Release P Version 2.
- Modify P to P'
- Test P' for new functionalities
- Perform Regression Testing on P' to ensure that the code carried from P behaves correctly
- Release P'

So whenever we have modified program P' we need to re-execute the test cases T. In long run, add of running previous Test cases increase the number of Test cases. So Instead of running all

previous test cases, we select some of them on the basis of some criteria such as execution trace and dynamic slicing [4].

II. SAMPLE CODE

```
main(){
int x,y,p;
scanf("%d%d",&x,&y);
if(x>y){
p=g(x,y);
printf("%d",p);
}
}

int g(int a, int b){
if(a==(b+1)){
a=a+1;
return(a*a);
}else
return(b*b);
}
```

Control flow graph for sample code

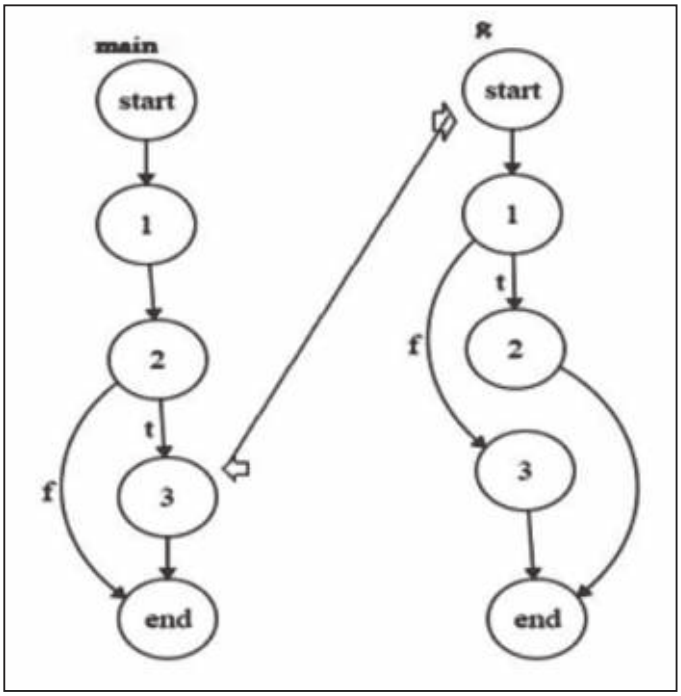

IV. TEST CASE SUITE FOR PROGRAM P

Consider the following test cases that was run to test version 1 program P

T = {
t1= < x=4; y = 3>
t2= < x= 6; y = 4>
t3= < x = 2; y = 5>
}

These are minimum required test case to execute the each statement at least once.

V. EXECUTION TRACE FOR TEST SUITE T

Execution Trace is the nodes in execution on a particular test case.

Test Case	Execution Trace
t1	main.start,main.1,main.2, main.3,g.start,g.1,g.2,g. end,main.3,main.end
t2	main.start,main.1,main.2,main.3,g.start,g.1,g.3,g.end, main.3,main.end
t3	main.start,main.1,main.2,main.end

VI. TEST VECTOR

A test vector for node n, is set of tests traverse the node n

Function	Test Vector				
	Start	1	2	3	End
main	t1,t2,t3	t1,t2,t3	t1,t2,t3	t1,t2	t1,t2,t3
g	t1,t2	t1,t2	t1	t2	t1,t2

VII. VERSION 2: MODIFY PROGRAM P TO P'

Suppose we do some change the function g()

```
int g(int a, int b){
if(a==(b+2)){ //here is change
a=a+1    ;
return(a*a);
}else
return(b*b);
}
```

So change is at if condition a==(b+2) in P' instead of a==(b+1) of program P

VIII. TEST CASE SELECTION/MINIMIZATION

As we noticed the change happen at the Node g.1 in the control flow graph, CFG. Initially we have Test suite T,

T = {
t1= < x=4; y = 3>
t2= < x= 6; y = 4>
t3= < x = 2; y = 5>
}

for program P.

As per the Test Vector we generate, only the test case t1 and t2 is traversing the node g.1 for P'

So minimized Test suite for Regression Testing is:

T' = {

t1= < x=4; y = 3>

t2= < x= 6; y = 4>

}

IX TEST CASE PRIORITIZATION USING STATEMENTCOVERAGE

Now we have minimized test suite

T' = {

t1= < x=4; y = 3>

t2= < x= 6; y = 4>

}

Now as per modified program P'

Test case t2 is satisfying the condition a=(b+2) and covering more statement [a=a+1; return(a*a);] than test case t1 [return(b*b);]

We can give priority to test case t2 over test case t1 because executing more statement earlier to rectify more error as early as possible [2,3].

X. CONCLUSION

As in paper we have proposed the way to minimize the number of test cases that are need to execute during Regression Testing after modification of Program P to P' and give the priorities to selected test cases on the basis of statement coverage. We found that Instead of 3 test cases only 2 test cases required during Regression Testing and to execute the test case covering more statements earlier is more beneficial as it have higher probability to find more errors that the test case covering less statement.

REFERENCES

[1] Mathur, A.P., "Foundations of Software Testing", Pearson, 2008

[2] Muhammad Shahid and Suhaimi Ibrahim," A New Code Based Test Case Prioritization Technique", International Journal of Software Engineering and Its Applications, Vol.8, No.6 (2014), pp. 31-38.

[3] K.K. Aggrawal, Yogesh Singh, A. Kaur, " Code coverage based technique for prioritizing test cases for regression testing," ACM SIGSOFT Software Engineering Notes, vol. 29 Issue 5 September 2004.

[4] Leung, K.N., White, L., "Insights into Regression Testing", Proc. *IEEE International Conference on Software Maintenance* (ICSM), pp. 60-69, 1989.

A Modified PTS Scheme for PAPR Reduction in OFDM System with Low Complexity

Monica Kathuria
Deptt. Of ECE
MIT
Moradabad, India

Pankaj Sharma
Deptt. Of ECE
MIT
Moradabad, India

Umesh Gupta
Deptt of ECE
Meri College of Engg. &Tech
Sampla, India

ABSTRACT
Orthogonal Frequency Division Multiplexing (OFDM) is the most desired and attractive among the various broadband wireless communication system because of its robustness against multipath fading. However even after its so many advantages OFDM has been able to deliver upto its potential due to its "High Peak to Average Power Ratio (PAPR)" which causes power inefficiency in RF section of the transmitter effecting the throughput. The soul purpose of this paper is to provide the most effective PAPR reduction technique while doing amendments in the Partial Transmit Sequence and is termed as the modified Partial Transmit Sequence which overcomes the limitation of conventional system in which a property of cyclically shifting of IFFT is used which doesn't require the side information and provides a system with low complexity.

Keywords
PAPR, PTS, IFFT, CCRR.

1. INTRODUCTION
Orthogonal frequency division Multiplexing (OFDM) is a Multicarrier modulation technique where multiple data streams are modulated with mutually orthogonal carrier. In OFDM a high rate data stream is divided into a various number of lower rate data streams which would eventually get transmitted over a number of subcarriers simultaneously [1]. These subcarriers are overlapped with each other in order to increase the spectral efficiency hence providing desired resource utilization. One of the major attractive and effective feature of OFDM is its efficiency in utilization of the available network spectrum also stating its capability to effectively utilize the various other desired resources. Among the different effective and advantageous attributes some of the most popular are as its immunity to the inter-symbol interference, its robustness with respect to multipath fading and ability for effectively transfer high data rates. Due to its high spectrum efficiency and channel robustness it is used in digital audio/videos for high speed communication .The major drawback of OFDM is high PAPR which causes nonlinear distortion. Many techniques has been designed to overcome this PAPR issue in which conventional PTS is an attractive and most adopted method [2].

In this paper we proposed modified partial transmit sequence to reduce the peak-to-peak-average ratio (PAPR) in orthogonal division multiplexing (OFDM) system. The proposed technique uses the cyclically shifting property of IFFT which doesn't require the explicit transmission of side information which is required in conventional partial transmit sequences (PTS) technique [3]. The paper is comprised of following sections: In section II an introduction of PAPR in OFDM system has been highlighted which is followed by the proposed method in section III in which conventional and modified Partial Transmit Sequence is shown for improving the computational complexity an analysis has been done in this section. Its results are shown in section IV which is carried on MATLAB.This is followed by the conclusion in section V.

2. PAPR IN OFDM SYSTEM
Consider the N input blocks of length N which is given as $(x_n, n = 0,1, \dots \dots N-1)$.Each symbol modulates a single set of subcarriers $(f_n, n = 0,1,2, \dots N-1)$.The chosen subcarriers are orthogonal and given as $f_n = n\Delta f$ in frequency domain where $\Delta f = {}^{1}/_{NT}$,T is the duration of symbol. Thus, the transmitted OFDM signals is given as:

$$\chi(\mathrm{t}) = \frac{1}{\sqrt{N}} \sum_{k=0}^{N-1} X_k e^{j2\pi f_k t},\ 0 \le t \le NT \qquad (1)$$

Where j=√ (-1), Figure 1 shows the block diagram of OFDM system.

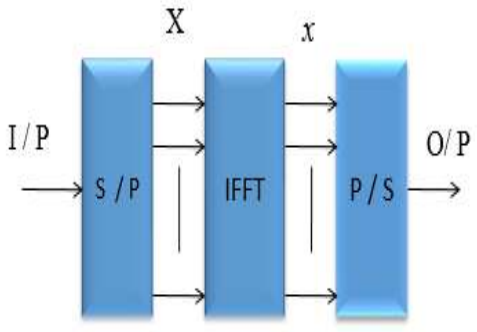

Figure1. Block diagram of basic OFDM system

PAPR in OFDM signal is defined as the ratio of maximum instantaneous power and its average power which is given as:

$$PAPR = \frac{max|x(t)|^2}{E|x(t)|^2} \qquad (2)$$

Where E denotes the expectation operator.PAPR and in dB it is calculated and given as $PAPR = 10\log_{10}(PAPR)$.

3. PROPOSED METHOD

3.1 Conventional Partial Transmit Sequence (C-PTS)

Conventional Partial Transmit Sequence C-PTS is the most halsen technique for the reduction of PAPR in OFDM system. The PTS model is shown in figure in 2 .X denotes the data block and given as a vector:

$$X = [X_0, X_1, \ldots \ldots X_{N-1}]^T \qquad (3)$$

The above vector X is divided into M disjoint subblocks and represented by vector:

$$\{ X_m, m = 1,2,3 \ldots . M \}$$

$$X = \sum_{m=1}^{M} X_m \qquad (4)$$

All the subcarrier that are presented in another subblock. An IFFT is employed as:

$$x = IFFT\{X\} \qquad (5)$$

Applying phase rotation sector to each subblock:

$$b_m \in \{ \pm 1, \pm j \} \qquad (6)$$

Where $b_m, m = 1,2,3 \ldots . M$, we can set weighting factor $b_1 = 1$,where the optimum phase sequence is analyzed which minimizes PAPR of the OFDM signal[4,5], then-

$$x' = [x_1, x_2, \ldots . x_m] \begin{bmatrix} b_1 \\ b_2 \\ \vdots \\ b_m \end{bmatrix}$$

$$x' = \sum_{m-1}^{M} b_m x_m \qquad (7)$$

And $\{ b_1, b_2, \ldots\ldots\ldots, b_m \} = \arg\min[\max |\sum_{m-1}^{m} b_m, x_m|^2]$

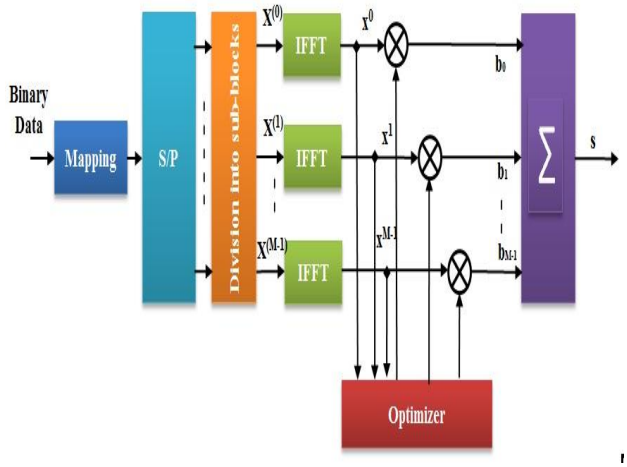

Figure 2. Block diagram of Conventional PTS

3.2 Modified PTS Scheme (M-PTS)

This scheme is the amended version of conventional PTS scheme as it lowers the complexity of the transmitter and the receiver without the help of side information Unlike the C-PTS ,this modified version generates a sequence by cyclically shifting the signals and then combining them together and given as [6,7]:

$$\bar{x} = \sum_{m=1}^{M} \bar{x}^m(k) \qquad (8)$$

Where the shifting number is ***k***, for sub-block signals x^m and $\bar{x}^m(k)$ is:

$$\bar{x}^m(k) = circular(x^m, k)$$
$$= \left[x^m(k), \ldots, x^m(LN-1), x^m(0), \ldots, x^m(k-1)\right] \qquad (9)$$

For directly computing the signal the equation we can use the equation (8) when they have only different in sub-block m .

$$x2 = x1 - \left(x^m - \bar{x}^m(k)\right) \qquad (10)$$

Thus the subblocks can be generated by using the equation 10 and the sequence should be chosen with the minimum value of PAPR for transmission [8]. Figure 3 depicts the OFDM structure with the modified PTS scheme.

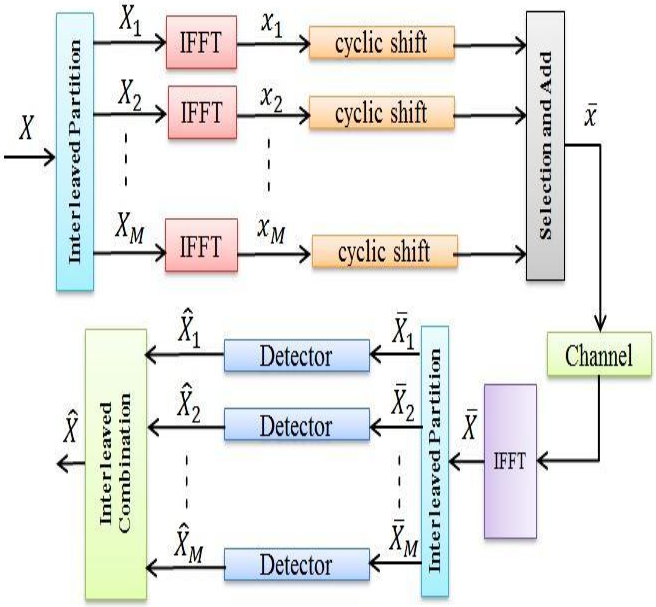

Figure 3. Block diagram of M-PTS Scheme

In this the property of cyclically shifting of IFFT is utilized which operates on each subblocks individually for shifting the number k as the cyclically shifting signal which have the eminent phase constellation in frequency domain and at the receiver, detector determines the shift number k according to the phase constellations for the signal received after FFT without using the side information. Thus the computational complexity is achieved by using Cooley-Tukey algorithm with this interleaved partition method.

3.3 Analysis of Computational Complexity for the C-PTS and the M- PTS

The computational complexity for the C-PTS and the modified PTS has been analyzed for transmitter and the receiver.

3.3.1 Computational Complexity for the Transmitter

In this section the computational complexity of the proposed scheme is compared with the C-PTS and other low complexity PTS schemes.

When the number of subcarriers is $N = 2^n$ and the oversampling factor is $L = 2^l$ .The numbers of complex multiplications and complex additions required for the conventional PTS scheme can be express as follows:

The LN -point IFFT requires $LN/2\log_2(LN)$ numbers of complex multiplication (n_{mul}) and $LN\log_2(LN)$ numbers of complex addition (n_{add}) thus for the C-PTS the total n_{mul} and n_{add} are given as $LN/2\log_2(LN/M)$ and $LN\log_2(LN/M)+W^{(M-1)}(M-1)LN$ respectively.

While for the modified PTS scheme, the total n_{mul} and n_{add} are given as $LN/2\log_2(LN/M)$ and $LN\log_2(LN/M)+W^{(M-1)}2LN$, respectively.

3.3.2 Computational Complexity for the Receiver

The computational complexity for both receivers of modified PTS and C-PTS are divided in two parts-

(i) A LN -point FFT operation and

(ii) The detector

The overall computational complexity for the C-PTS scheme is:

$$n_{mul} = LN/2\log_2(L^2N^2/M)+(Q+2)N$$
$$n_{add} = LN\log_2(L^2N^2/M)+W^{(M-1)}(M-1)LN+2QN$$

While the overall computational complexity for the modified PTS scheme is:

$$n_{mul} = LN/2\log_2(L^2N^2/M)+(Q+2)WN$$
$$n_{add} = LN\log_2(L^2N^2/M)+W^{(M-1)}2LN+2QWN$$

The computational complexity reduction ratio (CCRR) of the modified PTS scheme over the C-PTS scheme is defined as [8,9,10]:

$$CCRR = \left(1-\frac{\text{Complexity of the modified PTS}}{\text{Complexity of the C - PTS}}\right)\times 100\%$$

In table 1 the comparison for the different values of CCRRs is shown in between C-PTS and the M-PTS for different values of M & N.

Table 1. Computational Complexity Reduction Ratio

Comparison	CCRR	
Subblock	M=8	M=16
Complex Addition	71.01%	86.3%
Complex Multiplication	72.66%	87.12%

4. SIMULATION RESULTS

The analysis has been done with the help of MATLAB and several simulations results are assess which describes that modified PTS shows better performance in comparison to C-PTS. In this QPSK modulation scheme is used. The evaluation of the performance is analysed in terms of complementary cumulative distribution function.

Table 2. Simulation Parameters

PARAMETERS	VALUE
Modulation	QPSK
Number of subcarriers (N)	256
Number of sub-blocks (M)	8,16
Channel	AWGN
Oversampling factor (L)	4
Phase factor possible values (W)	4 (1,-1,j,-j)
HPA model	SSPA

Figure 4 shows the Simulation Results of Conventional PTS.

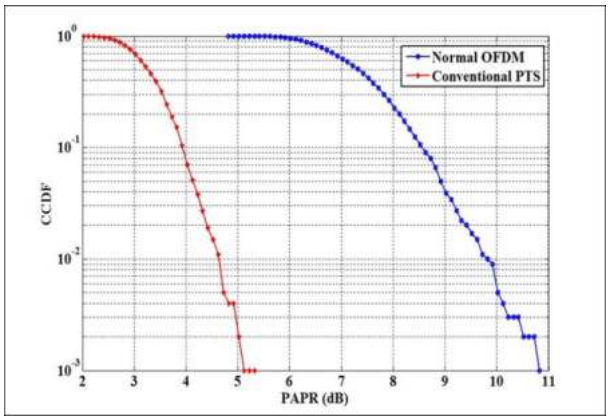

Figure 4. PAPR performance of C-PTS and normal OFDM

In Figure 5 comparison between the proposed modified PTS scheme (C-PTS) with conventional PTS scheme is shown and we found that CCDF of proposed C-PTS scheme is superior.

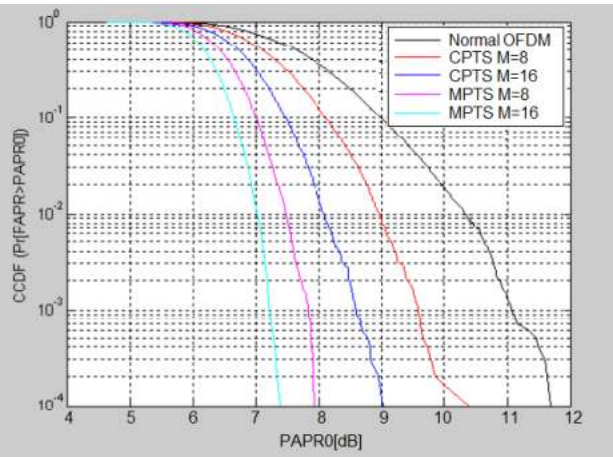

Figure 5. PAPR performance of MPTS, CPTS and normal OFDM for N=256, M=8 &16

5. CONCLUSION

In this paper, a modulated PTS scheme with reduced complexity has been proposed. In this approach cyclically shifting property of IFFT is used which doesn't require side information for the transmission. With this technique the complexity has been reduced in comparison with the conventional partial transmit sequence and the PAPR reduction performance is improved with increase in the number of sub-blocks M due to increase in the number of values.

6. REFERENCES

[1] Jae Hong Lee Seung Hee Han, "An Overview of peak-to-average power ratio reduction techniques for multicarrier transmission," IEEE Wireless Communications, pp. 56-65, April 2005.

[2] Yiyan Wu Tao Jiang, "An Overview: Peak-to-Average Power Ratio Reduction Techniques for OFDM Signals," IEEE transactions on broadcasting, vol. 54, no. 2, june 2008.

[3] Muller, S. H. and J. B. Huber, "OFDM with reduced peak-to average power ratio by optimum combination of partial transmit sequences," IEEE Electron. Lett., Vol. 33,368-369, Feb. 1997.

[4] S. H. Muller and J. B. Huber, "OFDM with reduced peak-to-average power ratio by optimum combination of partial transmit sequences," *Electron. Lett.*, vol. 33, pp. 368–369, 1997.

[5] S. H. Han and J. H. Lee, "PAPR reduction of OFDM signals using a reduced complexity PTS technique," *IEEE Sig. Proc. Lett.*, vol. 11, no. 11, pp. 887-890, Nov. 2004.

[6] L. J. Cimini Jr. and N. R. Sollenberger, "Peak-to-average power ratio reduction of an OFDM signal using partial transmit sequences,"IEEE Commun. Lett., vol. 4, no. 3, pp. 86-88, Mar. 2000.

[7] Abdelsalam Sayed Ahmed,Mona Shokair,El Sayed El Rabaie, "PAPR Reduction for LFDMA using a reduced Complexity PTS Scheme," The online Journal on Electronics and Electrival Engineeing,Vol.04 No.02,pp. 524-530.

[8] L. Wang, O. Yuan and H. C. Chen, "A low-complexity peak-to average power ratio reduction technique for OFDM-based systems," IEEE VTC 2004-Fall, 2004, vol. 6, pp. 4380-4384.

[9] Ghassemi, A.; Gulliver, T.A., "A Low-Complexity PTS-Based Radix FFT Method for PAPR Reduction in OFDM Systems," IEEE Transactions on Signal Processing, vol.56, no.3, pp.11611166,March 2008.

[10] Pooria Varahram, Borhanuddin Mohd Ali, Senior Member, IEEE, "Partial Transmit Sequence Scheme with New Phase Sequence for PAPR Reduction in OFDM Systems", IEEE Transactions on Consumer Electronics, Vol. 57, No. 2, May 2011.

[11] Chenyang Yang,Gang Wu, Shaoqian Li, and Geoffrey Ye Li Taewon Hwang, "OFDM and Its Wireless Applications: A Survey," IEEE Transactions on Vehicular Technology, Vol. 58, No. 4, pp. 1673-1694, May 2009.

[12] Tao Jiang and Yiyan Wu, "An Overview: peak to average power ratio reduction technique for OFDM system," IEEE Transactions on Broadcasting, vol. 54, no.2,pp. 257-268, June 2008.

[13] Y.Wu and W. Y. Zou, "Orthogonal frequency division multiplexing: A multi-carrier modulation scheme," IEEE Trans. Consumer Electronics, Vol. 42, No. 3, pp. 392-399, August 1995.

[14] W. Y. Zou and Y. Wu, "COFDM: An overview," IEEE Trans. Broadcasting," Vol. 41, No.1, pp. 1-8, March 1995.

[15] Ramjee Prasad, "OFDM for Wireless Communications systems", Artech House Publishers, 2004.

[16] Breiling, M., Muller-Weinfurtner, S. H., and Huber, J. B., "SLM peak- power reduction without explicit side information," IEEE Communications Letters, vol. 5, pp. 239-241, June 2001.

[17] R. W. Bauml, R. F. H. Fischer, and J. B. Huber, "Reducing the peak-to- average power ratio of multicarrier modulation by selected mapping," Electron. Lett., vol. 32, pp. 2056–2057, Oct. 1996.

[18] G.Tong Zhou and Liang Peng, "Optimality condition for Selected Mapping in OFDM ," IEEE Transactions on signal processing, vol. 54,no.8, pp. 3159-3165, Aug. 2006.

[19] Seung Hee Han and Jae Hong Lee, " An overview of peak-to-average power ratio reduction techniques for multicarrier transmission," IEEE Wireless Communications, Vol.12,No.2, pp.56 – 65, 2005.

[20] D Wulich, and L Goldfeld, "Reduction of peak factor in orthogonal multicarrier modulation by amplitude limiting and coding," IEEE Transactions. Communication, vol. 47, no. 1, pp 18-21, January 1999.

Rajul Misra* and G. L. Pahuja

Fuzzy Logic Based Rotor Health Index of Induction Motor

DOI 10.1515/ijeeps-2015-0032

Abstract: This paper presents an experimental study on detection and diagnosis of broken rotor bars in Squirrel Cage Induction Motor (SQIM). The proposed scheme is based on Motor Current Signature Analysis (MCSA) which uses amplitude difference of supply frequency to upper and lower side bands. Initially traditional MCSA has been used for rotor fault detection. It provides rotor health index on full load conditions. However in real practice if a fault occurs motor can not run at full load. To overcome the issue of reduced load condition a Fuzzy Logic based MCSA has been designed, implemented, tested and compared with traditional MCSA. A simulation result shows that proposed scheme is not only capable of detecting the severity of rotor fault but also provides remarkable performance at reduced load conditions.

Keywords: MCSA, Fuzzy Logic, SQIM

1 Introduction

MCSA is one of the most widely used methods for online diagnosis and detection of motor faults. It does not require estimation of motor parameters and the simplicity of current sensors. Their installation makes it an attractive tool. Many studies have been performed on MCSA [1–5]. Many simulation studies with faulty motor models have been suggested to observe the spectrum of stator currents for each fault condition. By using mathematical equations many models of broken rotor parts and inter turn short circuited stator windings have been implemented, tested, and then abnormal harmonics of stator currents have been obtained [6–12]. Many types of air-gap eccentricities caused by cracked bearings or bending axes have been modeled and simulated [13–16]. Simulation results showed SQIM's fault status that was similar to real fault of broken motors. It has been observed from simulations results that not only stator current has been extracted for MCSA but also speed, torque, flux, and rotor current have been calculated to observe the motor status. Some researchers also have developed methods for motor diagnosis using MCSA with advanced signal-processing techniques. Eigen analysis based frequency estimation has been suggested for high resolution spectral analysis. Wavelet signal processing has been used in spectral analysis for efficiently extracting information of motor faults from stator current spectrums [17, 18]. Online monitoring of motor conditions has been proposed to observe motor parameters, such as, stator resistance and inductance [19]. MCSA methods have recently been successfully applied to diagnose the rotor faults of large induction motors used in the industrial field. From these useful results, MCSA techniques have become the standard of online motor diagnosis. Although MCSA is one of the most powerful and attractive tools for diagnosing motor faults, it has some limitations that degrades the performance and accuracy of a motor diagnosis. Firstly, it requires high precision of slip frequency information to guarantee the reliability of diagnosis results. Secondly, stator current data should be sampled after motor speed arrives at the steady state. The variation of motor speed during the sampling operation invalidates the sampled data. Finally, the unspecified harmonic numbers in the equations of abnormal harmonics induce ambiguous results from MCSA based diagnosis methods. In this paper, Fuzzy logic based MCSA has been proposed to detect the rotor faults efficiently. The proposed scheme is based on Upper side band (USB) and Lower sideband (LSB), and finally rotor health index has been determined. The rest of the paper is organized as follows: in Section 2 various rotor faults have been discussed, Section 3 focuses on the basic fundamentals of MCSA, in Section 4 experimental and simulation studies have been carried out and finally conclusions are drawn in last section.

2 Rotor fault

Induction motor failures through rotor faults are common in many industrial applications. Many researches

***Corresponding author: Rajul Misra,** EED – NIT Kurukshetra, Hariyana, India, E-mail: rajulmisra71@gmail.com
G. L. Pahuja, EED – NIT Kurukshetra, Hariyana, India, E-mail: pahuja.gl@gmail.com

undertaken have identified numerous stresses and their causes [20]. Faults in rotor can be categorized, namely, rotor eccentricity, breakage of end-rings, breakage of rotor cage bars and rotor bow. These faults lead to some secondary failures that may cause severe malfunction of motor. Rotor faults are briefly illustrated as follows:

2.1 Rotor eccentricity

Rotor eccentricity is most common fault occurs mainly due to mechanical stresses e.g. shaft misalignment, load unbalance, bend in rotor shaft, wear and tear in bearings, manufacturing defects and mispositioning of the stator or rotor. Because of a constant radial force, shaft misalignment displaced the rotor position from its routine position which yields asymmetric air-gap between rotor and stator [21]. Air gap eccentricity can be classified into static and dynamic type. Commonly occurring causes of static air gap eccentricity are stator core ovality, incorrect positioning of stator core, and bearing at installation. In static air gap eccentricity, the position of the minimal radial air gap length is fixed and invariant with time. On the other hand dynamic air –gap eccentricity is a condition in which the center of the rotor is not positioned at the center of rotation. Hence the position of the minimal radial air gap rotates with the rotor. Bent shaft, worn bearings, asymmetric thermal expansion of the rotor etc. are the causes of dynamic air –gap eccentricity. Eccentricity in air gap causes ripple torque, unbalanced magnetic pull and lowers the power factor. Its results can be seen in speed pulsations, vibration, acoustic noise, bearing wear and tear and rotor deflection. This increases the risk of stator rotor rub, which can cause severe damage in the stator or rotor core, conductors and insulation [22, 23].

2.2 Breakage of end-rings

The rotor bars of IM are short-circuited on the both sides by end-rings. Substandard castings of aluminum rotors, and/or poor end-ring joints during manufacturing are the sources of the end-ring faults. Once the fault occurs, localized overheating may develop in the cage. Under faulty condition of induction motor, high centrifugal force is produced which causes drastic increase in the speed and current fluctuations [24].

2.3 Breakage of rotor bars

The rotor bars can be partially or completely cracked under running condition of motor due to stresses and improper rotor geometry design. The bar breakage is the major fault in the rotor of IM. Once a bar cracks, the condition of the nearby bars also deteriorates due to the increased stresses. To avoid such a cumulative destructive process, the fault should be detected at early stage [25]. A DOL online starting duty cycle for which the rotor cage winding was not designed to withstand is the main reason of breakage of rotor bars. If breakage of rotor bars rises due to the centrifugal force, the bar will contact the stator winding and finally damage it. In a severe case, the broken pieces of the rotor bar may damage the stator windings or laminations during operation [26]. Broken rotor bar leads to a shaft vibration, bearing failures, air gap eccentricity, destructive sparking, excessive vibration and noise during the motor startup [26, 27]. In addition a broken rotor bar causes unbalanced currents and torque pulsation and therefore average value of torque decreases [28, 29].

2.4 Rotor bow

Due to an asymmetrical heating or cooling of the symmetrical rotor, and/or to an axial symmetry thermal distribution of an asymmetrical rotor, a bow in the rotor can occurs [30]. The rotor bow causes significant problems in the other parts of motor, depending on where the bend occurs [31]. Bows in the rotor can be classified into two types namely local and extended bows [30]. A local bow occurs when an asymmetrical heating is localized in the part with a small length whereas the extended bow occurs when asymmetrical heating extends to a certain length of the rotor [31].

3 MCSA

MCSA is the most general method which is used for fault detection in stator as well in rotor faults [32–38]. In this method the information fetched by stator current sensors is utilized to analyze the behavior of motor. This approach uses the lower and upper twice-slip-frequency sidebands around the fundamental frequency when a rotor asymmetry occurs. This occurrence may be accounted for as the result of a backward rotating field induced by the rotor fault [39]. These LSB and USB are

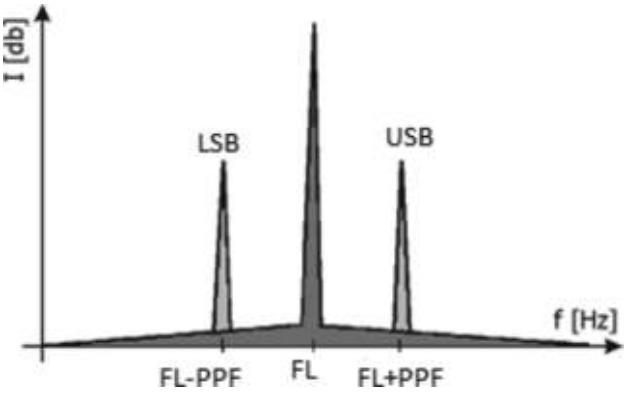

Figure 1: Ideal current spectrum.

majorly affected due to the rotor broken bars. An ideal current spectrum for healthy motor is shown in the Figure 1, which shows twice slip frequency sidebands due to broken rotor bars around the main harmonic.

A decibel (dB) versus frequency spectrum is used to give wide dynamic range and to detect the unique current signature patterns that are the characteristics of different faults. On the basis of current patterns the condition of the rotor is identified. A rotor fault in motor mainly depends upon slip frequency and pole pass frequency (PPF). The slip frequency is the difference between normal speed and actual speed. Generally in motor the number of poles is known and PPF can be determined. The peaks of sidebands can be determined by the eq. (1)

$$F_L \pm PPF \tag{1}$$

where F_L is line frequency The difference in amplitude between the line frequency peak and the pole passing frequency sidebands is an indication of the rotor bar health. The difference of greater than 60 dB indicates an excellent rotor bar condition. As the rotor bars start degrade (i. e. high resistance joints are present or a crack starts developing), the rotor impedance rises therefore the current drawn at the PPF frequency rises, misleading to an increase in the amplitude of the PPF peaks in the current spectrum. A difference of about 48 dB would indicate the presence of high resistance joints whereas a difference of about 35 dB would indicate multiple broken bars. For healthy motor amplitude difference should be high. An estimation of number of broken bars (broken bar factor) can be obtained from the eq. (2) [40].

$$n = \frac{2R}{\left(10^{\frac{N}{20}} + p\right)} \tag{2}$$

Where n is the index (estimate of number of broken bars), R is number of rotor slots, N represents average dB difference between USB and LSB and p is the pole pairs. This index is determined on full load operation and it has to be modified since one may performed the experiments on reduced load. After applying the correction factor for reduced load and particular motor design (commercially sensitive and could not be shared with author) finally index can be determine. Often, there is an expert knowledge available in plant. Expert operators know about the health of the motor. Therefore it is desirable to use this knowledge for extracting the rotor health. An expert can not usually express his knowledge in precise numerical terms but knowledge can be formulated by using words from natural language like excellent, good, alert and damaged etc. In the present work Fuzzy logic based MCSA has been designed, implemented and discussed in detailed in next section.

4 Experimental and simulation study

An Experimental study of fourteen (14) cases has been carried out for rotors faults and analyzed rigorously at Jindal Steel & Power Limited, Raigarh, India. Out of all collected case studies, the results of two cases have been reported. The specifications of reported IMs are tabulated in Table 1, as follows:

Case study – 1
In this case the value of PPF is 0.573 Hz. A fault in rotor (breakage in rotor bars) produces USB and LSB around

Table 1: Specification of IMs.

Case study	KW rating	Full load current (Amps)	Power factor	No. of rotor bars	Load (%)	PPF (Hz)	USB (dB)	LSB (dB)	Index
1	661	72	0.810	58	68.5	0.573	−38.4	−41.8	1.9635
2	480	54	0.893	88	85.7	0.963	−61.9	−65.8	0.02455

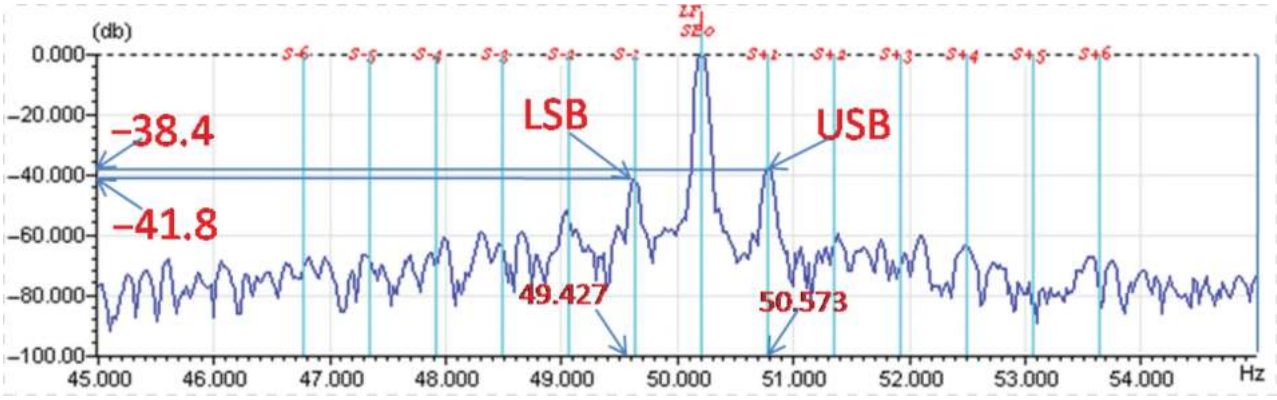

Figure 2: Current pattern for case 1 (Faulty).

the shaft rate harmonics. The differences in amplitude between the line frequency peak to USB and LSB are indications of the rotor bar health. Current signature of motor is shown in Figure 2, and it is observed form the current pattern that the values of USB and LSB are −38.4 and −41.8 respectively and rotor health index has been determined as 1.9635.

For healthy motor amplitude difference should be high. The difference of greater than 60 dB indicates an excellent rotor bar condition. Under faulty condition of the motor (i.e. high resistance joints or cracks in rotor bar), the rotor impedance rises. Due to this, the current drawn at the PPF frequency increases, misleading to an increase in the amplitude of the PPF peaks in the current spectrum. A difference of about 45 dB would indicate the presence of high resistance joints whereas difference of about 35 dB would indicate multiple broken bars. As the value of index is very high which shows faulty condition of the rotor.

Case study – 2

In this case the PPF is 0.963 Hz. The current signature is shown in Figure 3. By observing the signature it is well cleared that FL is 50 Hz and two peaks around the FL have been observed at 50.963 Hz and 49.037 Hz which can also be calculated theoretically from eq. (1). The values of USB and LSB are found to be −65.8 and −61.9 and rotor index has been calculated as 0.0245. The difference in magnitude is greater than 60 dB which shows the healthy condition of the motor.

To verify the effectiveness of Fuzzy based MCSA system all simulation has been carried out on MATLAB R2010a. In the present work Fuzzy based MCSA system has been proposed in which Mamdani Fuzzy inference system has been designed and implemented. Fuzzy membership functions are constructed by observing the data set. LSB and USB are inputs and five (05) triangular membership functions have been considered for each as

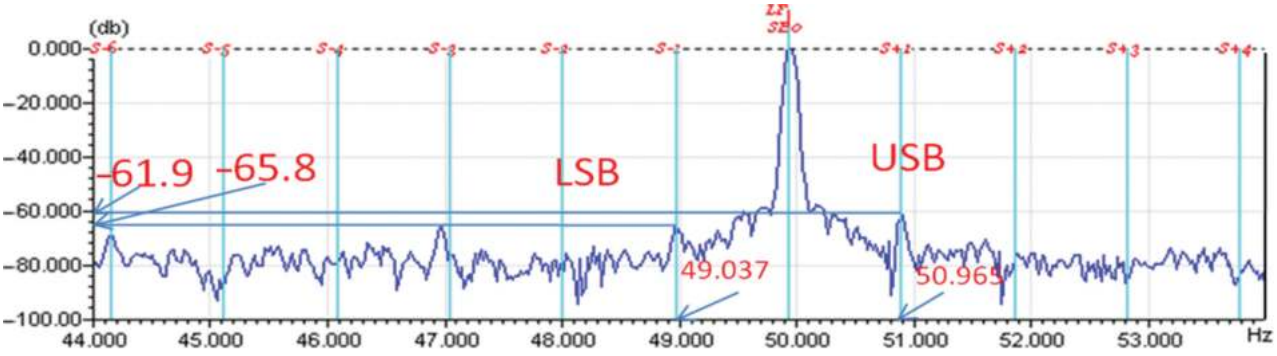

Figure 3: Current pattern for case 2 (Healthy).

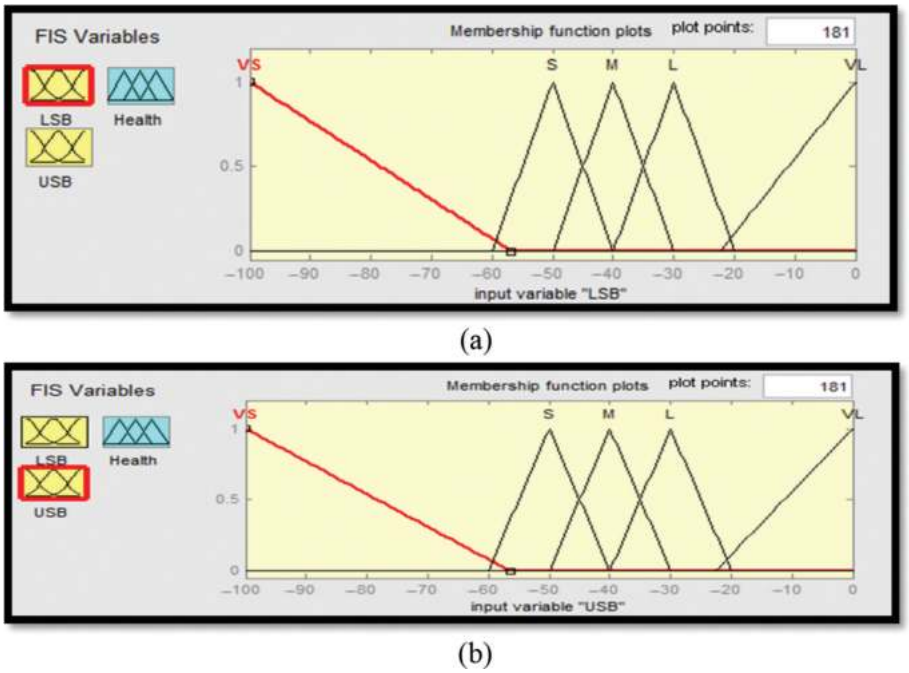

Figure 4: Input membership functions. (a) LSB. (b) USB.

Very Small (VS), Small (S), Medium (M), Large (L) and Very Large (VL). The inputs membership functions are shown in Figure 4.

Rotor health Index is considered as output which has been constructed by trapezoidal and triangular membership functions. For index linguistic variables are Excellent, Good, Alert and Damaged. Centroid method has been considered for defuzzification of the output. The output membership function is shown in Figure 5.

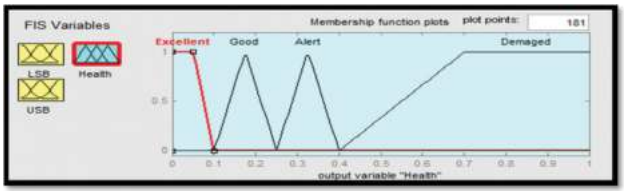

Figure 5: Output membership functions.

Index related to rotor health of motor are tabulated in Table 2.

The rule base is tabulated in Table 3.

The snapshot of Fuzzy rule viewer and surface viewer are shown in Figures 6 and 7 respectively.

The simulated results are obtained and compared with experimental results in Table 4.

Table 2: Rotor health index.

SN	Index	Rotor health
1	0.0–0.10	Excellent
2	0.1–0.25	Good
3	0.25–0.40	Alert
4	>0.40	Damaged

Table 3: Rule base.

LSB / USB	VS	S	M	L	VL
VS	Damage	Damage	Damage	Damage	Damage
S	Damage	Damage	Alert	Damage	Alert
M	Damage	Alert	Alert	Good	Alert
L	Alert	Alert	Good	Good	Excellent
VL	Alert	Alert	Good	Excellent	Excellent

By observing the Table 4, it is cleared that from SN 1 to 9 the experimental indices and simulated indices are almost same and it is already mentioned in Table 2, that with the index of greater than 0.4 the fault severity level of motor increases which considered damaged rotor health and by observing SN 10 to 14 it is clear that the proposed Fuzzy based MCSA system also indicates worst rotor health.

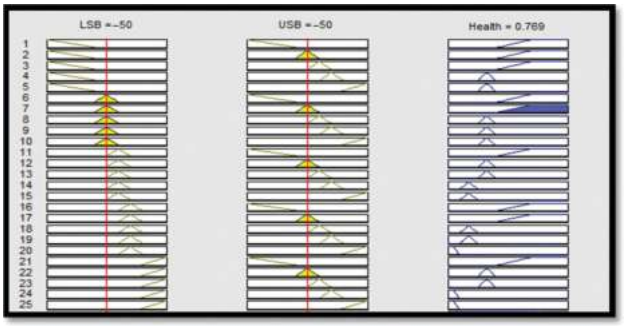

Figure 6: Fuzzy rule viewers.

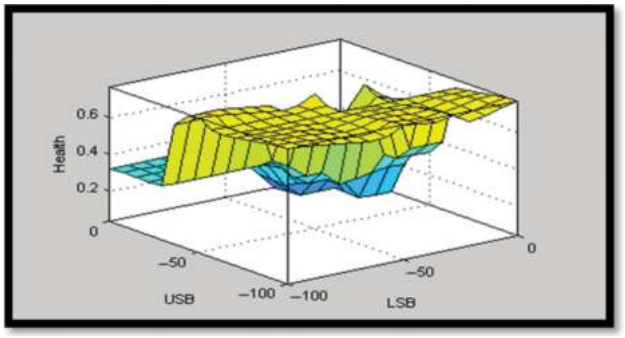

Figure 7: Surface viewer.

5 Conclusions

In this paper several rotor faults have been explored and Mamdani Fuzzy based MCSA scheme has been proposed. The proposed scheme utilizes the information of USB and LSB and provides rotor health index. Conventional MCSA provides the output (rotor health index) at full load condition but one has to add correction factor for determining rotor health index at actual load condition. However in actual practice when faults occurs machine can not run at full load condition Therefore in present work a number of case studies have been carried out at reduced load conditions. It has been concluded from the simulation results that the proposed scheme is able to detect the faults and provides rotor health index without any correction factor.

References

1. Thomas WT, Fenger M. Current signature analysis to detect induction motor faults. IEEE Ind Appl Mag 2001;7:26–34.
2. Nandi S, Toliyat HA. Condition monitoring and fault diagnosis of electrical machine-a review (IEEE IAS Annual Conference. Vol 1, 197–204, 1999).
3. Ye Z, Wu B. A review on induction motor online fault diagnosis (Proc. Int. conf. IEEE-PIEMC.Vol 3, 1353–8, 2000).
4. El Hachemi Benbouzid M. A review of induction motors signature analysis as a medium for faults detection. IEEE Trans Ind Electron 2000;47:984–93.
5. Stone G, Kapler J. Stator winding monitoring. IEEE Ind Appl Mag 1998;4:15–20.
6. Toliyat HA, Lipo TA, White JC. Analysis of concentrated winding induction machine for adjustable speed drive applications-Part 1 (motor analysis). IEEE Trans Energy Convers 1991;6:679–83.
7. Toliyat HA, Lipo TA. Transient analysis of cage induction machines under stator, rotor bar and end ring faults. IEEE Trans Energy Convers 1994;10:241–7.
8. Xiaogang L, Yuefeng L, Toliyat HA, El-Antably A, Lipo TA. Multiple coupled circuit modeling of induction machines. IEEE Trans Ind Appl 1995;31:311–18.
9. Milimonfared J, Kelk HM, Nandi S, Minassians AD, Toliyat HA. A novel approach for broken-rotor-bar detection in cage induction motors. IEEE Trans Ind Appl 1999;35:1000–6.

Table 4: Comparison of results.

SN	IMrating (KW)	Load (%)	LSB	USB	Index (experimental)	Index (simulated)	Error	Rotor health
1.	650	73.50	−80.3	−76	0.0437	0.045	−0.0013	Excellent
2.	350	105.20	−83.7	−73.4	0.0547	0.04379	0.01091	
3.	360	84.80	−55.7	−69.9	0.2387	0.2429	−0.0042	Good
4.	350	85.50	−56.9	−67.2	0.2584	0.2299	0.0285	
5.	650	70.30	−57	−63.5	0.2612	0.2656	−0.0044	Alert
6.	270	89.60	−57.3	−61.3	0.2917	0.2938	−0.0021	
7.	650	64.00	−55.7	−59.3	0.3178	0.325	−0.0072	
8.	180	52.80	−57.7	−60	0.3223	0.325	−0.0027	
9.	650	66.40	−56.9	−57.5	0.3238	0.32	0.0038	
10.	550	79.30	−62.1	−49	0.8683	0.5715	0.2968	Damaged
11.	550	68.50	−52.8	−59.9	0.9019	0.3555	0.5464	
12.	661	65.00	−45.2	−56	1.4489	0.6465	0.8024	
13.	661	68.00	−43.3	−44.1	2.6594	0.7265	1.9329	
14.	350	77.50	−37.7	−39.7	5.0883	0.7903	4.298	

10. Nandi S, Toliyat HA. Novel frequency-domain-based technique to detect stator interturn faults in induction machines using stator induced voltages after switch-off. IEEE Trans Ind Appl 2002;38:101–9.
11. Joksimovic G, Penman J. The detection of interturn short circuits in the stator windings of operating motors (Proc IEEE IECON, Vol 4, 1974–9, 1998).
12. Tallam RM, Habetler TG, Harley RG. Transient model for induction machines with stator winding turn faults. IEEE Trans Ind Appl 2002;38:632–7.
13. Toliyat HA, Arefeen MS, Parlos AG. A method for dynamic simulation of air-gap eccentricity in induction machines. IEEE Trans Ind. Appl 1996;32:910–18.
14. Nandi S, Ahmed S, Toliyat HA. Detection of rotor slot and other eccentricity related harmonics in a three phase induction motor with different rotor cages. IEEE Trans Energy Convers 2001;16:253–60.
15. Joksimovic GM, Durovic MD, Penman J, Arthur N. Dynamic simulation of dynamic eccentricity in induction machines-winding function approach. IEEE Trans Energy Convers 2000;15:143–8.
16. Schoen RR, Habetler TG, Kamran F, Bartfield RG. Motor bearing damage detection using stator current monitoring. IEEE Trans Ind Appl 1995;31:1274–9.
17. Benbouzid MEH, Vieira M, Theys C. Induction motors' faults detection and localization using stator current advanced signal processing techniques. IEEE Trans Power Electron 1999;14: 14–22.
18. Kyusung K, Parlos AG. Induction motor fault diagnosis based on neuropredictors and wavelet signal processing. IEEE/ASME Trans Mechatron 2002;7:201–19.
19. Wiedenbrug WJ, Ramme A, Matheson E, Jouanne VA, Wallace AK. Modern online testing of induction motors for predictive maintenance and monitoring. IEEE Trans Ind Appl 2002;38:1466–72.
20. Bonnett AH, Soukup GC. Cause and analysis of stator and rotor failures in three-phase squirrel-cage induction motors. IEEE Trans Ind Appl 1998;28:921–37.
21. Cameron JR, Thomson WT, Dow AB. Vibration and current monitoring for detecting airgap eccentricity in large induction motor (Proc IEE Electric Power Appl, 155–60, 1986).
22. Nandi S, Toliyat HA, Li X. Condition monitoring and fault diagnosis of electrical motors – A review. IEEE Trans Energy Convers 2005;20:719–29.
23. Faiz J, Ojaghi M. Different indexes for eccentricity faults diagnosis in three-phase squirrel-cage induction motors: a review. Mechatronics 2009;19:2–13.
24. Thomson WT, Gilmore RJ. Motor current signature analysis to detect faults in induction motor drives – fundamentals, data interpretation and industrial case histories (Proc 32nd Turbomachinery Symposium, Houston, TX, USA, 145–56, 2003).
25. Nandi S, Bharadwaj R, Toliyat HA, Parlos AG. Study of three phase induction motors with incipient rotor cage faults under different supply conditions (Proc IEEE Industry Applications Conference, 34th IAS Annual Meeting, 1922–1928, 1999).
26. Culbert IM, Rhodes W. Using current signature analysis technology to reliably detect cage winding defects in squirrel-cage induction motors. IEEE Trans Ind Appl 2007;43:422–8.
27. Zhang P, Du Y, Habetler TG, Lu B. A survey of condition monitoring and protection methods for medium-voltage induction motors. IEEE Trans Ind Appl 2011;47:34–46.
28. Bachschmid N, Pennacchi P, Tanzi E. Cracked rotors. Berlin, Heidelberg: Springer-Verlag, 2010, ISBN 978-3-642-01484–0.
29. Ilonen J, Kamarainen JK, Lindh T, Ahola J, Kalviainen H, Partanen J. Diagnosis tool for motor condition monitoring. IEEE Trans Ind Appl 2005;41:963–71.
30. Pennacchi P, Bachschmid N, Vania A, Zanetta GA, Gregori L. Use of modal representation for the supporting structure in model-based fault identification of large rotating machinery: part 1 – theoretical remarks. Mech Syst Sig Process 2006;20:662–81.
31. Pennacchi P, Bachschmid N, Vania A, Zanetta GA, Gregori L. Use of modal representation for the supporting structure in model-based fault identification of large rotating machinery: part 2 – application to a real machine. Mech Syst Sig Process 2006;20:682–701.
32. Henao H, Martis C, Capolino GA. An equivalent internal circuit of the induction machine for advanced spectral analysis (Conf. Rec. IEEE-IAS Annual. Meeting, vol. 2, Pittsburgh, PA, 739–45, 2002).
33. Henao H, Martis C, Capolino G, Radulescu M. Harmonic characteristics of an induction machine connected to a distribution network (Proc IEEE IECON'02, vol. 2, Seville, Spain, 1008–13, 2002).
34. Henao H, Capolino GA. A circuit-oriented model of induction machine for diagnosis (Proc SDEMPED, Carry-le-Rouet, France, 277–82, 1997).
35. Milimonfared J, Kelk HM, Nandi S. A novel approach for broken rotor bar detection in cage induction motors. IEEE Trans Ind Appl 1999;35:1000–6.
36. Kliman GB, Koegl RA. Noninvasive detection of broken rotor bars in operating induction motors. IEEE Trans Energy Convers 1988;3:873–9.
37. Nandi S, Toliyat HA. Condition monitoring and fault diagnosis of electrical machines – a review (Conf. Rec. IEEE-IAS annual. meeting, vol 1, 197–204, 1999).
38. Thomson WT, Fenger M. Current signature analysis to detect induction motor faults. IEEE Ind Appl Mag 2001;7:26–34.
39. Bellini A, Filippetti F, Franceschini G, Tassoni C, Kliman GB. Quantitative evaluation of induction motor broken bars by means of electrical signature analysis. IEEE Trans Ind Appl 2001;37:1248–55.
40. Thomson WT, Rankin D. Case histories of rotor winding fault diagnosis of induction motor (Proc 2nd International Conference on Condition Monitoring, University College of Swansea, Wales, UK, 1987).

Asian Journal of Multidisciplinary Studies

ISSN: 2321-8819 (Online)
2348-7186 (Print)
Impact Factor: 0.92
Volume 3, Issue 5, May 2015

Rethinking Colonial Discourse in *The Mimic Men*

Sangeeta Mahesh
Asst. Professor of English
Moradabad Institute of Technology, Moradabad

Abstract: *This paper highlights the portrayal of newly independent colonies by V.S. Naipaul in his novel, The Mimic Men. In his early novels Naipaul was mainly engaged in remembering his personal experiences in the fictional form in an attempt to visualize his own displacement. With the writing of House, the problems had been partly resolved. Now he did not want to confine himself as a regional writer, so he wrote some of his novels to establish himself as a universal writer. In Mimic Men, he has portrayed not only the problems of alienation but also the struggle of the people to gain recognition and identity. In The Mimic Men, through the character of Mr. Ralph, the protagonist of the novel, he has tried to focus on broader post colonial themes of power and freedom. His failures at the level of personal life are indicative of a larger national failure. In this novel V.S. Naipaul has given expression to the chaos, confusion and disorder prevailed in the contemporary colonial society. The social analysis which he attempts in The Mimic Men is not confined to the West Indies but extends to the entire Third World. Mimic is one of the most optimistic of Naipul's later novels. At the end of the novel, Ralph Singh can still claim that he has "cleared the decks" and prepared himself for fresh action.*

Key words: Mimic men, colonial discourse, identity crisis, power, independence, Ralph singh, alienation

The Mimic Men starts that phase of Naipaul's fiction writing which portrays newly independent colonies. The themes of alienation, homelessness and mimicry still preoccupy Naipaul, but the view point has changed. They are now seen as a universal condition of the modern world afflicting both colonized and colonizers alike. The other themes like the broader post-colonial themes of power and freedom and recolonization also start appearing in his novels. While the displaced colonials of the earlier novels saw England as the land of opportunities and escape to England meant an escape from all miseries, in The *Mimic Men,* however, London is exposed for what it is – a mirage, a mere illusion – and the 'promised land' turns out to be equally mischievous. ChampaRao Mohan says, "Thematic continuity is maintained through a much more comprehensive treatment of the concept of identity. For, with political independence another dimension has been added making Ralph Singh's search for an identity in *Mimic*, a more complex affair as he has to locate himself within the new socio-political framework" (81)

Naipaul brings out the predicament of Ralph Singh, the protagonist of the novel, to be the same as that of any modern man including an ex-colonizer. The novel is told in the form of memoirs by the main character, who is implicitly criticized by what he actually shows about himself. It starts and ends in the present with the narrative shifting back and forth in time between Ralph Singh's childhood, student life in London, his return to the island, his political career and exile in London. In that way a series of compressed events are joined together in a sequence of contrasting events to develop a unified plot.

Ralph Singh, the protagonist-narrator of the novel, is the representative of a generation which gains power at independence and can only mimic the authenticity of selfhood. His failures at the level of personal life are indicative of a larger national failure. Ralph Singh sets out to write down his experiences with the hope of fashioning an order out of the various unrelated adventures and encounters through which he had gone through. The story he records can be described as tracing Ralph Singh's transition from innocence to experience and his passage from external disorder to personal harmony. By interpreting and analyzing his own experiences he hopes to find some order within the chaos of the present and the uncertainty of the 'picture in the contemporary colonial society'. The social analysis which he attempts in *The Mimic Men* is not confined to the West Indies but extends to the entire Third World.

> It was my hope to give expression to the restlessness, the deep disorder with the great explorations, the overthrow in three continents of established social organizations' the unnatural bringing together of people. But the work will not now be written by me. I am too much a victim of that restlessness which was to have been my subject. And it must also be confessed that in that dream of writing I was attracted less by the act and the labour than by the calm and the order which the act would have implied. (32)

The novel is not in the form of a linear, chronological memoir because the narrator in his attempts to salvage his wrecked life imposes a deliberate order on the events and experiences of his life to reconstruct the meaning of his life. In this novel, Naipaul attains a quality of total detachment which expresses his maturity as a writer. And this quality is indispensable for a writer, working as a critic of societies and cultures.

Singh's memoirs come to us in three parts. In the first part Singh records his disillusionment with London, his marriage with Sandra, an English girl, their return to Isabella followed by Singh's rise in business and finally the breakdown of his marriage. In the second part Singh reverts back to his childhood while in the final section of the novel he gives an account of his political career.

Singh comes to London, full of hopes, thinking it to be the centre of his world, where he is at last to find fulfillment. Singh confesses that while at Isabella, the island of his birth, he had been painfully aware of his ambiguous New World background. “To be descended from generation of idlers and failures, an unbroken line of the unimaginative, unenterprising and oppressed, had always seemed to me to be a cause for deep, silent shame." (83) Singh's frank account of his childhood reveals the materialistic nature of the society of Isabella, where it is considered a disgrace to be poor. Singh's father is a poor school teacher and so Singh prefers to lay claim to his mother’s family only because they are among the richest in the island. In Isabella, even children live dual lives and the borne-down by secrets. Singh’s childhood is burdened with secrets he longs to be rid of. The duality is introduced into their lives because in Isabella, as in any colonial society, the school and the home remain two separate hemispheres.

In school every boy lived with a fantasy of his own and concealed the real life of the home. That is why, Hok, one of Singh's classmates ignores his mother on one occasion when he is with his classmates. When this is reported to the teacher he is outraged and makes Hok go back and wish her. Hok breaks down into tears because he feels exposed and Singh provides the reasons: "It wasn't only that the mother was black and of the people, though that was a point; it was that he had been expelled from that private hemisphere of fantasy where lay his true life." (97) The pressure that a colonial society exerts on the psyche of even small boys is expressed through the episode. It is clear from what Singh says that it is they who lead them to deny the reality around them:

> Anything that touched on everyday life excited laughter when it was mentioned in a classroom: the name of a street, the name of street-corner foods. The laughter denied our knowledge of these things to which after the hours of school we were to return. We denied the landscape and the people we could see out of open doors and windows, we who took apples to the teacher and wrote essays about visits to temperate farms. Whether we dissected a hibiscus flower or recited the names of Isabellan birds, school remained a private hemisphere. (95)

Singh too, fashions his own fantasies in which he imagines that his life is a shipwrecked chieftain on an unknown shore, "awaiting rescue, awaiting the arrival of ships of curious shape to take him back to mountains." (111) Eden, Singh’s classmate has his own dreams of a "remote land where he, the solitary Negro among an alien pretty people, ruled as a sort of sexual king" (151). Singh tries out other ways of overcoming his sense of inadequacy. For instance, he starts calling himself “Ralph” rejecting even his real name which is “Ranjit”, as if a change of name would make him a different person. This becomes one of his 'heavy secrets" and keeps him in a constant fear of discovery at home. Such instances provide an adequate commentary on the society which drives even children to such acts of deception. We are reminded once again that the sense of one’s reality lying elsewhere is a typical malady of the colonized people. We realize too, that the only alternative left to colonials, who deny their reality is mimicry.

Singh's conclusions about Isabella are strikingly similar to those arrived at by Naipaul in *Passage*. In Singh's words: "To be born on an island like Isabella, an obscure New World transplantation, second-hand and barbarous, was to be born to disorder." (118) He thus resolves to leave Isabella and make a fresh start in London. However, because of his father's religio-political movement his plans of escape gets delayed and the connection he had tried to suppress only gets further strengthened. Later on, it becomes the pretext on which his own political career commences.

The political agitation started by Singh's father begins quite abruptly. One afternoon, Singh's father fails to return home from work and the next thing they know is that he has become "a preacher, a leader with a growing frenzied following" (125). However, after creating a sensation, the movement dies out having neither philosophy nor a cause to keep it sustained. Singh, who has to face embarrassments in school because of his father's political movement feels betrayed. By this time, though, the insularity of the school has been broken. In spite of his indifference towards his father, Singh finds it difficult to remain totally detached from the movement because the role of "the son of a leader suddenly found" is thrust upon him. Nevertheless, Singh's attitude towards the whole affair remains ambivalent. As he himself confesses: "With some boys I was as detached as before about my father's movement, though their

criticism still pained me. And then I could not reject the conspiratorial devotion of the others."(132) At the same time Singh feels repulsed by the devotion offered to him by Browne and the others, who have begun to look upon him as their Messiah's son.

The killing of Tamango, the favorite race horse for the Malay Cup which marks the culmination of Singh's father's movement, horrifies Singh. What horrifies Singh is not just the killing, but the fact that it is done in the ritualistic manner of the "Asvamedha" the ancient horse sacrifice, which in Singh's imagination is "a thing of beauty, speaking of the youth of the world, of untrodden forests and unsullied streams, of horses and warrior-youths in morning light .... " (140) When even his private world of fantasy is intruded into and rendered obscene, Singh experiences an urgent need for withdrawal. An acute existential fear grips Singh when, while on a beach holiday, he witnesses a drowning accident. This is his first lesson about the "weakness of the flesh." A deep fear of extinction haunts him. Even when he is in his grandfather's solid and strong house, he begins to jump on the floor and lean against the walls to test their strength. On one occasion while he is watching the afternoon show, it suddenly begins to rain heavily. He runs home in panic but is relieved to find his house safe. Paradoxically however, he also feels disappointed and he explains that it is "the disappointment of someone who had been denied the chance of making a fresh start, alone." (153) About this time an incestuous relationship develops between Singh and Sally, his cousin. His grandfather's house had been a refuge for Singh while his grandfather lived. With his Grandfather's death however, the house begins to be invaded by Cecil's friends with whom Singh finds himself ill at ease. He now seeks refuge in the clandestine relationship with Sally. It is this relationship that defines all his other relationships with women. For, in every other relationship he experiences either triumph or humiliation but never the "mutual acceptance" found in the first. In this as well as in Eden's dream of ruling as a sort of sexual king, we witness the extent to which colonialism has corrupted even the most apolitical of all relationships-the relation between the sexes. This testifies that in the colonial ethos every relationship is reduced to the colonial binary of Domination and Subordination. Men like Singh are the products of colonialism, damaged both at the psychological and spiritual levels.

Singh's long-awaited release from Isabella finally comes when he is accepted by the London School. On coming to London he takes a room in a boarding house owned by a Jew. His first experience of Snow turns bitter when he goes into the attic of the boarding house to get a better view of the snow fall, but gets a peep into his late landlord's secret life of pleasure. He feels all the magic of the city go away with this exposure of the forlornness of the city and the people who live in it. In London, Singh experiences a deeper fragmentation and instead of the flowering of personality, he encounters a greater confusion. There is the same sense of isolation and absence, of correlation between the people and the landscape:

> Those of us who came to it lost some of our solidity; we were trapped into fixed, flat postures. And, in this growing dissociation between ourselves and the city in which we walked, scores of separate meetings, not linked even by ourselves, who became nothing more than perceivers: Everyone reduced, reciprocally, to a succession of such meetings, so that first experience and then the personality divided bewilderingly into compartments. Each person concealed his own darkness. (27)

Throughout the novel, Naipaul conveys the idea that identity is a feeble entity for colonials. Singh first gets this insight when his grandfather is insulted by some labourers. Though they are just labourers, their insult deeply affects Singh's grandfather and Singh gets his first political lesson: "A man was only what he saw of himself in others .... " (100) In London, Singh seeks reassurance in Lieni's eyes and gets into the role of the extravagant colonial that she fashions for him. To rid himself of his inner emptiness he begins to visit brothels. He is on the verge of a mental breakdown when Sandra, whom he has known for some time, leads him to propose to her. Singh is attracted by the aura of good luck about her as well as her sense of sureness and precision which he himself lacks. In reality however, Sandra's position is no better than Singh's. Though she belongs to the metropolis, she too is a drifter and like Singh has rejected her family. At the moment she asks Singh to marry her, she is just about as uncertain about her future because having failed a qualifying examination, the route of escape through education is no longer available to her.

Soon after marriage Singh and Sandra leave for Isabella, but at the port itself Singh's mother creates an embarrassing scene by refusing to accept Sandra and instead of going home, they go to a hotel. Singh finds the post-war Isabella greatly changed. It no longer seems mean and constricting. Singh and Sandra attach themselves to a "neutral, fluid group" of young men who have studied abroad and have "expatriate and fantastically cosmopolitan wives or girl friends." (55) In this society, Singh experiences a solidity, feeling for the first time that his character is not "what others took it to be, but something personal and ordained." (57) Sandra too feels avid and appreciative. Singh makes a fortune by developing the land his grandfather has left him. However, the island life soon begins to tire Sandra and she withdraws into her shell. Something also goes

wrong between the couple and they drift away from each other. Singh relapses into his old habit and starts seeking pleasure in affairs outside marriage. As Singh later reflects it was the barrenness of their relationship which promised no growth, that led to the rift between them. He nevertheless, holds himself responsible for not doing anything to save the marriage. He realizes that he had let Sandra sink into despair, when even a mere physical demonstration of anger could have revived the relationship.

In her own despair, Sandra starts hurting the racial susceptibilities of people for,every thing in the island has begun to seem inferior to her. In the meanwhile, the construction of Singh's house gets completed, but it has ceased to have any meaning for either of them. The house-warming party ends in unpleasantness when the guests suddenly get into a destructive mood and start breaking things. The party underscores the deep, disorder that forms, the reality of societieslike Isabella. Singh leaves the party in a fit of rage and by thetime he returns the guests have left. He silently retires tohis room as by this time he and Sandra have started living inseparate rooms, and no longer share a relationship whereconsolation can be sought or given. After the house-warmingparty the rift between them widens. Sandra takes the ultimate step by leaving the island. She leaves behind a note for Singh in which she writes: "The Niger is a tributary of that Seine" (80)This highlights the racial difference between them.

Soon after Sandra's departure, Singh led on by Browne, his former school friend, embarks on his political career. Browne, who is now the editor of "The Socialist" plans to celebrate the anniversary of the dock worker's exodus from the city as the first gesture towards independence and urges Singh to contribute the main article about his father. The article is written and with the publication of the anniversary issue of the new-look socialist, their political movement gets launched. They win the elections and Browne becomes the Prime Minister while Singh is made a Cabinet Minister. It is only on coming to power that Singh comes to realize the futility inherent to the New World politician's situation. Singh's failure to bring about the nationalization of the sugar estates provokes race riots and he is forced to make his escape to London. It is only when he begins writing his memoirs that Singh reflects on his political career and comes to understand the fraudulence of power in the emergent nations of the Third World which lack order. The political career of the colonial politician finds an apt portrayal in the following passage:

> The career of a colonial politician is short and ends brutally. We lack order. Above all, we lack power, and we do not understand that we lack power. We mistake words and the acclamation of words for power; as soon as our bluff is called we are lost. Politics for us is a do - or-die, once-for-all charge. Once we are committed we fight more than political battles; we often fight quite literally for our lives. Our transitional or makeshift societies do not cushion us. There are no universities or City houses to refresh us and absorb us after the heat of battle. For those who lose, and nearly everyone in the end loses, there is only one course: flight. Flight to the greater disorder, the final emptiness ; London and the home countries. (8)

The Third World's penchant for foreign goods also comes under criticism. This aspect is reflected in the failure of the only purely local endeavour of canning local fruit. Singh observes: "It hadn't occurred to anyone concerned to find out whether local people wanted local fruit tinned...." (215) In the ultimate analysis, the crux of the problem is identified in the nature of the society itself :

What exists instead of society is only a kind of "controlled chaos." Movements like the one carried out by Singh's father might not have had philosophy or a cause but at least there had been one positive outcome: It had shocked people out of their wits by generating disorder in the ostensible order. What the post-independence politicians did was just antithetical. By the outwards semblance of order that they offered, they deluded people into believing that there was order. By hiring English secretaries the ministers of the post-independence period offered their people "the spectacle of the black man served by the white . . . "(210)This was the revolution they claimed to have created.

In spite of all the images of shipwreck, *Mimic* is one of the most optimistic of Naipul's later novels. At the end of the novel, Singh can still claim that he has "cleared the decks" and prepared himself for fresh action. He is even confident that it will be the action of a "free man." Through the act of writing his memoirs, Singh has come to understand and accept the finality of his displacement and is now well-equipped to begin afresh.

Reference :

Mohan, ChampaRao, *Post Colonial Situation in the Novels of V.S. Naipaul* (New Delhi : Atlantic, 2004).
Naipaul, V.S., *The Mimic Men* (Harmondsworth : Penguin, 1969).

IJRD International Journal of Research & Development Organisation

Journal Of Electrical And Electronics Engineering

SMART GAS CYLINDER

Mohit Kumar[1], Pragati Gupta[2], Mohd Wamiq[1], Abhishek Kumar[1]
UG Scholars [1] , Assistant Professor [2]
Department of Electronics & Communication Engineering, Moradabad Institute Of Technology, Moradabad
mohitkumar260694@gmail.com, guptapragati30@gmail.com, www.wamiqgreat786@gmail.com,
abhishekkumar1992.as@gmail.com

ABSTRACT

In this brief we are going to design smart gas cylinder which is capable of detection of leakage gas. The proposed design is basically inspired from the fire accidents due to the leakage of gas. This system is built using combination of microcontroller and GSM. The system has been design and implemented in a cost effective way so that commercialized user will take benefit from it.

KEYWORDS

Microcontroller, LPG, Gas Sensor, Alarm, GSM, Gas Monitoring System.

1.INTRODUCTION

The liquefied petroleum gas is finding wide usage in homes, industries and in automobiles as fuel because of its desirable properties which include high calorific value, produces less soot, produces very less smoke and does not cause much harm to the environment. However there is a serious problem about their leakage in the air. The gases being heavier than air do not disperse easily and may lead to suffocation when inhaled also when gas leakage into the air may lead to explosion. Due to the explosion of LPG the number of deaths has been increased in recent years. To avoid this problem there is a need for a system to detect and also prevent leakage of LPG. The proposed system reduces the customer burden. It will monitor gas level in the cylinder, when the gas level reaches below it sends SMS alert to the user. It uses a MQ5 gas sensor which can detect LPG gas and a microcontroller to alert when the levels of gas detected is beyond safety limit. The alert mechanism in the proposed system includes an LED indication, buzzer and an SMS sent to the stored numbers with the help of GSM. This system is designed for use in homes which use LPG or natural gas; however it can be used in industries and other applications involving the gas cylinders.

2.SYSTEM STRUCTURE & OPERATION

Fig (1). shows the system block diagram and Fig (2). Shows the system circuit diagram. The system mainly consists of LPG leakage detection system and Microcontroller with GSM module. The main function of gas leakage detection module which consist of gas sensor to continuously detect the gas leakage in the air. For the gas leakage detection a solid state gas sensor MQ5 is used. MQ5 gas sensor which offers many advantages like long lifetime, low cast, reliable and high sensitive to LPG. In gas sensors Tin dioxide is the most common material. MQ5 gas sensor less sensitivity to air but high sensitivity to combustible gases.

When target LPG gas or combustible gases exist in the environment the conductivity of gas sensor increases and whose conductivity is less in the air. When using MQ5 gas sensor sensitivity is very necessary. We calibrate the detector for 300 to 5000 ppm of LPG and Natural Gas.

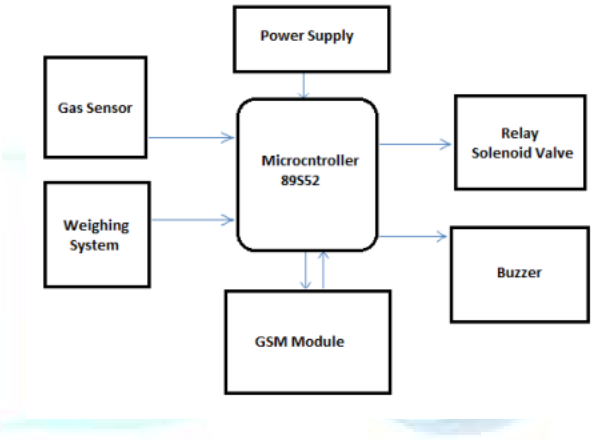

Fig (1). BLOCK DIAGRAM

The sensor works with 5volt power supply. When the concentration of gas in the air exceeds the certain level then activate the audio visual alarm which includes LED, Buzzer and send the message to the consumer by using GSM module. The GSM module is used to send short messages when gas leakages. Any number of mobile numbers can be included to which SMS must be sent about the above mentioned details. This wireless module is used to alert the consumer even when they are away from home. An audio-visual alarm provided to immediately alert the people at home in abnormal condition. As added feature it monitors the weight of the gas in cylinder. When the weight of the gas is less than or equal to 2 Kg, a logic high pulse is fed to a port pin of microcontroller. As this pin goes high, microcontroller will send a booking message to distributor of format, "REG_AMARGAS_12345". An indication SMS will be sent sto the consumer if found the gas level reaches below or gas in the cylinder is going to empty. The microcontroller forms the heart of the entire system controlling all processes that take place.

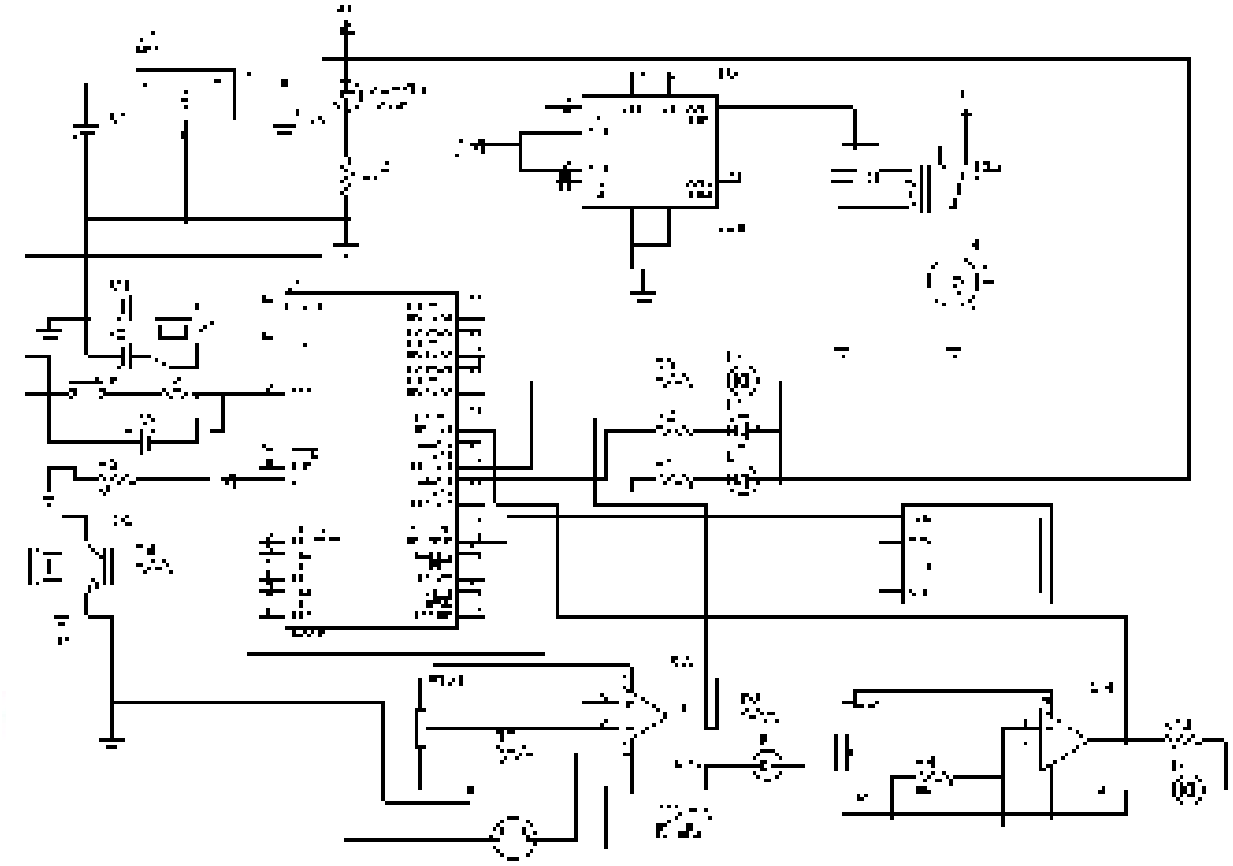

Fig (2). CIRCUIT DIAGRAM

3. RESULT

Overall system was designed and tested by introducing the small amount of LPG near gas sensor module. The system detect the level of gas in the air if it exceeds the safety level then send a SMS to the consumer using GSM modem and activate the audio-visual alarm which includes LED, Buzzer to alert the user at home in abnormal condition and to take the necessary action and the system continuously monitors the level of the LPG present in the cylinder and if the gas level reaches below then activate the LED and send a SMS to the consumer using GSM modem.

4. CONCLUSION

These design innovations will allow to navigate in kitchen to accomplish task with safety. This will greatly simplify the gas leakage control problem and give the house a full safety.

5. ACKNOWLEDGEMENT

This work is supported by Moradabad Institute Of Technology, Moradabad, U.P., India. We are thankful to Mr. Kshitij Shinghal (H.O.D., E&C Engg.) & Associate Dean, MIT Moradabad for his support and to Mrs. Pragati Gupta (Assistant Professor, E&C Deptt.) for their guidance and precious time.

6. REFERENCES

[1] Sunithaa.J, Sushmitha.D, "Embedded control system for LPG leakage detection and prevention" International Conference on Computing and Control Engineering (ICCCE 2012), 12 & 13 April, 2012.

[2] V.Ramya, B. Palaniappan, "Embedded system for hazardous gas detection and alerting" International Journal of Distributed and Parallel Systems (IJDPS) Vol.3, No.3, May 2012.

[3] Mr. Sagar Shinde, Mr. S.B. Patil, Dr. A.J. Patil, "Development of movable gas tanker leakage detection using wireless sensor network based on embedded system", International Journal of Engineering Research and Applications (IJERA) ISSN: 2248-9622 Vol. 2, Issue 6, November- December 2012.

[4] Luay Friwan, Khaldon Lweesy, Aya Bani-Salma, Nour Mani, "A Wireless Home Safety Gas Leakage Detection System", IEEE 2011.
[5] S. Rajitha, T. Swapna, "Security alert system using GSM for gas leakage" International Journal of VLSI and Embedded Systems-IJVES.
[6] GSM: "Architecture, protocols and services" by Jorg Eberspacher, Christian, Hansjoerg vogel, Christian Hartmann, John Wiley Son Ltd, 2009.
[7] Taufiq Noor Machmuda, "LPG Gas Detector and leak prevention based microcontroller.
[8] A. CheSoh, M.Sc.; M.K. Hassan, M.Eng.; and A.J. Ishak, M.Sc. "Vehicle gas leakage detector".
[9] W. Chung, and D. Lee, "Real time muti-channel gas leak monitoring system using CPLD chip" Sensors and Actuators B, Vol. 77, pp. 186- 189, 2001.
[10] Nakano, S.; Goto, Y.; Yokosawa, K.; Tsukada, K, "Hydrogen gas detection system prototype with wireless sensor networks", Proc. Of IEEE Conference on Sensors, pp. 1-4, 2005.
[11] Nasaruddin, N.M.B.; Elamvazuthi, I.; Hanif, N.H.H.B.M, "Overcoming gas detector fault alarm due to moisture", Proc. Of IEEE Student Conference on Research and Development, pp. 426-429, 2009.

IGS Mumbai Chapter

Extended Abstract Volume of International Geotechnical Engineering Conference on Sustainability in Geotechnical Engineering Practices and Related Urban Issues, September 23-24, 2016, Mumbai, India.

SIMSG ISSMGE
ISSMGE

CAPACITY AUGMENTATION OF RED MUD POND USING INDUSTRIAL WASTES

Parvathi G. S.[i], Amitava. Ghosh[ii]

i. Scientist, Geotechnical Engineering Division, Central Road Research Institute, New Delhi, India, +918171503754, parvathigsengg@gmail.com
ii. Retd. Scientist, Geotechnical Engineering Division, Central Building Research Institute, Roorkee, India, +9412071577, aghoshcbri@yahoo.co.in

Keywords: Red mud, Composite reinforced earth wall, geogrid

EXTENDED ABSTRACT

For augmenting the capacity of red mud pond No. 4 at Muri, of Hindalco Industries, it was decided to make a mechanically stabilized earth wall of 10m height above the existing lateral embankment of the pond. This will result in extending the life of red mud pond for 5 more years. A feasible and flexible structure with cost effectiveness has been considerations for the toe protection of the existing embankment. But the main challenge for the construction of the reinforced earth wall above the existing pond is the slope instability and poor foundation soil. The existing embankment slope was first stabilized using a composite reinforced earth wall of 12m height. This needs a base width of minimum 10m, for resisting the base sliding failure. Where ever, there is a space constraint for the construction of 10m wide reinforced soil, gabion gravity retaining wall were constructed. Since gabion wall had greater unit weight and better interaction with foundation soil than reinforced soil, it required only 6m base width. Thus saving more space, but has higher cost than RE wall. This toe protection wall is being rested on a rock stratum. Because of this good foundation soil, it has been able to build a gabion wall of 12m height. To drain out the water from the red mud pond, Geosynthetic composite drain was recommended behind the RE wall. This will act as a separator too. External and internal stability checks for both types of walls have been done using Geo5 software. Figure 1 shows the layout of proposed structures for slope protection and capacity augmentation. Slope stability analysis considering both the toe wall and capacity augmenting wall also have done using the slope stability module of Geo5 software.

The existing embankment is made of silty soil, which is in fully consolidated stage, as of now. It has a 1V:2H slope. This earthen embankment crust now acts as an unpaved road for the plying of trucks to dump the fresh red mud waste. For capacity augmentation also, the composite RE wall has been recommended. Composite RE wall is nothing but conventional type RE wall with gabion box facing element. It has been decided that this wall shall be made of industrial waste only, as there is no availability of sand or any other high frictional soil nearby the site. The existing dry mud can be utilized effectively if reinforced with high strength geogrids. Since red mud is a heavy material, to reduce the unit weight of backfill, 50% fly ash has also been recommended to mix with red mud. The soil mixture has been extensively tested in laboratory for its engineering and physical properties. Some of the parameters of red mud fly ash mix, used for the design of RE wall are given in table 1. For arresting the pull out failure, it became essential to give a geogrid length of 14m. This is due to the poor adhesion of geogrid with the backfill soil.

Table 1: Reinforced earth wall design parameters

Optimum Moisture Content:		36.2%
Maximum dry density		1.385 g/cc
Specific Gravity		2.87
Permeability		$1.829*10^{-6}$ cm/s
Shear Strength Parameters:	Unsaturated :	$\varphi = 21^0$ C=18 kPa
	Saturated:	$\varphi = 16^0$ C=9 kPa

Lot of precautions has been taken to design this capacity augmenting wall. The main concern was the pore pressure/water pressure dissipation within the backfill, as this may create additional pressure on the composite RE wall facing element. For preventing this proper drainage measures have adopted. For the dissipation of pore pressure behind the wall, geosynthetic composite drain has been adopted. For preventing the infiltration of runoff water/rain water to the wall, a proper drainage system with geomembrane and granular blanket with vegetative soil on the top of them has been adopted.

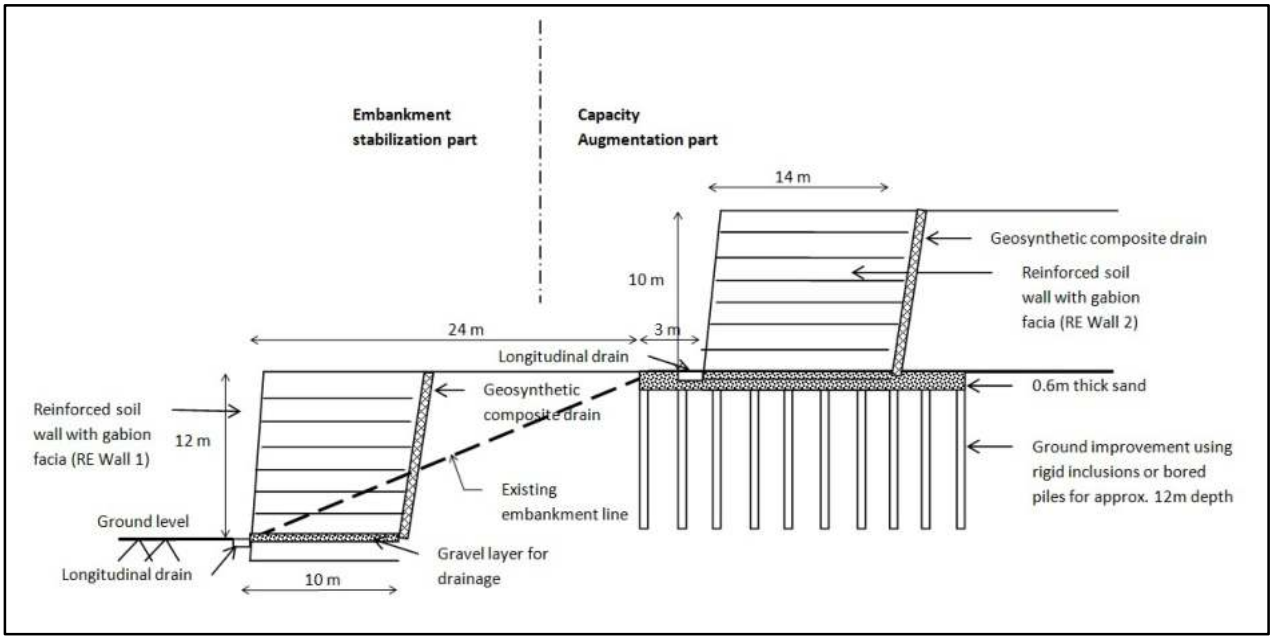

Fig 1. Layout of proposed structures for slope protection and capacity augmentation

The second challenge was the poor foundation soil for this wall, as it has to be made partly on the existing embankment, which is made of clayey silt and partly on fresh red mud deposit, both having very less shear strength to support the structure above. Semi rigid inclusion using displacement technique has been adopted for ground improvement.

This composite RE wall with red mud system makes the optimum utilization of space and materials available. This paper presents the specifics of this project, soil parameters and the design concepts of composite RE wall with red mud as backfill material.

REFERENCES

1) BS: 8006 – 2010 "Code of practice for strengthened / reinforced soils and other fills"
2) Hatami K., et al. (2001) - Static Response of reinforced Soil Retaining Walls with Non uniform Reinforcement, *The International Journal of Geomechanics*, Vol. 1 No. 4, 477-506
3) Hatami K., et al. (2000), Numerical Study of retaining walls with non-uniform reinforcement. *Proceedings of Eurogeo 2000: 219-224, Bologna.*
4) IS 1893 (2000) "Criteria for earthquake resistant design of structures"
5) Juran I. et al. (1990). Strain compatibility analysis for geosynthetics reinforced soil walls, *Journal of Geotechnical Engineering, ASCE*, vol. 116 N° 2: 312-327
6) Koerner, R. M. (1998)"Designing with Geosynthetics", Fourth Edition.
7) Lambe W. T. and Whitman R. V.(1979), "Soil Mechanics-SI Version", Wiley- India
8) Pietro P.Di. (2002)- Design and construction of soil reinforced structures using composite reinforcement systems: modern and cost effective alternatives for high walls and slopes, *Proceedings of the Seventh International Conference on Geosynthetics, 7-ICG*

International Geotechnical Engineering Conference on Sustainability in Geotechnical Engineering Practices and Related Urban Issues, IGS Mumbai Chapter & ISSMGE
23rd-24th Sept. 16

Capacity Augmentation of Red Mud Pond using Industrial Wastes

Parvathi G. S.
Scientist
CSIR-CRRI
New Delhi

Prof. Amitava Ghosh
Retd. Cheif Scientist
CSIR-CBRI
Roorkee

Introduction

- Red Mud Pond of Hindalco Industries is located in Muri, Ranchi
- Yearly production of red mud waste is around 2.25 lac Cubic meter
- The height of the existing bund is 12m from the ground level with 1V:1H slope and a crest width of 5m
- Capacity of the Pond (~10000sqm area for RMP # 4) was nearing its exhaustion and methods for augmenting the capacity has been thought about

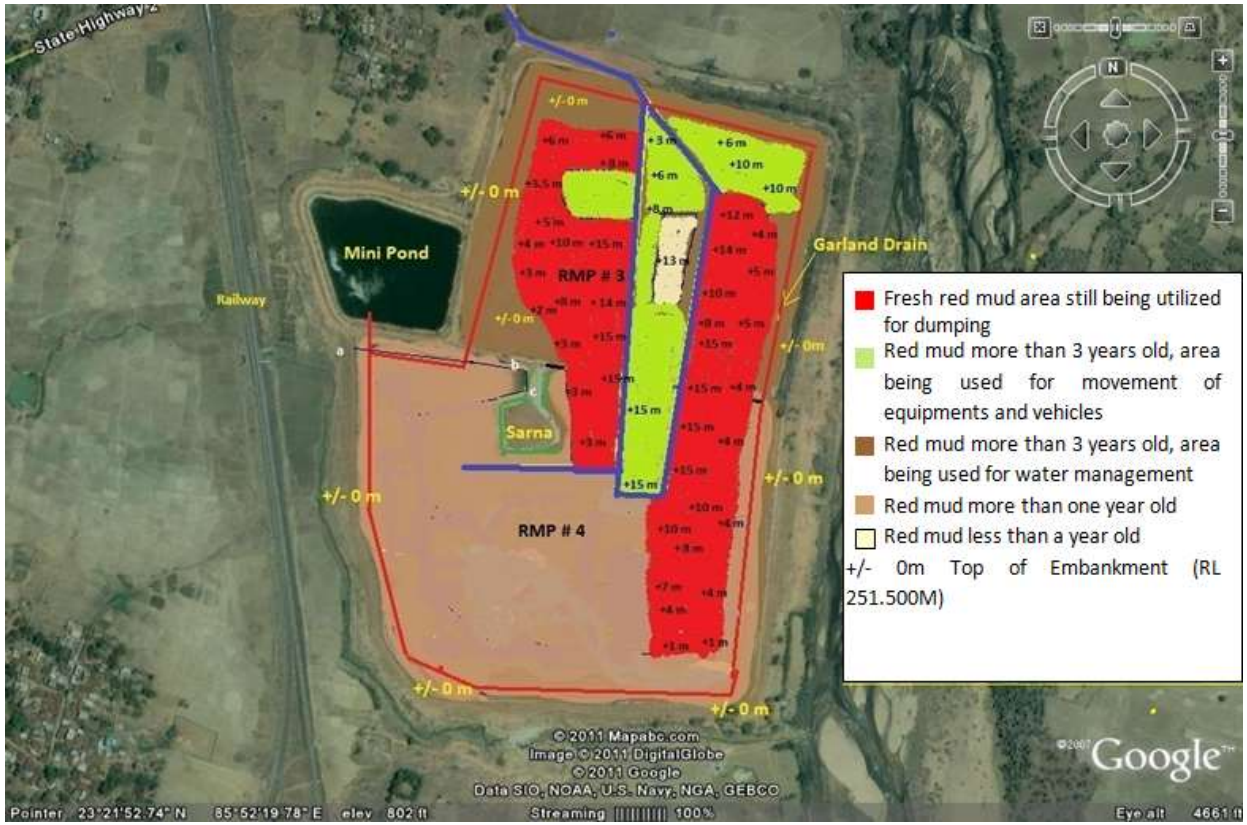

Challenges and Benefits

- For any dumping above the existing pond, the main challenge is the extreme soft nature (SPT N~0) of wet red mud and ground water level inside the pond
- Unavailability of sand / good frictional soil for construction
- There is a natural stream going along the west side of pond and further space constraints on other sides

- The existing embankment/bund is more than 15 years old and is in consolidated stage.
- There a presence of weathered rock strata at a depth of 2m from the ground level
- Availability of industrial wastes like red mud and fly ash which are alkaline in nature

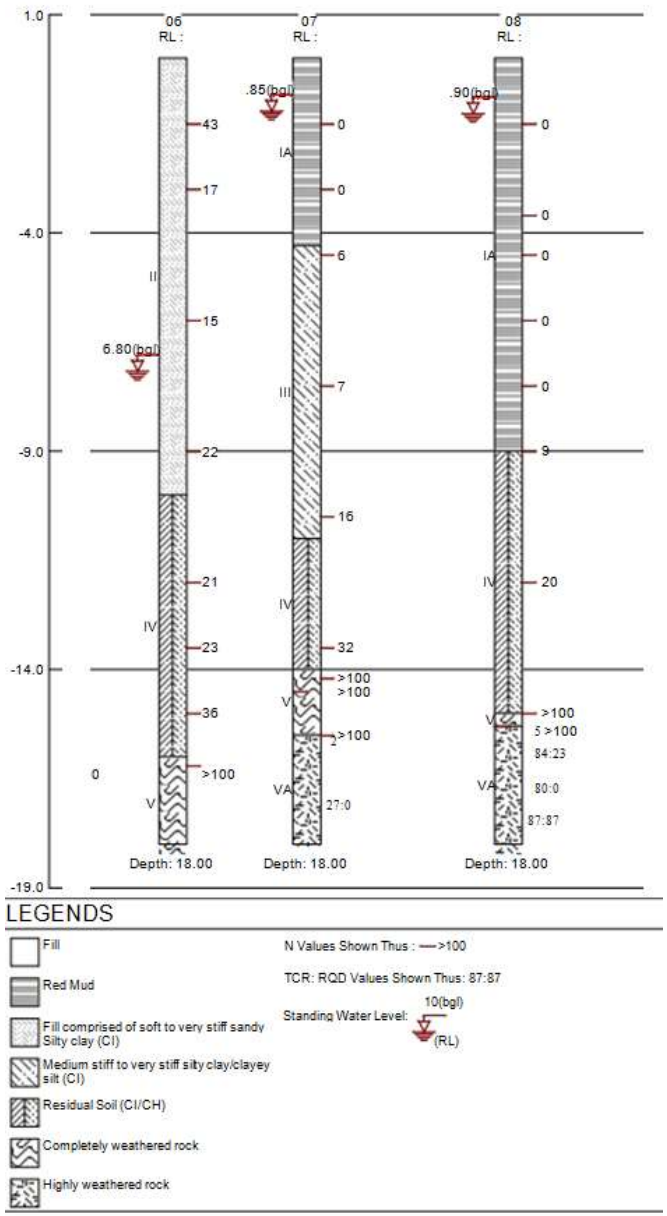

Geotechnical Properties of soils

Properties	Grain Size Analysis (%)			G	Unit weight (kN/m³)		Shear Strength Parameters		K (cm/sec)	Consolidation Properties	
	Sand	silt	clay		Ybulk	Ysat	C (kPa)	Φ (°)		Cc	Cv (cm2/s)
Red Mud (At 97% MDD & OMC	3	70	27	3.05	19.8	21.5	18	18	$2.9*10^{-7}$	0.13	$1.33x10^{-3}$
Red Mud (Insitu Condition)	3	70	27	3.05	19.40	19.40	14 (max)	0	$4.26*10^{-5}$	-	-
Embankment soil	34	49	17	2.6	20.5	21	12	21	$5.78*10^{-6}$	-	-
Foundation/ Residual soil	84	13	0	2.7	18	20	30	10	$3.43*10^{-6}$	-	-
Fly ash (At 97% MDD & OMC	08	78	14	2.08	13.4	-	6	27	$8.12*10^{-6}$	0.11	$1.04x10^{-3}$

Stability Analysis of the existing embankment

- Stability analysis of the existing embankment was done in slope/w software with the geometry shown below

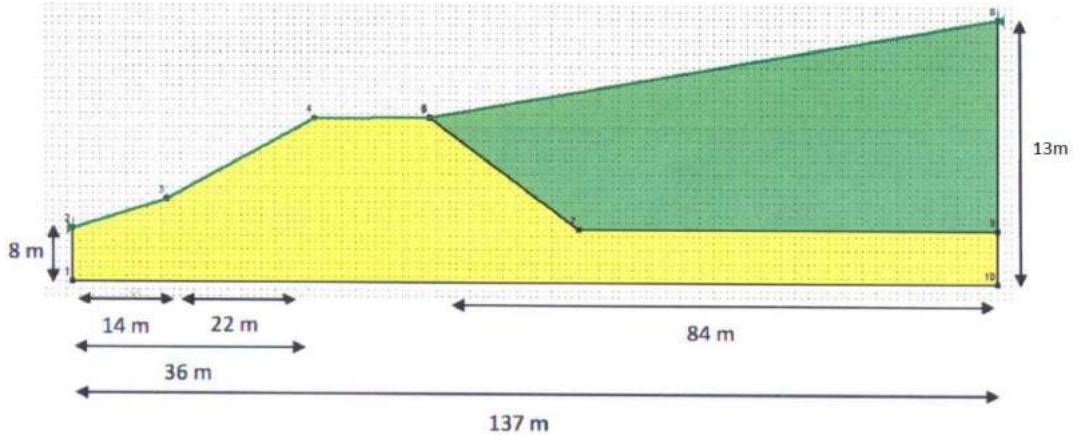

Condition	FOS
Static	1.37
Steady seepage	1.02
Pseudo-static	1.22

Solution

- A retaining wall system above the existing bund is planned for increasing the capacity of the pond along with ground improvement measures.
- To stabilize the existing embankment another retaining wall at the toe of existing bund has also been proposed
- The toe retaining wall is being proposed on three sides of the pond
- This benefits in confining and retaining the red mud within the boundary limit as well as protect the environment by constructing a structure that is in sync with the natural surroundings.
- A capacity increment of 16 lac cubic meter was possible considering both the RE wall, resulting in an extension of life 7.2 years for the pond

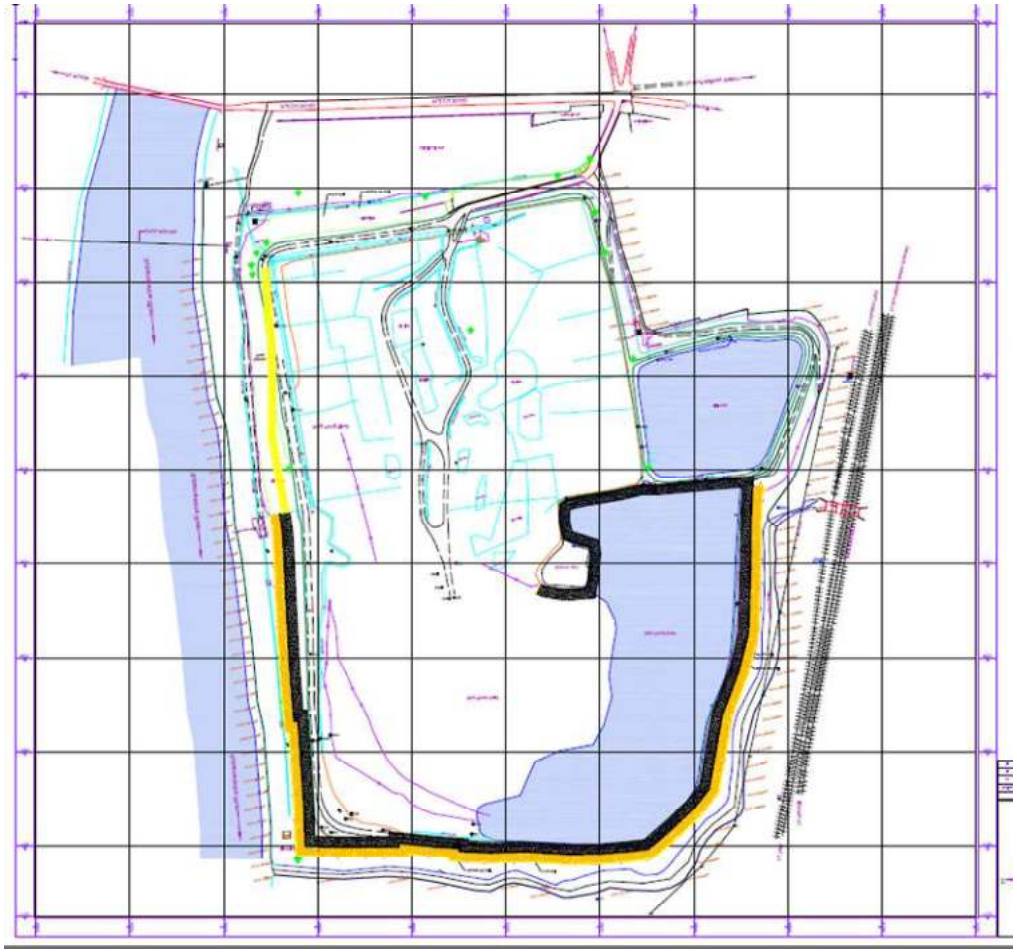

Solution

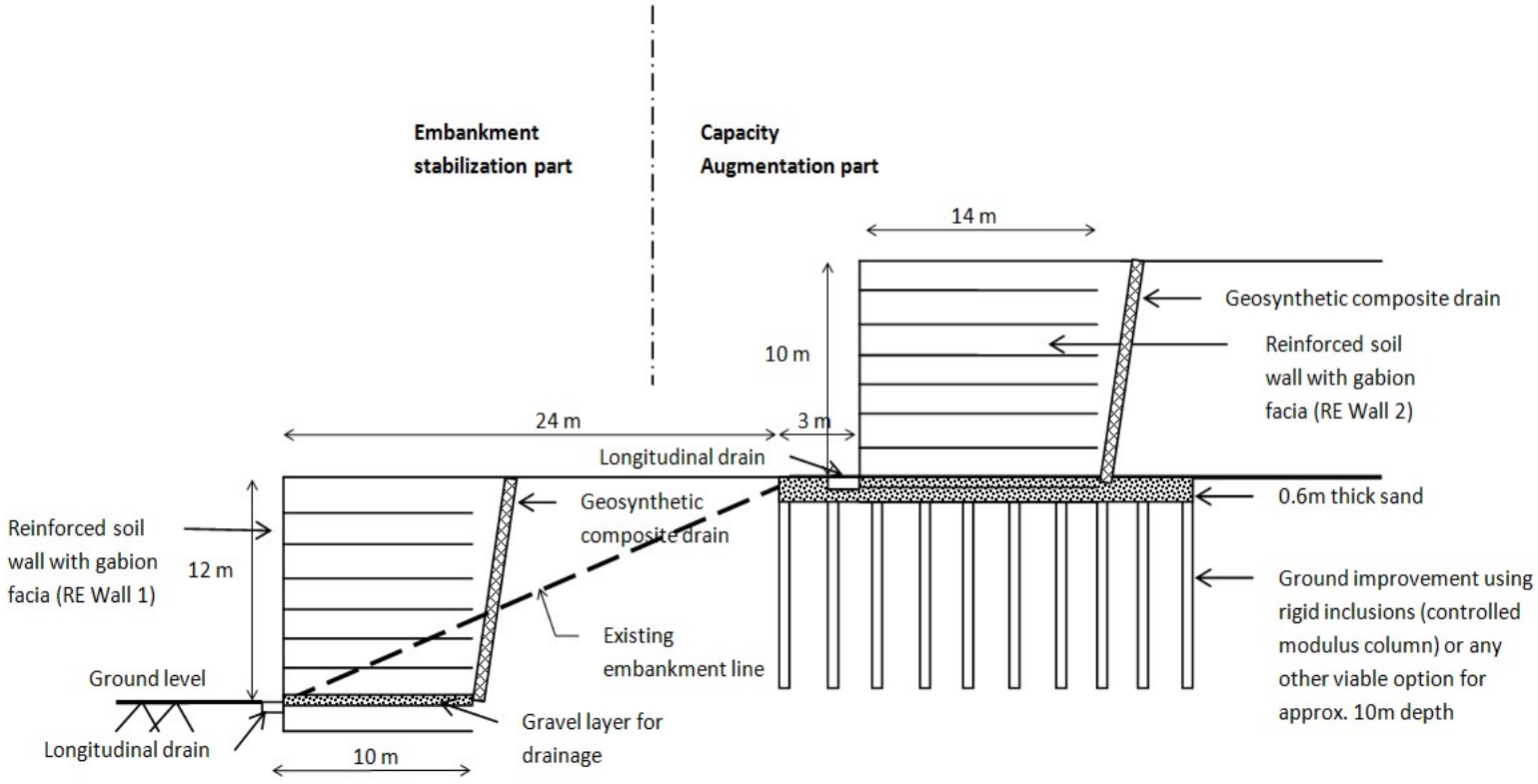
Embankment
stabilization part
Capacity
Augmentation part
14 m
Geosynthetic composite drain
Reinforced soil
wall with gabion
facia (RE Wall 2)
10 m
24 m
3 m
Longitudinal drain
Geosynthetic
composite drain
0.6m thick sand
Reinforced soil
wall with gabion
facia (RE Wall 1)
12 m
Ground improvement using
rigid inclusions (controlled
modulus column) or any
other viable option for
approx. 10m depth
Existing
embankment line
Ground level
Gravel layer for
drainage
Longitudinal drain
10 m

Details of Structure-1

- Composite RE wall system was adopted for toe protection retaining wall system with red mud-fly ash mix as fill material.
- A live load of 12kPa of approach road has been considered above the backfill for the analysis
- High strength geogrid of 200kN/m has been used with vertical spacing varying from 0.5m to 2 m.

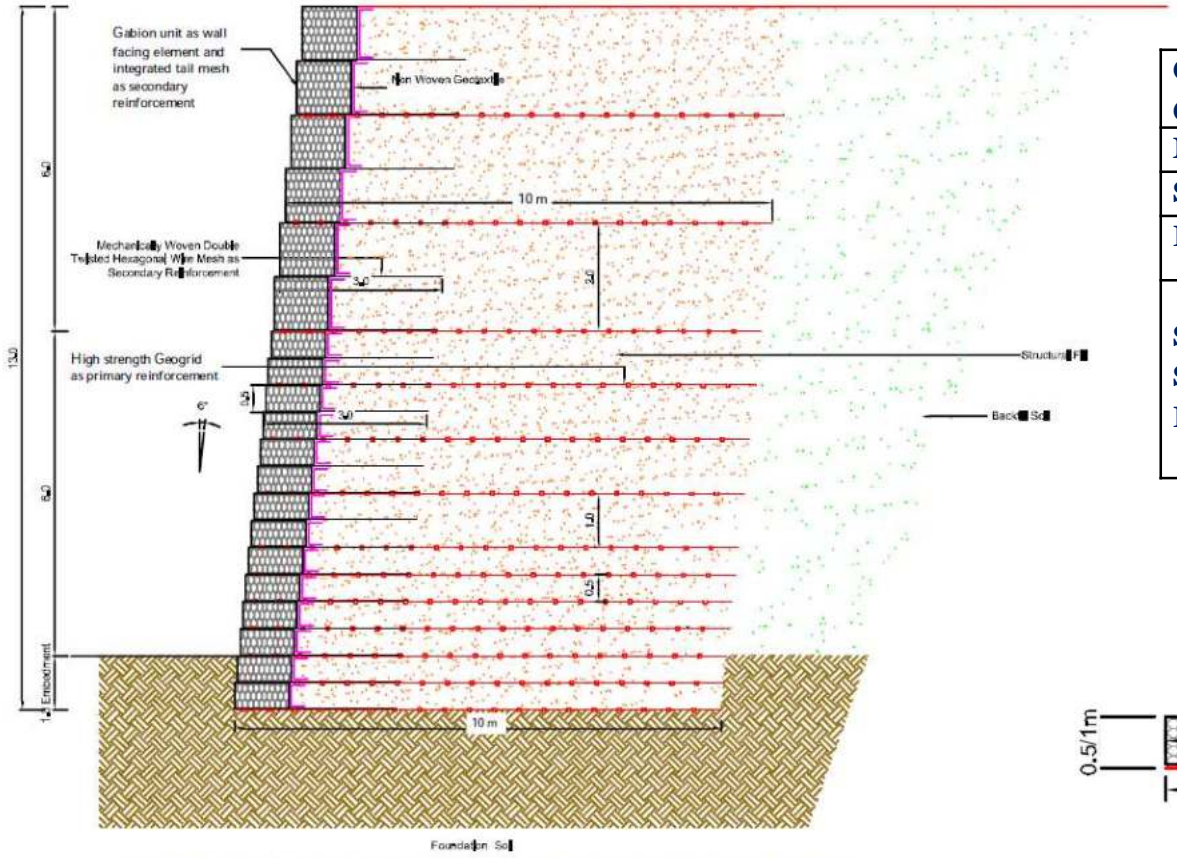

TYPICAL CROSS-SECTION OF 12M HIGH COMPOSITE SOIL REINFORCED WALL

Optimum Moisture Content:		36.2%
Maximum dry density		1.385 g/cc
Specific Gravity		2.87
Permeability		$1.829*10^{-6}$ cm/s
Shear Strength Parameters:	Unsaturated :	$\varphi = 21^0$ C=18 kPa
	Saturated:	$\varphi = 16^0$ C=9 kPa

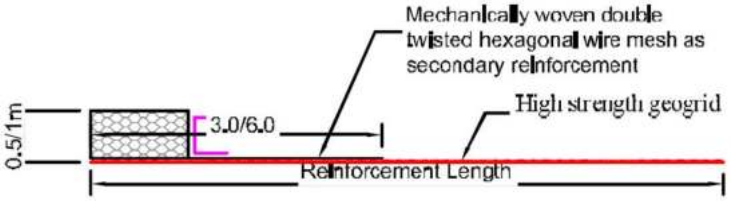

DETAILS OF SINGLE UNIT

Stability analysis of Structure-1 (Geo 5)

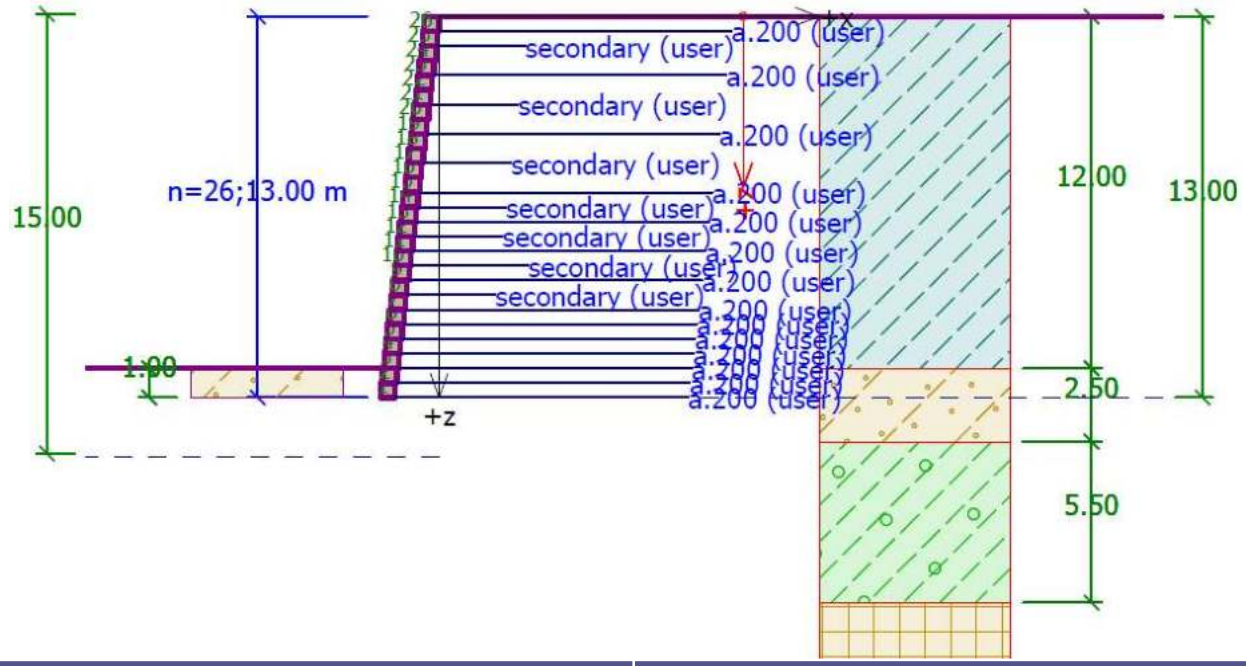

Condition		FOS
Bearing		7.74
Overturning		13.4
Slip		4.78
Slope stability		1.96
Internal stability	Tensile strength	1.73 (lowest)
	Pull out	1.96 (lowest)

Details of Structure-2

- Gabion wall of height 13m was adopted for toe protection retaining wall system where there is a space constraint.
- A live load of 12kPa of approach road has been considered above the backfill for the analysis
- Gabion boxes of 0.5m and 1m height were used for the construction.

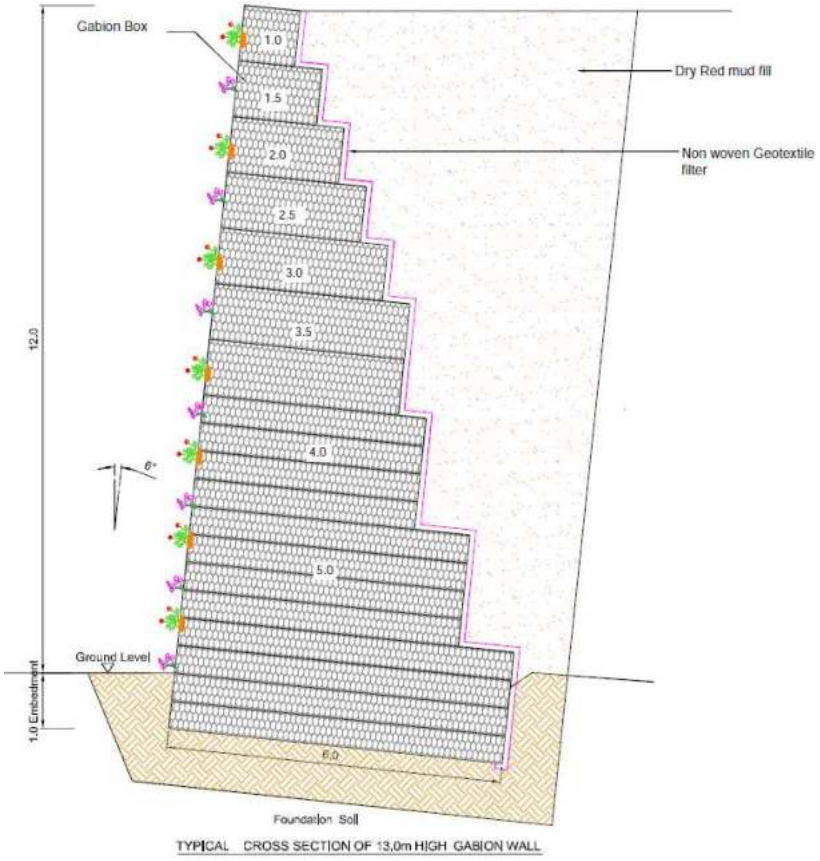

TYPICAL CROSS SECTION OF 13.0m HIGH GABION WALL

Stability analysis of Structure-2 (Geo 5)

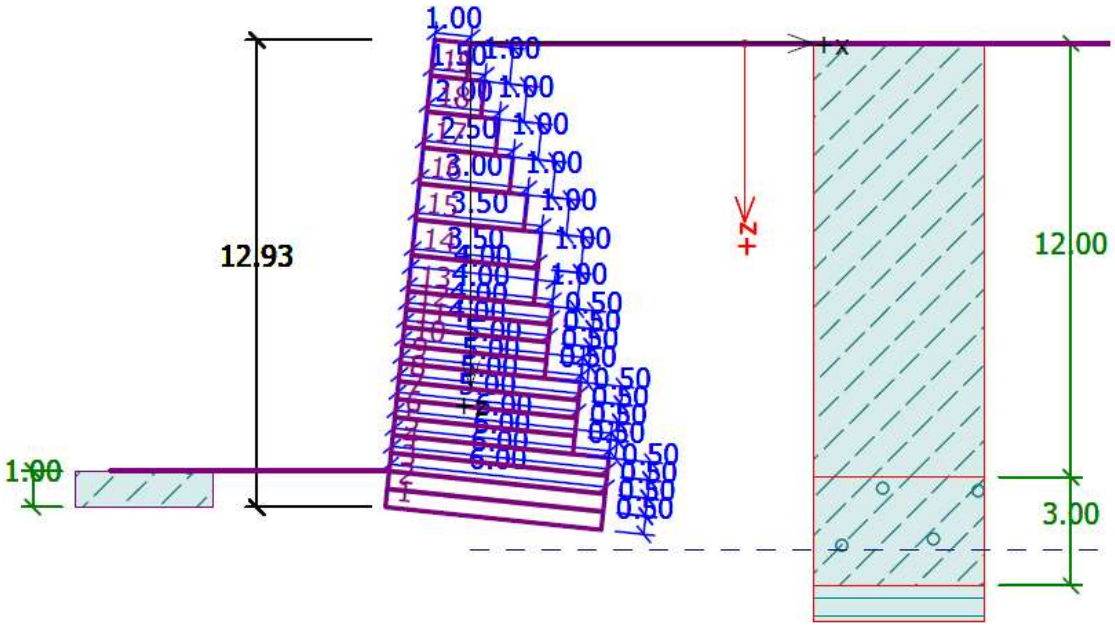

Condition		FOS
Bearing		4.43
Overturning		2.97
Slip		3.45
Slope stability		1.77
Joint stability	Bearing	1.83 (lowest)
	Overturning	3.16 (lowest)
	Slip	3.02(lowest)

Details of Structure-3

- Composite RE wall system of height 10m was adopted for Capacity Augmentation above existing bund red mud-fly ash mix as fill material.
- A live load of 12kPa of approach road has been considered above the backfill for the analysis
- High strength geogrid of 250 and 200kN/m has been used with vertical spacing varying from 0.5m to 2 m.
- This wall rests partially above the bund and partially on virgin red mud pond. Ground improvement using rigid inclusion/controlled modulus column (CMC) of 12m deep was used to ensure safe bearing capacity and slope stability

Stability analysis of Structure-3 (Geo 5)

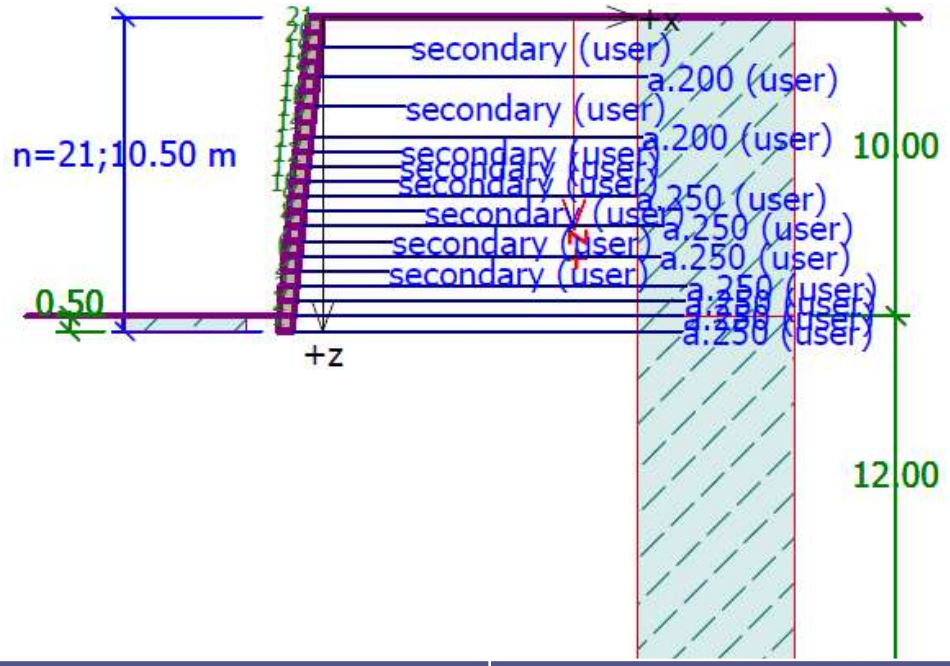

Condition		FOS
Bearing		3.97
Overturning		16.9
Slip		3.16
Slope stability		1.96
Internal stability	Tensile strength	2.24 (lowest)
	Pull out	2.59 (lowest

Global stability Analysis (Geo 5)

FOS for global stability at static condition is obtained as 1.39>1.3

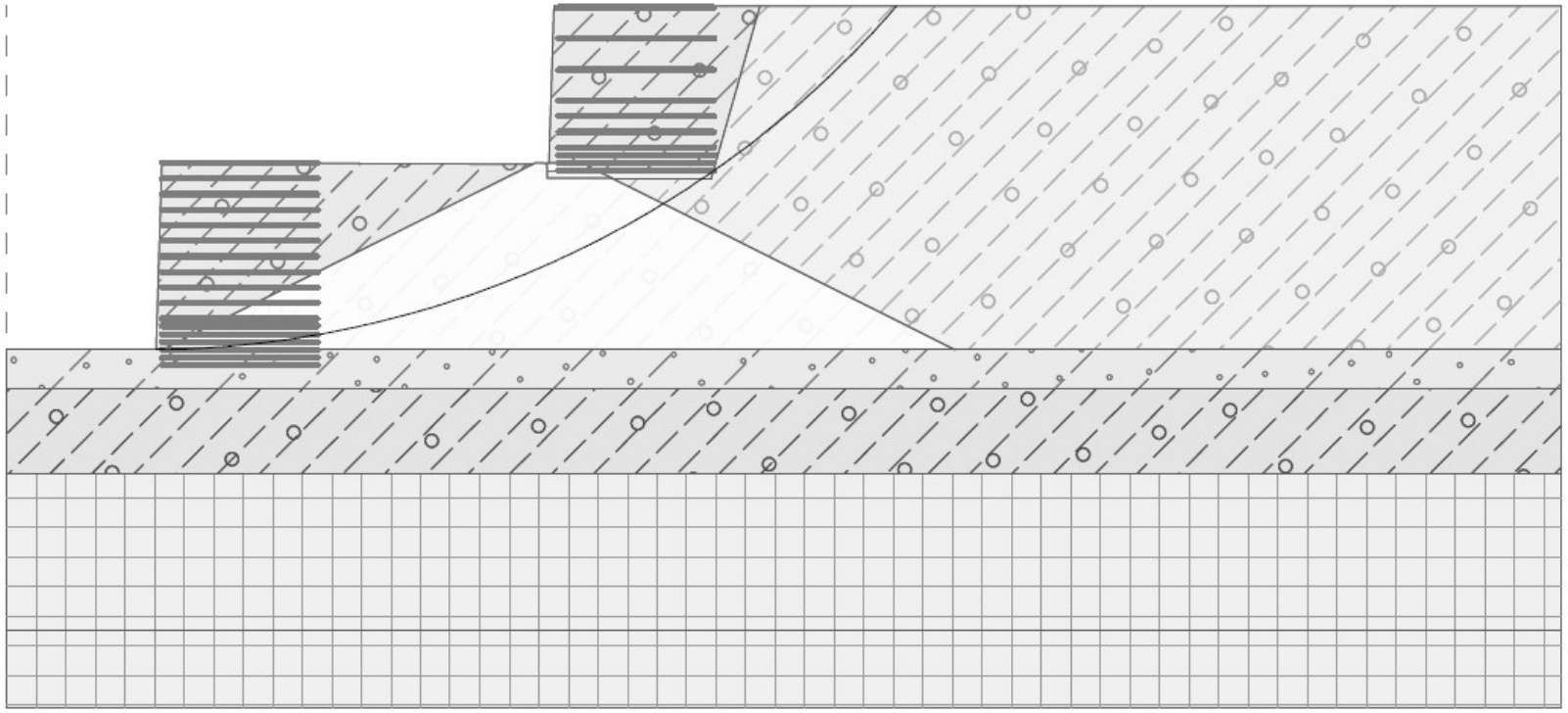

Concerns and solutions

Pore pressure/water pressure dissipation within the backfill, as this may create additional pressure on the RE wall facing element.	Proper drainage measures : -For the dissipation of pore pressure behind the wall, geosynthetic composite drain has been used -For preventing the infiltration of runoff water into the wall, a drainage system with geomembrane and granular blanket with vegetative soil on the top of them has been adopted.
Poor Foundation soil	Rigid inclusion/CMC using displacement technique has been adopted for ground improvement.
Durability of Reinforcements	Red Mud is alkaline in Nature, so reduction factors of geogrid was considered for high alkaline environment


02 06 2014


25 06 2014

Conclusions

- Exhaustion of red mud pond capacity was a major concern as Muri is a sensitive area and difficult to find a new dumping land
- Composite RE wall system of 10m height along with ground improvement was successfully installed at the site ensuring the stability conditions
- For toe protection composite RE wall system of 12m height was constructed
- Wherever Space constraint is encountered Gabion wall is being constructed for toe protection
- A capacity increment of 16 lac cubic meter was possible considering both the RE wall, resulting in an extension of life 7.2 years for the pond
- This solution makes optimum utilization of space and materials available

Thank You

An Empirical Study of Medical Tourism in India

Name of Author: DR. SACHIN AND MR. RAHUL SINGH

ABSTRACT

Medical Tourism in India is a developing concept whereby people from world over visit India for their medical and relaxation needs. Most common treatments are heart surgery, knee transplant, cosmetic surgery and dental care. The reason India is a favorable destination is because of it's infrastructure and technology in which is in par with those in USA, UK and Europe. India has some of the best hospitals and treatment centers in the world with the best facilities. Since it is also one of the most favorable tourist destinations in the world, Medication combines with tourism has come into effect, from which the concept of Medical Tourism is derived.

Following are the two basic objectives of my paper:

1. To examine the medical tourism in India and its future prospects.
2. To analyze the cost benefit medical services in India.

Key words:

Medical facility, Tourism, cost benefits, Treatment Centers, medicotourism packages

Introduction

Medical tourism can be broadly defined as provision of 'cost effective' private medical care in collaboration with the tourism industry for patients needing surgical and other forms of specialized treatment. This process is being facilitated by the corporate sector involved in medical care as well as the tourism industry both private and public. Medical or Health tourism has become a common form of vacationing, and covers a broad spectrum of medical services. It mixes leisure, fun and relaxation together with wellness and healthcare. The idea of the health holiday is to offer you an opportunity to get away from your daily routine and come into a different relaxing surrounding. Here you can enjoy being close to the beach and the mountains. At the same time you are able to receive an orientation that will help you improve your life in terms of your health and general well being. It is like rejuvenation and clean up process on all levels - physical, mental and emotional. Many people from the developed world come to India for the rejuvenation promised by yoga and Ayurvedic massage, but few consider it a destination for hip replacement or brain surgery. However, a nice blend of top-class medical expertise at attractive prices is helping a growing number of Indian corporate hospitals lure foreign patients, including from developed nations such as the UK and the US. As more and more patients from Europe, the US and other affluent nations with high medicare costs look for effective options, India is pitted against Thailand, Singapore and some other Asian countries, which have good hospitals, salubrious climate and tourist destinations. While Thailand and Singapore with their advanced medical facilities and built-in medical tourism options have been drawing foreign patients of the order of a couple of lakhs per annum, the rapidly expanding Indian corporate hospital sector has been able to get a few thousands for treatment. But, things are going to change drastically in favour of India, especially in view of the high quality expertise of medical professionals, backed by the fast improving equipment and nursing facilities, and above all, the cost-effectiveness of the package.

Research Methodology

It is a descriptive paper which is based on the secondary data. Data collected from the various sources like news papers, magazines, internet, books etc.

Medical Tourism Packages available for India

Several Medical Packages are available to suit patient needs. The medical package suitable for a patient depends on past treatment and current condition, based on which the most appropriate treatment will be made available.

Some of the medical Packages available are for :

- Dental Care
- Eye Care
- Heart Care
- Heart Surgery
- Health Check Up
- Cosmetic Treatment
- Orthopaedic Surgery

Medical Tourism in India for Dental Care

There are several Dental Care packages available. However, these will be based on the requirements of the person and his holiday needs.

Please find below a small cost comparison of dental treatment procedures between USA and India. There is a huge difference between the pricing (about 7/8 times when we speak of Top-end dentists).

Dental procedure	***Cost in USA ($)***		***Cost in India ($)***
	General Dentist	***Top End Dentist***	***Top End Dentist***
Smile designing	*-*	*8,000*	*1,000**
Metal Free Bridge	*-*	*5,500*	*500**
Dental Implants	*-*	*3,500*	*800**
Porcelain Metal Bridge	*1,800*	*3,000*	*300**
Porcelain Metal Crown	*600*	*1,000*	*80**
Tooth impactions	*500*	*2,000*	*100**
Root canal Treatment	*600*	*1,000*	*100**
Tooth whitening	*350*	*800*	*110**
Tooth colored composite fillings	*200*	*500*	*25**
Tooth cleaning	*100*	*300*	*75**

** These figures do not suggest the actual cost. Actual cost of treatment varies from case to case.*

Some of the facilities offered by the dental clinics are :

- Dental Scanning - Intra mouth
- Surgical Intervention under general anaesthesia
- Whitening of teeth
- Ceramic caps without gold under microscopic control
- Prosthesis on the implant
- Vertical and horizontal bone grafting
- Gum Grafting
- Palatal orthodontics
- Fluoride treatment for children
- Maxillary surgery
- Over denture
- Combined prostheses with milling

Medical Tourism in India for Eye Care

The cost different for most eye care procedures varies as high as 8-10 times from that of USA and UK. Some of the treatments available are :

Eye Lasik Refractive Packages
Lasik Eye Surgery
Eye Care Treatment
Lasik Treatment
Refractive Surgery India
Laser Refractive Surgery
Refractive Eye Correction Package
Natural Eye Care Treatment
Vision and Eye Care
Eye Refractive Care Packages

Medical Tourism Packages in India for Heart Care

India offers world-class healthcare that costs substantially less than those in developed countries, using the same technology delivered by competent Specialists attaining similar success rates. Hospitals in India use some of the best know-how and technology and the procedures include cardiothoracic, neurology, gastrointestinal, orthopaedic, renal, obstetric, ENT, opthalmology, dental, plastic, cosmetic and tumour surgeries.

A heart care surgery which costs in the region of USD 30,000 in USA can cost as low as USD 8,000 in India. This clearly states the price difference that exists in India when compared to the west.

Conditions operated on include:

- Valvular diseases
- Arrhythmias

- Coronary artery disease
- Hypercholesterolemia
- Family history of coronary disease
- Hypercholesterolemia
- Heart disease symptoms

Some of the procedures available are:

- directional coronary atherectomy
- rotablation
- coronary artery stenting
- intravascular ultrasound
- balloon valvuloplasty
- Non-surgical closure of holes in the heart such as ASD, VSD and PDA.

Medical Tourism Packages in India for Heart Surgery

A heart care surgery which costs in the region of USD 30,000 in USA can cost as low as USD 8,000 in India. This clearly states the price difference that exists in India when compared to the west.

Cardiac care has become a specialty in India with institutions like the Escorts Heart Institute and research Centre, All India Institute of Medical Sciences and Apollo Hospital becoming names to reckon with. They combine the latest innovations in medical electronics with unmatched expertise in leading cardiologists and cardo-thoracic surgeons. These centers have the distinction of providing comprehensive cardiac care spanning from basic facilities in preventive cardiology to the most sophisticated curative technology. The technology is contemporary and world class and the volumes handled match global benchmarks. They also specialize in offering surgery to high risk patients with the introduction of innovative techniques like minimally invasive and robotic surgery.

Renowned Indian hospitals like Apollo and Escorts Heart Institute are equipped to handle all phases of heart diseases from the elementary to the latest clinical procedures like interventional cardiac catherisation and surgical cardiac transplants. Their success rate at an average of 98.50% is at par with leading cardiac centers around the world.

Leading heart centers like The Escorts Heart Institute have Cardiac Care Units with sophisticated equipment and investigative facilities like Echocardiography with coloured Doppler, Nuclear Scanning and Coronary Angiography. The Jayadeva Institute of Cardiology in Bangalore, the Cardiology Hospital in Kanpur, the Heart Hospital in Calicut and the Sree Sudihindra Medical Mission Hospital in Cochin are some hospitals in India devoted exclusively to cardiac treatment.

Surgical treatment packages are offered in following areas:

» Cardiac Surgery And Cardiology
» Open Heart Surgery
» Angiographies
» Angioplasties
» Paediatric Cardiac Surgery
» Paediatric Intervention
» Cardiology Robotic Surgery

Some other procedures available are:

» directional coronary atherectomy
» rotablation
» coronary artery stenting
» intravascular ultrasound
» balloon valvuloplasty
» non-surgical closure of holes in the heart such as ASD, VSD and PDA.

Medical Tourism Packages in India for Health Check-ups

Many common and life-threatening conditions can be treated successfully if detected early. Many leading hospitals in India have health check-up programmes that screen every part of the body meticulously and professionally. A proper health check-up scans your bio-history, interprets signals and provides the opportunity for the proverbial "stitch in time". A heart check-up constituting echocardiography, consultation by a senior cardiologist, blood test, general test and haemogram can go a long way in ensuring a healthy heart. The test can be done at any of the leading cardiac hospitals or private clinics.

A comprehensive health check-up contains the following tests:

- Doctors consultation and full medical examination
- Blood tests
- Complete Haemogram (hb, TLC, DLR, ESR, Haemotocrit, Peripheral Smear)
- Blood group (ABO, RH)
- Blood Sugar
- Blood Urea
- Serum Uric Acid
- Serum Creatinine
- Serum Cholesterol
- Lipid Profile
- Urine and Faeces Exmimation
- X-Ray Chest PA
- ECG
- Exercise Stress Test (TMT)
- Stress Screening by Psychologist
- Eye Examination
- Gynaecologist Consultation and Pap Smear Test
- Post Check-up consulation
- Optional Test

Medical Tourism Packages for Cosmetic Surgery

A new dimension of the medical field taking off in India is cosmetic surgery which utilises some of the latest techniques in corrective procedures. Some disfigurations corrected include hair restoration (hair implants, hair flaps, and scalp reductions), rhinoplasties (reshaping or recontouring of the nose), stalling of the aging process (face life, cosmetic eyelid surgery, brow lift, sub-metal lipectomy for double chin), demabrasions (sanding of the face,) otoplasty for protruding ears, chin and cheek enlargement, lip reductions, various types of breast surgery and reconstruction and liposuction.

Non-invasive surgical procedures like streotactic radiosurgery and radiotherapy for brain tumours are practised successfully.

Medical Tourism Packages in India for Orthopaedic Surgery

A number of orthopedic procedures are available such as hip and knee replacement, the Illizarov technique, limb lengthening, Birmingham Hip resurfacing technique (which scores over conventional hip replacements and is still unavailable even in the US) etc.

Many hospitals specialize in latest techniques and treatments such as minimal invasive surgery, cartilage and bone transplantation, spine surgery and limb sparing surgery. All kinds of musculo-skeletal problems ranging from Arthiritis to sports injuries, to complex broken bones, bone tumors and childhood conditions like scoliosis are treated most effectively.

A wide range of spinal surgeries including fixation, stabilization and fusion are regularly undertaken.

Bone Marrow Transplant

Major hospitals in India have oncology units comprising surgical oncology, medical and radiation therapy as well as the crucial Bone Marrow Transplantation (BMT). The BMT unit with high pressure hipa filters has helped achieve a very high success rate in the various types of transplantation.

Cord Blood Transplant and Mismatched Allogeneic Stem Cell Transplant have been performed successfully, a feat that is remarkable and significant, considering the fact that the treatment costs one-tenth of what it does in the west. Special surgeons are available for individual organs. Plastic surgeons of repute provide treatment for head and neck cancer, breast cancer and other malignancies. Facilities offered include tele-therapy which includes simulation work stations to ensure high precision and safety during treatment at the 18 MV linear accelerator or telecobalt machines, brachy therapy and 3-D planning systems. In orthopaedics, the Ilizarov technique is practised for the treatment of limb deformities, limb shortening and disfiguration.

Joint Replacement Surgery

Shoulder/hip replacement and bilateral knee replacement surgery using the most advanced keyhole or endosopic surgery and anthroscopy is done at several hospitals in India including the Apollo Hospital, Sir Ganga Ram Hospital and Holy Family Hospital in Delhi, Bombay Hospital, Leelavati and Hinduja Hospital in Mumbai and the Madras Institute of Orthoepaedics and Trauma Sciences. Some hospitals like Apollo in Delhi have Operation Theatres with Laminar Air Flow System which compares with the best in the USA and the UK. A knee joint replacement costs about 3000 pounds in India wheras in the UK, a similar surgery using the same implants and medical consumables costs around 10,000 pounds.

Hospitals in India

India offers world-class healthcare that costs substantially less than those in developed countries, using the same technology delivered by competent Specialists attaining similar success rates.

- AIIMS
- Apollo Hospital
- B.M.Birla Heart Research Centre
- Christian Medical College
- Tata Memorial Hospital
- Apollo Cancer Hospital

- Indraprastha Medical Corporation
- Institute Cardiovascular Diseases

Holiday Destinations in India

In a country as diverse and complex as India, it is not surprising to find that people here reflect the rich glories of the past, the culture, traditions and values relative to geographic locations and the numerous distinctive manners, habits and food that will always remain truly Indian.

Beaches in India

Thousands of sun-deprived tourists visit India because it incredibly has the most diverse varieties of beaches anywhere in the world. Placid backwaters and lagoons, bays and rough lava-rocked seas, marine estuaries with fish, crashing surf, powdery golden sand or palm fringed shores - Incredible India has them all.

The West Coast with the Arabian Sea and the East Coast with the Bay of Bengal offer many a verdant vistas to the traveller. The coasts of India have their own seafood cuisine, relaxing spas, diving and water sports and great places to stay for a balmy holiday.

Hill Stations and Retreats

India offers several Hill Stations with excellent tourist attractions and facilities.

Royal Retreats

Having had a glorious past ranging from old civilizations to the more recent kingdoms, India offers royal retreats which are nowhere to be seen elsewhere. Staying at beautiful palaces with lush green fields, huge borders etc., make some of these retreats a memory of a lifetime.

Some of the Holiday destinations covered by us are :

- Agra
- Rajasthan
- Kerela
- Goa

- Delhi
- Mumbai (Bombay)
- Karnataka

Analysis and interpretation

Cost Comparison - India vs United Kingdom (UK)

Significant cost differences exist between U.K. and India when it comes to medical treatment. Accompanied with the cost are waiting times which exist in U.K. for patients which range from 3 months to over months.

India is not only cheaper but the waiting time is almost nil. This is due to the outburst of the private sector which comprises of hospitals and clinics with the latest technology and best practitioners.

Nature of Treatment	**Approximate Cost in India ($) ***	**Cost in other Major Healthcare Destination ($)***	**Approximate Waiting Periods in USA / UK (in months)**
Open heart Surgery	4,500	> 18,000	11-Sep
Cranio-facial Surgery and skull base	4,300	> 13,000	8-Jun
Neuro-surgery with Hypothermia	6,500	> 21,000	14-Dec

Complex spine surgery with implants	4,300	> 13,000	11-Sep
Simple Spine surgery	2,100	> 6,500	11-Sep
Simple Brain Tumor -Biopsy -Surgery	 1,000 4,300	 > 4,300 > 10,000	8-Jun
Parkinsons -Lesion -DBS	 2,100 17,000	 > 6,500 > 26,000	11-Sep
Hip Replacement	4,300	> 13,000	11-Sep

Cost Comparison - India vs United States of America (USA)

Significant cost differences exist between U.K. and India when it comes to medical treatment.

India is not only cheaper but the waiting time is almost nil. This is due to the outburst of the private sector which comprises of hospitals and clinics with the latest technology and best practitioners.

Procedure Charges in India & US (US $):

Procedure	***Cost (US$)***	
	United States	India
Bone Marrow	2,50,000	69,000

Transplant		
Liver Transplant	3,00,000	69,000
Heart Surgery	30,000	8,000
Orthopedic Surgery	20,000	6,000
Cataract Surgery	2,000	1,250

Here's a brief comparison of the cost of few of the Dental treatment procedures between USA and India

Dental procedure	*Cost in US ($)**		*Cost in India ($)**
	General Dentist	Top End Dentist	Top End Dentist
Smile designing	-	8,000	1,000
Metal Free Bridge	-	5,500	500
Dental Implants	-	3,500	800
Porcelain Metal Bridge	1,800	3,000	300
Porcelain Metal Crown	600	1,000	80
Tooth impactions	500	2,000	100
Root canal Treatment	600	1,000	100
Tooth whitening	350	800	110
Tooth colored composite fillings	200	500	25
Tooth cleaning	100	300	75

Conclusion

Medical tourism is likely to be the next major foreign exchange earner for India as an increasing number of patients, unwilling to accept long queues in Europe or high costs in the US, are travelling to the country to undergo surgery, according to a media report Medical tourism is on the rise with more people from the United States, Europe and the Middle East seeking Indian hospitals as a cheap and safe alternative, says an article in an upcoming issue of Bloomberg Markets magazine. The report says Indian doctors are setting up what could be a medical renaissance in their country and the next great boom for the Indian economy. Many Indian hospitals are coming together to improve the quality of health care, boost first impressions and aiming for $2.3 billion in annual revenue by 2012, it says. Instead of paying $2,00,000 for a mitral valve surgery in the US, a patient could travel to India and receive the same treatment for $6,700.Similarly, rather than paying 15,000 pounds Sterling for hip resurfacing in the UK, a patient can get the same procedure for 5,000 pounds in India, including surgery, airfare and hotel stay, the magazine says.

Authors Detail

Dr Sachin Bhardwaj Asst Prof Department of Management MIT Moradabad Email: sachinmba04@gmail.com M: 9675954299	Rahul Singh Asst Prof Department of Management MIT Moradabad Email: rsrmit@gmail.com M: 9411245948

Int J Mech Mater Des
DOI 10.1007/s10999-017-9369-2

Influence of porosity on the flexural and vibration response of gradient plate using nonpolynomial higher-order shear and normal deformation theory

Ankit Gupta · Mohammad Talha

Received: 3 January 2017 / Accepted: 28 March 2017

Abstract The present article deals with flexural and vibration response of functionally graded plates with porosity. The basic formulation is based on the recently developed non-polynomial higher-order shear and normal deformation theory by the authors'. The present theory contains only four unknowns and also accommodate the thickness stretching effect. The effective material properties at each point are determined by two micromechanics models (Voigt and Mori–Tanaka scheme). The governing equations for FGM plates are derived using variational approach. Results have been obtained by employing a C^0 continuous isoparametric Lagrangian finite element with eight degrees of freedom per node. Convergence and comparative study with the reported results in the literature, confirm the accuracy and efficiency of the present model and finite element formulation. The influence of the porosity, various boundary conditions, geometrical configuration and micromechanics models on the flexural and vibration behavior of FGM plates is examined.

Keywords Porosity · Nonpolynomial higher-order shear and normal deformation theory · Flexural · Vibration · Voigt · Mori–Tanaka

A. Gupta (✉) · M. Talha
School of Engineering, Indian Institute of Technology Mandi, Mandi, Himachal Pradesh 175005, India
e-mail: erankit04@gmail.com

1 Introduction

Over the last three decades, composite materials, have been the dominant emerging materials. The diversified applications of composite materials have grown steadily, penetrating and conquering new markets persistently. Further, the need of composite for the structural application has placed a high emphasis on the use of new and advanced materials which can be tailored microstructurally as per the requirement. Functionally graded materials (FGMs) are also a class of composites that have a continuous variation of material properties from one surface to another (Gupta et al. 2015). The gradation of properties in an FGM reduces the thermal stresses, residual stresses, and stress concentrations found in conventional composites.

Prediction of the realistic response of any structural component depends on its structural kinematics. In this regard, first plate theory was proposed by Kirchhoff (1850), known as Classical plate theory (CPT). This theory does not include transverse shear and normal stress hence, delivers irrational results for the thick plate. To conquer this limitation, displacement and stress based first order shear deformation theory (FSDT) was proposed by Mindlin (1951) and Reissner (1945) respectively. In FSDT, the shear correction factor is used to define the proper shear stress distribution. Its value depends on the geometric and loading conditions of the structure. To avoid

restriction associated with CPT and FSDT, several higher-order shear deformation theories (HSDT) have been proposed in the last two decades. In this framework, research carried out by Basset (1890), Lo et al. (1977), Levinson (1980), Murthy (1981), Kant et al. (1982) and Reddy (1984), can be treated as a benchmark in polynomial higher-order shear deformation theory. These polynomial HSDT used Taylor series coefficients to include the shear deformation. Therefore, these are relatively complex and computationally expensive.

To circumvent the aforesaid limitations, nonpolynomial higher-order shear deformation theories have been developed in which shear strain function is used to demonstrate the shear deformation. Touratier (1991), Soldatos (1992) and Karama et al. (2009) employed sinusoidal, sinusoidal hyperbolic and exponential shear strain function respectively. Recently, Mantari (2012) investigated the flexural response of FGM plate using new sinusoidal function based HSDT with five unknowns. Thai and Choi (2013) presented cubic, sinusoidal, hyperbolic, and exponential function based HSDT to study the static and vibration response of FGM plate. Authors divided the transverse displacement in the bending and shear component to reduce the number of unknowns. Belabed et al. (2014) proposed hyperbolic function based higher-order shear deformation theory with five unknowns to investigate flexural and vibration characteristics of FGM plate. Ameur et al. (2011) showed the closed form solution to investigate the bending response of FGM plate using trigonometric shear deformation theory with four unknowns. Atmane et al. (2010) developed a new higher shear deformation theory to investigate the free vibration analysis of simply supported functionally graded plates resting on a Winkler–Pasternak elastic foundation. Nguyen (2015) presented the closed form solution of static, vibration and buckling response of FGM plate using hyperbolic higher-order shear deformation theory with four unknowns. Zenkour (2005) presented the sinusoidal shear deformation plate theory to study buckling and free vibration of simply supported FG plates. Thai and Kim (2013) presented quasi-3D sinusoidal shear deformation theory with only five unknowns for bending behavior of simply supported FGM plates. The closed form solution of free vibration response of FGM plate using four-variable refined plate theory was given by Hadji et al. (2011).

Apart from the development of such theories, several kinds of literature are available in which implementation of these theories along with 3D exact solution are given to investigate static and dynamic characteristics of the composite plate. In this framework, Reddy (2000) proposed a finite element model based on the third-order deformation theory to investigate the static and dynamic responses of FGM plate under mechanical and thermal loading. Pandya and Kant (1988) presented isoperimetric finite element formulation to investigate the static response of advanced composite plate. The flexural response of the FGM plate using collocation multiquadric radial basis functions is investigated by Ferreira et al. (2005). Wu et al. (2010) developed a modified Pagano method for three-dimensional (3-D) analysis of simply-supported, functionally graded rectangular plates under magneto-electro-mechanical loads. Jha et al. (2013) presented a free vibration response of FG elastic, rectangular, and simply supported plates based on polynomial higher order shear/shear-normal deformations theories. Alipour et al. (2010) presented a semi-analytical solution to study the vibration response of two-directional-functionally graded circular plates, resting on elastic foundations. Authors implemented Mindlin's plate theory and the differential transformation technique to obtain the governing equations of motion. Kashtalyan (2004) presented the 3D elasticity solution for the flexural response of FGM plates, in which Young's modulus of the plate is assumed to vary exponentially through the thickness coordinate. Lal et al. (2012) used Reddy's third-order shear deformation theory to investigate the nonlinear bending response of FGM plate with random material properties. Prakash and Ganapathi (2006) used three-noded shear flexible plate element based on the field-consistency principle to study the free vibration and thermos-elastic buckling characteristics of circular FGM plates.

Talha and Singh (2010) investigated the static response and free vibration analysis of FGM plates using higher-order shear deformation theory with a special modification in the transverse displacement. Gupta et al. (2016a, b) used the polynomial higher order shear and normal deformation theory with 13DOF to analyze the vibration characteristics of FGM plate. Matsunaga (2009) presented Navier solution in the conjunction of two-dimensional higher-order theory to examine the flexural response

of FGM plate under thermal and mechanical loads. The free vibration analysis of plates made of FGMs with an arbitrary gradient was carried out by Benachour et al. (2011) using a four-variable refined plate theory. Mantari and Soares (2013) examined the bending response of FGM plates by using a new trigonometric higher order and hybrid quasi-3D shear deformation theories.

Mojdehi et al. (2011) presented the 3D elastic solution of FGM plates based on the MLPG method and MLS approximation. Authors found that the centroidal deflection of FGM plates lies in between those of a pure ceramic and a pure metallic plate for both static and dynamic loads. Xiang and Kang (2013) used a meshless method based on thin plate spline radial basis function for the flexural response of FGM plates based on various higher-order shear deformation theories. Qian et al. (2004) studied the static and dynamic deformation of thick functionally graded elastic plates by using higher order shear and normal deformable plate theories and meshless local Petrov–Galerkin method. Zenkour (2006) presented generalized shear deformation theory for the static response of FGM plates. Effective material properties were calculated by assuming a power-law. The comparative study of the effect of various gradation laws (power-law, sigmoid or exponential function) on the mechanical behavior of FGM plates under transverse load was carried out by Chi and Chung (2006). Vaghefi et al. (2010) showed a three-dimensional solution for thick FGM plates by utilizing a meshless Petrov–Galerkin method. An exponential function was assumed for the variation of Young's modulus through the thickness of the plate. Tamijani and Kapania (2012) used FSDT with element free Galerkin method to study the free vibration of an FG plate with curvilinear stiffeners. Zhu and Liew (2011) presented free vibration analyses of metal and ceramic FG plates with the local Kriging meshless method.

In addition, it is found from the literature (Ebrahimi and Zia 2015; Atmane et al. 2015) that during the fabrication process of FGMs, some microstructural defects i.e. micro-voids or porosities can accrue in the materials due to the large difference in solidification temperatures between the constituent materials. Wattanasakulpong and Ungbhakorn (2014), Wattanasakulpong et al. (2012) highlighted on the existence of porosities inside the FGM during multi-step sequential infiltration fabrication process. Therefore, it necessitates to include the porosity effect during computing the effective material properties of FGM plate. There are only a few reports available in the open literature dealing with the vibration and flexural analysis of FGM plate with porosity. Yahia et al. (2015) used higher-order shear deformation theories to study the wave propagation of an infinite FGM plate with porosities. The linear and nonlinear dynamic stability of a circular porous plate has been investigated to determine the critical loads in two separate studies by Magnucka-Blandzi (2010). Moreover, Mechab et al. (2016) have developed a nonlocal elasticity model for vibration of nanoplates made of porous FG material resting on elastic foundations.

Koiter (1959) and Carrrera et al. (2011) emphasized on the importance of thickness stretching effect on the structural response of the composite structure. From the aforesaid review, it is observed that most of the HSDT do not accommodate transverse normal strain which leads to the negligence of thickness stretching effect. It is also found that the available literature for the vibration and flexural response of FGM plates with porosity are relatively scarce. Therefore, the objective of the present work is set to investigate the flexural and vibration analysis of FGM plates with porosity using recently developed non-polynomial based higher-order shear and normal deformation theory by the authors' (Gupta and Talha 2016; Gupta et al. 2017). The present theory consists of a nonlinear variation of in-plane and transverse displacement along the thickness direction and also accommodate the thickness stretching effect. The effective material properties of FGM plate with porosity are computed using newly proposed model. To implement this theory, a suitable C^0 continuous isoparametric finite element with eight degrees of freedom (DOFs) per node is considered to minimize the computational complicacy. In order to compute the graded material properties, two micromechanics model (Voigt and Mori–Tanaka) is used with the conjunction of the power law. The influence of porosity volume fraction, volume fraction index, geometric configurations, and various boundary constraints on the flexural and vibration characteristics of FGM plates is investigated.

2 Mathematical formulation

The mathematical formulation of the actual physical problem of the FGM plates subjected to mechanical

loading is presented. An FGM plate with porosity having thickness 'h', length 'a', and width 'b' is considered and is shown in Fig. 1.

2.1 Constitutive equations and material properties

The Voigt model and Mori–Tanaka are used in the present study to compute the effective material properties of FGM plate.

2.1.1 Mori–Tanaka model

According to the Mori–Tanaka scheme (Mori 1973), the effective Young's modulus E_f and Poisson's ratio υ_f can be calculated using effective bulk modulus (K_f) and shear modulus (G_f) of the FGM plate as

$$\begin{aligned}\frac{K_f(z)-K_c}{K_m-K_c} &= \frac{V_m}{1+[1-V_m]\frac{3[K_m+K_c]}{[3K_c+4G_c]}}\\ \frac{G_f(z)-G_c}{G_m-G_c} &= \frac{G_f(z)}{1+[1-V_m]\left(\frac{G_m+G_c}{G_c+f_1}\right)}\end{aligned} \tag{1}$$

where, $f_1 = \frac{G_c[9K_c+8G_c]}{[6K_c+2G_c]}$ and K_c, G_c, K_m and G_m are the bulk modulus and shear modulus of ceramic and metal respectively. From Eq. (1), the effective material properties are represented as

$$E_f(z) = \frac{9K_f(z)G_f(z)}{3K_f(z)+G_f(z)}, \quad \upsilon_f(z) = \frac{3K_f(z)-2G_f(z)}{6K_f(z)+2G_f(z)} \tag{2}$$

2.1.2 Voigt model

The Voigt model is simple and has been adopted in most of the analyses of FGM structures (Gibson 1995). The effective material properties(p_e) in a specific direction (along with 'z') is determined by

$$\begin{aligned}V_m + V_c &= 1\\ p_e &= (p_c - p_m)V_c + p_m\end{aligned} \tag{3}$$

where, 'p_e' represents the effective material property (Young's modulus, mass density, Poisson's ratio), subscripts m and c represents the metallic and ceramic constituents, respectively. The volume fraction V_c is assumed to follow a simple power law in both the model as

$$V_c = \left(\frac{z}{h}+\frac{1}{2}\right)^n \tag{4}$$

where 'n' is the volume fraction index. To incorporate the porosity, a new mathematical expression is modeled with the help of slight modification in the

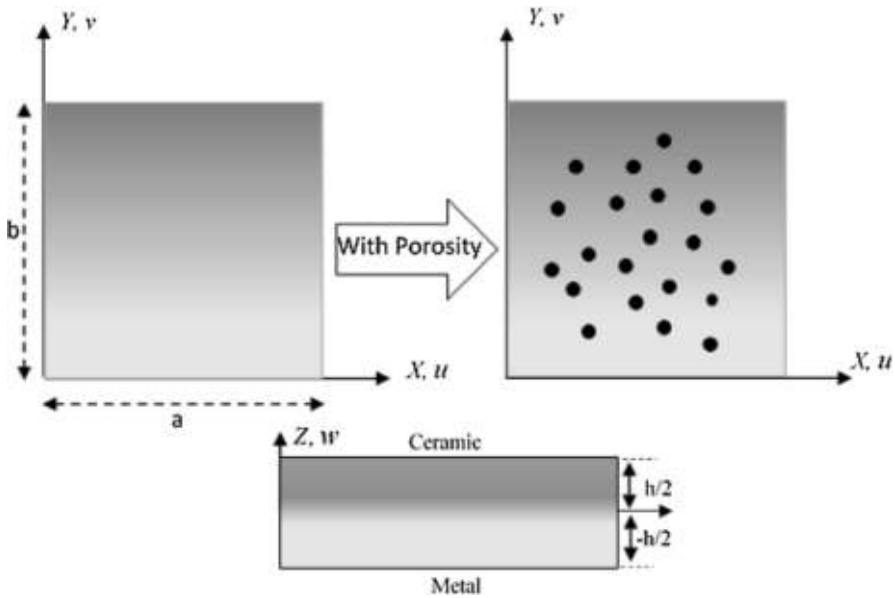

Fig. 1 The geometric configuration of FGM Plate with porosity

rule of mixture as given in Eq. (3). The material properties with porosity are anticipated to follow the power law in the present study and are expressed as

$$\begin{aligned} \mathrm{P} &= \mathrm{P}_c(V_c - \log(1+\lambda/2)) \\ &\quad + \mathrm{P}_m(V_m - \log(1+\lambda/2)) \end{aligned} \tag{5}$$

'λ' is termed as porosity volume fraction ($\lambda < 1$). $\lambda = 0$ indicates the non-porous functionally graded plate. The effective material property of porous FGM plate is given as

$$\begin{aligned} E(z) &= [E_c - E_m]\left(\frac{2z+h}{2z}\right)^n \\ &\quad - \log(1+\lambda/2)[E_c + E_m]\left[1 - \frac{2|z|}{h}\right] + E_m \\ \rho(z) &= [\rho_c - \rho_m]\left(\frac{2z+h}{2z}\right)^n \\ &\quad - \log(1+\lambda/2)[\rho_c + \rho_m]\left[1 - \frac{2|z|}{h}\right] + \rho_m \end{aligned} \tag{6}$$

The linear constitutive relations of an FG plate is given by Talha and Singh (2011):

$$\begin{Bmatrix} \sigma_{xx} \\ \sigma_{yy} \\ \sigma_{zz} \\ \tau_{yz} \\ \tau_{zx} \\ \tau_{xy} \end{Bmatrix} = \begin{bmatrix} C_{11} & C_{12} & C_{12} & 0 & 0 & 0 \\ C_{12} & C_{11} & C_{12} & 0 & 0 & 0 \\ C_{12} & C_{12} & C_{11} & 0 & 0 & 0 \\ 0 & 0 & 0 & C_{44} & 0 & 0 \\ 0 & 0 & 0 & 0 & C_{55} & 0 \\ 0 & 0 & 0 & 0 & 0 & C_{66} \end{bmatrix} \begin{Bmatrix} \varepsilon_{xx} \\ \varepsilon_{yy} \\ \varepsilon_{zz} \\ \gamma_{yz} \\ \gamma_{zx} \\ \gamma_{xy} \end{Bmatrix} \tag{7}$$

$$\begin{aligned} C_{11} &= E(z)(1+\upsilon)/(1-2\upsilon)(1+\upsilon) \\ C_{12} &= \upsilon E(z)/(1-2\upsilon)(1+\upsilon) \\ C_{44} &= C_{55} = C_{66} = E(z)/2(1+\upsilon) \end{aligned}$$

2.2 Displacement fields

A recently developed non-polynomial based higher-order shear and normal deformation theory by the authors' Gupta and Talha (2016), Gupta et al. (2017) is considered to investigate the realistic flexural and vibration responses of the porous graded plates as given in Eq. (8):

$$\begin{aligned} \bar{u}(x,y,z,t) &= u_o(x,y,t) - z\left(\frac{\partial w_b}{\partial x}\right) \\ &\quad - \psi\left[\sinh^{-1}\left(\frac{\kappa z}{h}\right) - \left(\frac{\kappa}{h}\right)z\right]\frac{\partial w_s}{\partial x} \\ \bar{v}(x,y,z,t) &= v_o(x,y,t) - z\left(\frac{\partial w_b}{\partial y}\right) \\ &\quad - \psi\left[\sinh^{-1}\left(\frac{\kappa z}{h}\right) - \left(\frac{\kappa}{h}\right)z\right]\frac{\partial w_s}{\partial y} \\ \bar{w}(x,y,z,t) &= w_b(x,y,t) + \kappa\cosh^2\left(\frac{\kappa z}{h}\right)w_s(x,y,t) \\ \text{Here, } \psi &= -\frac{h\cosh^2(\kappa/2)}{\sqrt{(1+\kappa^2/4)} - 1} \end{aligned} \tag{8}$$

where $\bar{u}$, $\bar{v}$ and $\bar{w}$ signifies the displacements of a point along the (x, y, z) coordinates. u_O, v_O, w_b and w_s are the four unknown displacement functions of mid-plane. The value of shape parameter 'κ' is deliberated in the post-processing phase and is evaluated as 3.4.

2.3 Strain–displacement relations

The non-zero linear strains associated with the displacement field in Eq. (8) is represented as,

$$\{\boldsymbol{\varepsilon}\}_{6x1} = [\mathfrak{M}]_{6x16}\{\bar{\varepsilon}\}_{16x1} \tag{9}$$

where $\{\bar{\boldsymbol{\varepsilon}}\}_{16x1}$ are the components of generalized strains. The non-zero strains are given below,

$$\begin{aligned} \begin{Bmatrix} \varepsilon_{xx} \\ \varepsilon_{yy} \\ \varepsilon_{zz} \\ \gamma_{xy} \\ \gamma_{xz} \\ \gamma_{yz} \end{Bmatrix} &= \begin{Bmatrix} \varepsilon^0_{xx} \\ \varepsilon^0_{yy} \\ \varepsilon^0_{zz} \\ \gamma^0_{xy} \\ \gamma^0_{xz} \\ \gamma^0_{yz} \end{Bmatrix} + z\begin{Bmatrix} \varepsilon^1_{xx} \\ \varepsilon^1_{yy} \\ 0 \\ \gamma^1_{xy} \\ 0 \\ 0 \end{Bmatrix} + f(z)\begin{Bmatrix} \varepsilon^2_{xx} \\ \varepsilon^2_{yy} \\ 0 \\ \gamma^2_{xy} \\ 0 \\ 0 \end{Bmatrix} \\ &\quad + \phi(z)\begin{Bmatrix} 0 \\ 0 \\ 0 \\ 0 \\ \gamma^1_{xz} \\ \gamma^1_{yz} \end{Bmatrix} + g(z)\begin{Bmatrix} 0 \\ 0 \\ 0 \\ 0 \\ \gamma^2_{xz} \\ \gamma^2_{yz} \end{Bmatrix} \end{aligned} \tag{10}$$

where, $f(z) = \psi\left[\sinh^{-1}\left(\frac{\kappa z}{h}\right) - \left(\frac{\kappa}{h}\right)z\right]$, $g(z) = \kappa\cosh^2\left(\frac{\kappa z}{h}\right)$, $\phi(z) = g'(z)$, $\varepsilon^0_{xx} = \frac{\partial u_0}{\partial x}$, $\varepsilon^0_{yy} = \frac{\partial v_0}{\partial y}$, $\varepsilon^0_{zz} = \left(2\kappa^2/h\right)w_s\cosh\left(\frac{\kappa z}{h}\right)\sinh\left(\frac{\kappa z}{h}\right)$, $\gamma^0_{xz} = -\left(\frac{\kappa\psi}{h}\right)\frac{\partial w_s}{\partial x}$, $\gamma^1_{xz} = \kappa\psi h$,

$\gamma_{xz}^2 = \kappa \frac{\partial w_s}{\partial x}.\ \gamma_{yz}^0 = -\frac{\kappa\psi}{h}\frac{\partial w_s}{\partial y},\ \gamma_{yz}^1 = \kappa\psi h,\ \gamma_{yz}^2 = \kappa\frac{\partial w_s}{\partial y},$
$\gamma_{xy}^0 = \frac{\partial u_0}{\partial y} + \frac{\partial v_0}{\partial x},\ \gamma_{xy}^1 = -\frac{\partial^2 w_b}{\partial x \partial y} - \frac{\kappa\psi}{h}\frac{\partial^2 w_s}{\partial x \partial y} - \frac{\partial^2 w_b}{\partial x \partial y} - \frac{\kappa\psi}{h}\frac{\partial^2 w_s}{\partial x \partial y},$
$\gamma_{xy}^2 = 2\psi\frac{\partial^2 w_s}{\partial x \partial y}\varepsilon_{xx}^1 = -\frac{\partial^2 w_b}{\partial x^2} - \left(\frac{\kappa\psi}{h}\right)\frac{\partial^2 w_s}{\partial x^2},\ \varepsilon_{yy}^1 = -\frac{\partial^2 w_b}{\partial y^2}$
$-\left(\frac{\kappa\psi}{h}\right)\frac{\partial^2 w_b}{\partial y^2},\ \varepsilon_{xx}^2 = \psi\frac{\partial^2 w_s}{\partial x^2},\ \varepsilon_{yy}^2 = \psi\frac{\partial^2 w_s}{\partial y^2}$

3 Solution methodology (finite element formulation)

3.1 Element selection

In the present finite element formulation, a C^0-continuous nine nodded isoparametric finite element with eight degrees of freedom per node (Fig. 2) is employed to discretize the plate geometry. Later, the generalized displacement vector and element geometry of the model at any point can be expressed in terms of shape functions as follows,

$$\{\Re\} = \sum_{i=1}^{nn} N_i\{\Re\}_i, x = \sum_{i=1}^{nn} N_i x_i, y = \sum_{i=1}^{nn} N_i y_i \qquad (11)$$

where $\{N_i\}$and$\{\Re_i\}$are the shape function and displacement vector of ith node respectively. 'nn' is the number of nodes per element and x_i, and y_i are the Cartesian coordinate of the ith node. The shape functions at an ith node of the nine noded elements are given as:

$$N_i = \begin{cases} \frac{1}{4}\left(\xi^2 + \xi_i\xi\right)\left(\eta^2 + \eta_i\eta\right), & for\ i = 1,2,3,4 \\ \frac{1}{2}\left(1-\xi^2\right)\left(\eta^2 + \eta_i\eta\right), & for\ i = 5,7 \\ \frac{1}{2}\left(\xi^2 + \xi_i\xi\right)\left(1-\eta^2\right), & for\ i = 6,8 \\ \frac{1}{2}\left(1-\xi^2\right)\left(1-\eta^2\right), & for\ i = 9 \end{cases} \qquad (12)$$

3.2 Continuity obligation

It is obvious from Eq. (9), that the in-plane displacement (i.e. $\bar{u}$ and $\bar{v}$) encompass transverse displacement derivatives $(\bar{w})$, which leads to the second order derivatives in the strain vector. Hence, it requires implementing C^1 continuity in the finite element modeling.

To eradicate the intricacy accompanying with these finite elements, the displacement field has been modified to make it appropriate for C^0 continuous element. In this framework, the transverse displacement derivatives exist in Eq. (8) are replaced as $\frac{\partial w_b}{\partial x} = \alpha_x$, $\frac{\partial w_b}{\partial y} = \alpha_y$, $\frac{\partial w_s}{\partial x} = \beta_x$, $\frac{\partial w_s}{\partial y} = \beta_y$ and $w_s = \beta_z$. After incorporating these modifications in the displacement field, four DOFs with C^1 continuity given in Eq. (8) are changed into eight DOFs with C^0 continuity as shown in Eq. (13).

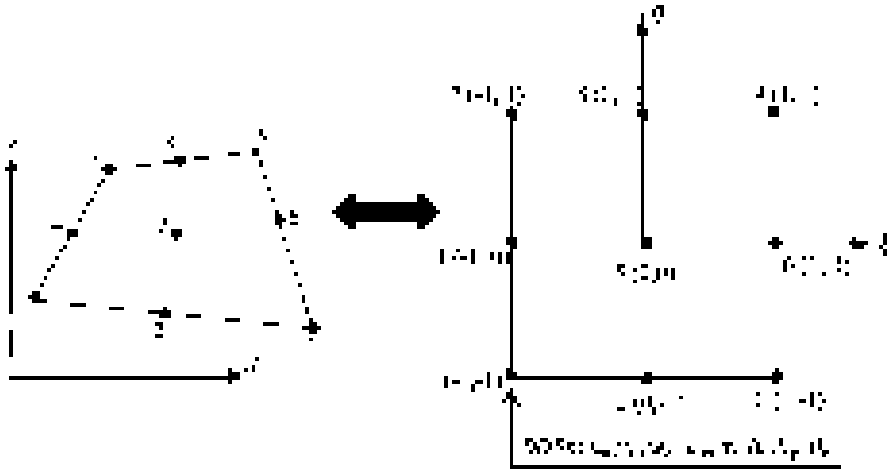

Fig. 2 Configuration of nine-noded finite element in natural coordinate system

$$\begin{aligned}\bar{u}(x,y,z,t) &= u_o(x,y,t) - z\left[\alpha_x + \left(\frac{\kappa\psi}{h}\right)\beta_x\right] \\ &\quad + \psi\sinh^{-1}\left(\frac{\kappa z}{h}\right)\beta_x \\ \bar{v}(x,y,z,t) &= v_o(x,y,t) - z\left[\alpha_y + \left(\frac{\kappa\psi}{h}\right)\beta_y\right] \\ &\quad + \psi\sinh^{-1}\left(\frac{\kappa z}{h}\right)\beta_y \\ \bar{w}(x,y,z,t) &= w_b(x,y,t) + \kappa\cosh^2\left(\frac{\kappa z}{h}\right)\beta_z(x,y,t)\end{aligned} \tag{13}$$

The basic field variables can be denoted mathematically as. In this procedure, the artificial constraints are introduced which are enforced variationally through a penalty approach as given in Eq. (15).

$$\begin{aligned}&\frac{\partial w_b}{\partial x} - \alpha_x = 0\,,\ \frac{\partial w_b}{\partial y} - \alpha_y = 0\,, \\ &\frac{\partial w_s}{\partial x} - \beta_x = 0 \text{ and } \frac{\partial w_s}{\partial y} - \beta_y = 0\end{aligned} \tag{14}$$

3.3 Energy equations

3.3.1 Strain energy of the plate

The strain energy of *i*th element of FGM plate is given by:

$$\begin{aligned}\Pi^e &= \frac{1}{2}\int_V \{\boldsymbol{\varepsilon}\}_i^T\{\boldsymbol{\sigma}\}_i dV = \frac{1}{2}\int_v \{\boldsymbol{\varepsilon}\}_i^T\left[\boldsymbol{Q_{ij}}\right]\{\boldsymbol{\varepsilon_i}\}dV \\ &= \frac{1}{2}\int_V \{\bar{\boldsymbol{\varepsilon}}\}_i^T[\mathfrak{M}]_i^T\left[\boldsymbol{Q_{ij}}\right][\mathfrak{M}]_i\{\bar{\varepsilon}\}_i dV \\ &= \frac{1}{2}\int_A \{\Re\}_i^T[\mathbf{B}]_i^T[\boldsymbol{D}][\mathbf{B}]_i\{\Re\}_i dA \\ &= \frac{1}{2}\{\Re\}_i^T[\boldsymbol{K}]_i\{\Re\}_i\end{aligned} \tag{15}$$

If '*ne*' is the number of elements used for meshing the plate, the strain energy of the plate is given as,

$$\prod = \sum_{e=1}^{ne}\Pi^{(e)}, \prod = \frac{1}{2}\sum_{e=1}^{ne}\{\Re\}^{(e)T}[\boldsymbol{K}]^{(e)}\{\Re\}^{(e)} \tag{16}$$

where $[\boldsymbol{K}]^{(e)}$ and $\{\Re\}^{(e)}$ are the linear stiffness matrix and displacement vector for the element, respectively.

3.3.2 Kinetic energy of the plate

The kinetic energy of FGM plate is given by:

$$\Delta = \frac{1}{2}\int_V \rho\{\dot{\boldsymbol{\Lambda}}\}^T\{\dot{\boldsymbol{\Lambda}}\}dV \tag{17}$$

where 'ρ'and $\{\boldsymbol{\Lambda}\}$ are the density and global displacement vector of the plate. The global displacement field model has represented as:

$$\{\boldsymbol{\Lambda}\} = [\bar{\mathbf{N}}]\{\Re\} \tag{18}$$

where the matrix $[\bar{\mathbf{N}}]$ is the function of thickness coordinate which is given in "Appendix". After substituting Eq. (18) into Eq. (17), the kinetic energy of an element is obtained as:

$$\begin{aligned}\Delta^e &= \frac{1}{2}\int_A\left(\int_Z \rho\left\{\dot{\Re}\right\}^T[\mathbf{N}]^T[\mathbf{N}]\left\{\dot{\Re}\right\}dz\right)dA \\ &= \frac{1}{2}\int_A\left\{\dot{\Re}\right\}^T[\mathrm{M}]^{(e)}\left\{\dot{\Re}\right\}dA\end{aligned} \tag{19}$$

Kinetic energy of vibrating plate for total number of element '*ne*' is given as

$$\Delta = \sum_{e=1}^{ne}\Delta^{(e)} \tag{20}$$

Here $[\mathrm{M}]^{(e)}$ is the inertia matrix of the element.

3.3.3 Work done due to transverse load

The external work done on the plate by uniformly applied load q_0 may be written as $W_{ext}^{(e)} = \int_A q_0(x,y)\{\boldsymbol{w}\}dA$

For the finite element formulation, the above equation can be written as

$$W_{ext} = \sum_{e=1}^{ne} W_{ext}^{(e)} \tag{21}$$

The total potential energy due to the applied load can be written as

$$\begin{aligned}V &= -W_{ext}^{(e)} = -\int_A \{\boldsymbol{\Lambda}\}^T\{\boldsymbol{\mathcal{F}}\}dA \\ &= -\{\boldsymbol{\Lambda}\}^{(e)T}\{\boldsymbol{\mathcal{F}}\}^{(e)} \\ \{\boldsymbol{\mathcal{F}}\}^{(e)} &= \{0 \quad 0 \quad Q \quad 0 \quad 0 \quad 0 \quad 0 \quad 0\}^T\end{aligned} \tag{22}$$

3.4 Governing equation

The governing equation for flexural and free vibration analysis of FG plate has been obtained using the principle of virtual work (Grover et al. 2013).

$$\int_{t_1}^{t_2} (\delta L) dt = 0 \tag{23}$$

where L is termed as Lagrangian and is demarcated as $L = \Pi - (\Delta + V)$. The final governing equation can be obtained by putting all the energy equations (Eqs. 16, 20 and 22) along with the energy function Π_c because of enforced artificial constraints during the conversion of C^1 continuity to C^0 continuity. This energy function $\Pi_c$is expressed as

$$\Pi_c = \frac{\gamma}{2} \iint \left[\begin{array}{c} \left(\frac{\partial w_b}{\partial x} - \alpha_x\right)^T \left(\frac{\partial w_b}{\partial x} - \alpha_x\right) + \left(\frac{\partial w_b}{\partial y} - \alpha_y\right)^T \left(\frac{\partial w_b}{\partial y} - \alpha_y\right) + \\ \left(\frac{\partial w_s}{\partial x} - \beta_x\right)^T \left(\frac{\partial w_s}{\partial x} - \beta_x\right) + \left(\frac{\partial w_s}{\partial y} - \beta_y\right)^T \left(\frac{\partial w_s}{\partial y} - \beta_y\right) \end{array} \right] dxdy \tag{24}$$

Using finite element approximation Π_c is represented as:$\Pi_c = \frac{\gamma}{2}\{\Re\}^T[\mathbf{K_c}]\{\Re\}$, where $[\mathbf{K_c}]$ is the stiffness matrix due to artificial constraints. After substituting theses value in Eq. (23), the governing equation is expressed as

$$\frac{1}{2}\int_{t_1}^{t_2} \delta\left[\left\{\dot{\Re}\right\}^T [\mathrm{M}]\left\{\dot{\Re}\right\} - \{\Re\}^T[\mathbf{K} + \gamma\mathbf{K_c}]\{\Re\}\right] dt = 0 \tag{25}$$

Above equations can be used to find the required governing equations for free vibration and flexural analysis by imposing the prerequisite boundary conditions as follows:

1. The generalized eigenvalue problem for free vibration of a system can be expressed as

$$[\mathrm{M}]\left\{\ddot{\Re}\right\} + [\mathbf{K} + \gamma\mathbf{K_c}]\{\Re\} = 0, \tag{26}$$

2. The generalized governing equation for flexural analysis may be expressed as

$$[\mathbf{K}]\{\Re\} = \{\boldsymbol{\mathcal{F}}\} \tag{27}$$

Table 1 Properties of the FGM components

Material	Properties		
	E (GPa)	ν	ρ (kg/m^3)
Aluminium (Al)	70	0.30	2707
Zirconia (ZrO_2)	151	0.30	3000
Alumina (Al_2O_3)	380	0.30	3800
Ti–6Al–4 V	105.5	0.294	4429
Silicon nitride (Si_3N_4)	327.27	0.24	2370

4 Numerical results and discussion

In this section, the model validation and numerical analyses for the flexural and vibration response of the FGM plate are performed using the finite element method. A uniform 6 × 6 mesh of nine noded C^o continuous elements is employed. To prevent the shear locking phenomena, the reduced integration technique is used to integrate terms related to the transverse shear stress. The description of material properties used in the analysis is provided in Table 1.

4.1 Convergence and validation of the present solution

Three test examples have been solved to show the efficacy and proficiency of the present solution along with the convergence and comparison studies. The obtained results are compared with those available in the literature. The numerical results are presented in the graphical and tabular form.

Example 1 The first example is performed for Al/Al_2O_3 square FGM plates with simply supported (SSSS) boundary condition for different values of the power law index '*n*'. The non-dimensional fundamental frequency $(\bar{\omega})$ obtained by present model are

Table 2 Comparison of linear frequency parameter $\left(\bar{\omega} = \omega(a^2/h)\sqrt{\rho_c/E_c}\right)$ for Al/Al_2O_3 (SSSS) FGM plate with different mesh size for $a/h = 10$

Mesh size	Volume fraction index 'n'				
	0	0.5	1	4	10
Present 2 × 2	5.9932	5.1375	4.6665	4.0139	3.7981
Present 3 × 3	5.9739	5.1274	4.6569	3.9894	3.7739
Present 4 × 4	5.8456	5.0100	4.5527	3.9247	3.7162
Present 5 × 5	5.8033	4.9672	4.5097	3.8935	3.6932
Present 6 × 6	5.7900	4.9560	4.4997	3.8846	3.6846
Belabed et al. (2014)	5.7800	4.9400	4.4900	3.8900	3.6800
% Difference	0.173	0.323	0.216	0.138	0.125

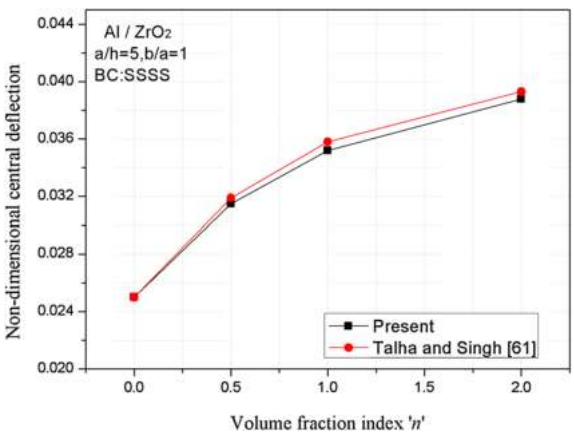

Fig. 3 Comparison of central deflection of Al/ZrO_2 FGM plate

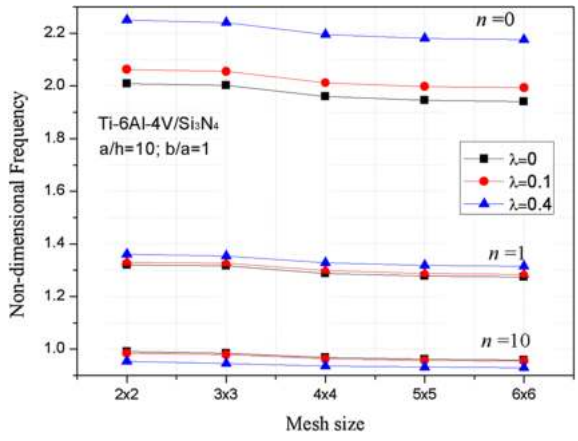

Fig. 4 Convergence for the non-dimensional frequency of FGM plate with porosity (λ: porosity volume fraction; n: volume fraction index)

compared with those given by Belabed et al. (2014) as shown in Table 2. In Ref (Belabed et al. 2014) higher - order shear and normal deformation theory with five unknowns has been used to investigate the vibration response of FGM plate. They employed Hamilton's principle to drive the governing equation of motion and frequency parameters have been calculated using Navier solution. The comparison study confirms that the present results are in excellent agreement with

Table 3 Comparison of frequency parameter of (CCCC) FGM plate (Ti–6Al–4V/Si_3N_4) for various volume fraction index 'n' and side to thickness ratio (M–T: Mori–Tanaka)

a/h	Volume fraction index 'n'									
	0		1		5		10		100	
	Voigt	M–T	Voigt	M–T	Voigt	M–T	Voigt	M–T	Voigt	M–T
5	7.6778	7.6778	5.1165	5.3330	3.9254	4.0103	3.6785	3.7331	3.2957	3.3089
10	10.0615	10.0615	6.6307	6.9037	5.2314	5.3369	4.9125	4.9938	4.3318	4.3513
20	11.0479	11.0479	7.2541	7.5461	5.8022	5.9159	5.4520	5.5476	4.7650	4.7880
30	11.3494	11.3494	7.4461	7.7440	5.9750	6.0914	5.6152	5.7150	4.8973	4.9213
50	11.5843	11.5843	7.5942	7.8964	6.1100	6.2283	5.7433	5.8463	5.0007	5.0256
100	11.7264	11.7264	7.6821	7.9866	6.1939	6.3130	5.8234	5.9285	5.0638	5.0893

Table 4 Comparison of frequency parameter of (SCSC) FGM plate (Ti–6Al–4V/Si_3N_4) for various volume fraction index '*n*' and side to thickness ratio (M–T: Mori–Tanaka)

a/h	Volume fraction index '*n*'									
	0		1		5		10		100	
	Voigt	M–T	Voigt	M–T	Voigt	M–T	Voigt	M–T	Voigt	M–T
5	6.3552	6.3552	4.3504	4.5337	3.3534	3.4277	3.0895	3.1554	2.7165	2.7260
10	8.2164	8.2164	5.4095	5.6308	4.2842	4.3698	4.0239	4.0915	3.5394	3.5557
20	8.8674	8.8674	5.8200	6.0533	4.6634	4.7544	4.3824	4.4598	3.8257	3.8443
30	9.0593	9.0593	5.9421	6.1792	4.7737	4.8664	4.4865	4.5666	3.9099	3.9292
50	9.2072	9.2072	6.0354	6.2752	4.8588	4.9528	4.5673	4.6494	3.9750	3.9949
100	9.2970	9.2970	6.0910	6.3322	4.9119	5.0063	4.6179	4.7014	4.0149	4.0351

Table 5 Comparison of frequency parameter of (SSSS) FGM plate (Ti–6Al–4V/Si_3N_4) for various volume fraction index '*n*' and side to thickness ratio (M–T: Mori–Tanaka)

a/h	Volume fraction index '*n*'									
	0		1		5		10		100	
	Voigt	M–T	Voigt	M–T	Voigt	M–T	Voigt	M–T	Voigt	M–T
5	5.1352	5.1352	3.3891	3.5271	2.6737	2.7275	2.5110	2.5523	2.2124	2.2227
10	5.7965	5.7965	3.8057	3.9581	3.0479	3.1073	2.8646	2.9149	2.5013	2.5135
20	5.9896	5.9896	3.9274	4.0834	3.1615	3.2226	2.9717	3.0251	2.5861	2.5991
30	6.0338	6.0338	3.9553	4.1120	3.1875	3.2490	2.9963	3.0504	2.6056	2.6187
50	6.0616	6.0616	3.9727	4.1299	3.2040	3.2657	3.0118	3.0664	2.6179	2.6311
100	6.0759	6.0759	3.9816	4.1390	3.2126	3.2745	3.0200	3.0749	2.6242	2.6375

those generated by Belabed et al. (2014) even though the present model consist only four unknowns. It is also clear from the convergence study that the performance of the present formulation is good in terms of solution accuracy and the rate of convergence with mesh refinement. Based on the convergence study, in the present analysis the results are obtained at (6×6) mesh size, and otherwise stated.

Example 2 In this example, the central deflection (w_c) of (SSSS) Al/ZrO_2 square FGM plates with varying volume fraction indexes (n) is computed and compared with the results given by Talha and Singh (2010). The material properties of the constituent material are $Em = 70$ GPa N/m^2, $\rho_m = 2702$ kg/m^3 for aluminium (Al), and $E_c = 151$ GPa, $\rho_c = 5700$ kg/m^3 for zirconia (ZrO_2). Talha and Singh (2011) used polynomial based higher-order shear deformation theory with thirteen DOF per node. It is clearly from the Fig. 3 that the solution accuracy is good for the static response for different values of volume fraction index.

Table 6 Comparison of frequency parameter of (CFSF) FGM plate (Ti–6Al–4V/Si_3N_4) for various volume fraction index '*n*' and side to thickness ratio (M–T: Mori–Tanaka)

a/h	Volume fraction index '*n*'									
	0		1		5		10		100	
	Voigt	M–T	Voigt	M–T	Voigt	M–T	Voigt	M–T	Voigt	M–T
5	3.9540	3.9540	2.6125	2.7213	2.0456	2.0871	1.9212	1.9516	1.7014	1.7110
10	4.4851	4.4851	2.9428	3.0618	2.3501	2.3958	2.2098	2.2478	1.9343	1.9443
20	4.6763	4.6763	3.0630	3.1855	2.4613	2.5085	2.3148	2.3557	2.0183	2.0278
30	4.7381	4.7381	3.1024	3.2262	2.4962	2.5440	2.3478	2.3895	2.0453	2.0574
50	4.7895	4.7895	3.1348	3.2595	2.5256	2.5739	2.3756	2.4180	2.0679	2.0768
100	4.8220	4.8220	3.1550	3.2802	2.5450	2.5935	2.3940	2.4370	2.0823	2.0941

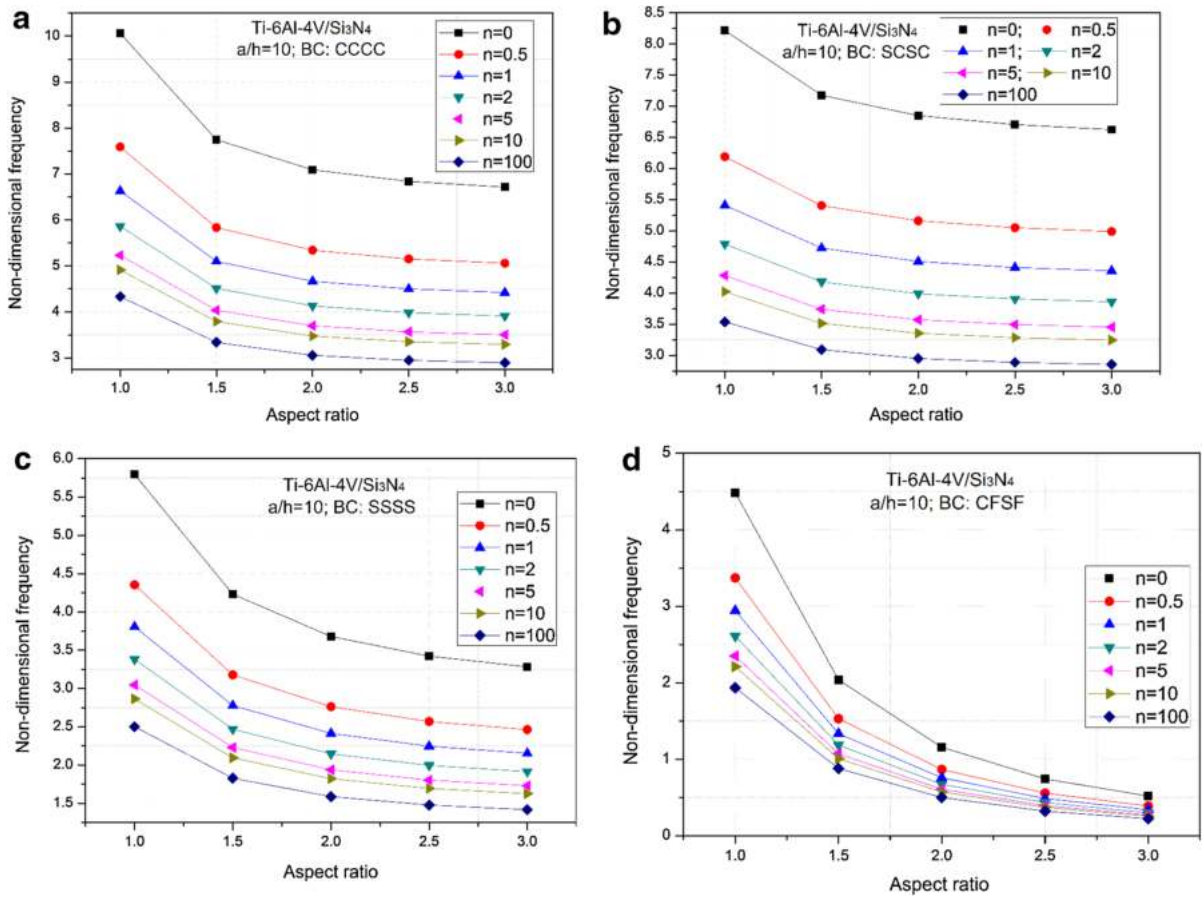

Fig. 5 Non-dimensional frequency versus aspect ratio for different volume fraction index '*n*'

Example 3 To verify the effectiveness of the present formulation in dealing with flexural and vibration analysis of FGM plate with porosity, a convergence study is conducted in terms of different mesh size. The analysis is performed for Simply supported Ti–6Al–4V/Si_3N_4 FGM plates having *a/h* ratio equals to 10 with various volume fraction indices ($n = 0$, 1 and 10). The material properties of the constituent material are $E_m = 105.7$ GPa, $\rho_m = 4429$ kg/m^3 for Ti–6Al–4V, and $E_c = 322.27$ GPa, $\rho_c = 2370$ kg/m^3 for Si_3N_4. Effective material properties of FGM plate with porosity have been calculated using the mathematical expression given in Eq. (6). The non-dimensional frequency parameter is calculated using mesh sizes from (2 × 2) to (6 × 6) for different volume fraction indexes '*n*'. It is clear from the Fig. 4 that the present solution shows the excellent convergence for the frequency parameter of FGM plate with porosity.

4.2 Parametric studies

In the view of the preceding discussion, it is observed that the present formulation delivers results which are in good agreement with various existing shear deformation theories of the FGM plate. In the subsequent section, the parametric studies have been carried out to explore the influence of various homogenization techniques, gradation rules, porosity volume fraction,

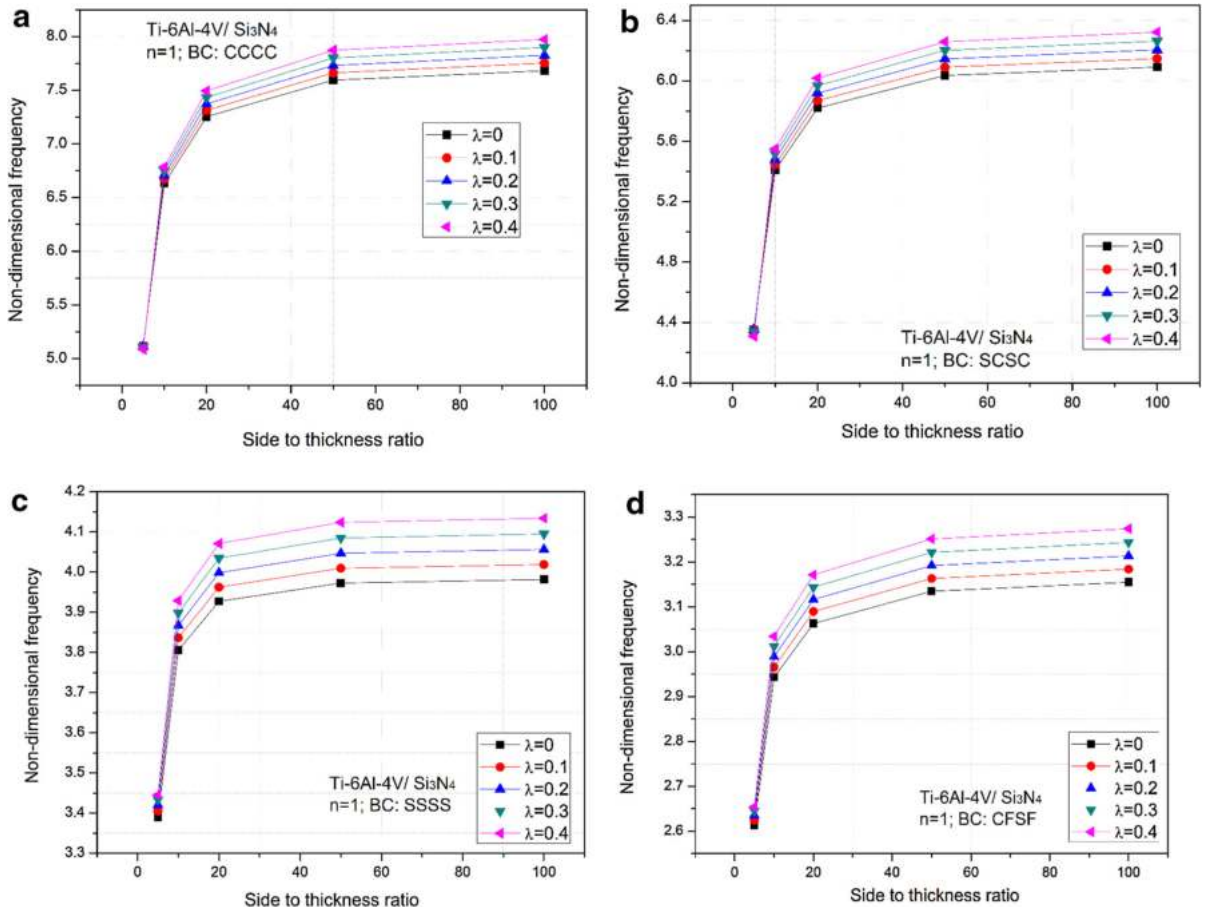

Fig. 6 Non-dimensional frequency versus side to thickness ratio for different porosity volume fraction (λ)

volume fraction index, and geometric configuration on the flexural and vibration response of FGM plate.

4.2.1 Vibration analysis of FGM plate

In Table 3, the frequency parameter of fully clamped square Ti–6Al–4V/Si_3N_4 FGM plate is presented for side to thickness ratio and volume fraction indexes (n). The influence of two micromechanics model (Mori–Tanaka and Voigt model) on the frequency parameter is also discussed in the results. The non-dimensional frequency parameter is assumed as $\left(\bar{\bar{\omega}} = \omega\left(a^2/h\right)\sqrt{\rho_c/E_c}\right)$. The material properties of the constituent material are $E_m = 105.7$ GPa, $\rho_m = 4429$ kg/m^3, $\upsilon_m = 0.298$ for Ti–6Al–4V, and $E_c = 322.27$ GPa, $\rho_c = 2370$ kg/m^3, $\upsilon_c = 0.25$ for Si_3N_4. It is perceived from the results that by increasing side to thickness ratio, the frequency parameter increases. It is also found that the frequency parameter decreases with increase in volume fraction index *'n'*. It is evident from the results that Voigt and Mori–Tanaka models delivers same results for an isotropic plate ($n = 0$), whereas very small changes are seen for the rest of the values of volume fraction index *'n'*. It is observed from the results that the maximum percentage difference between the two models is 4.23%.

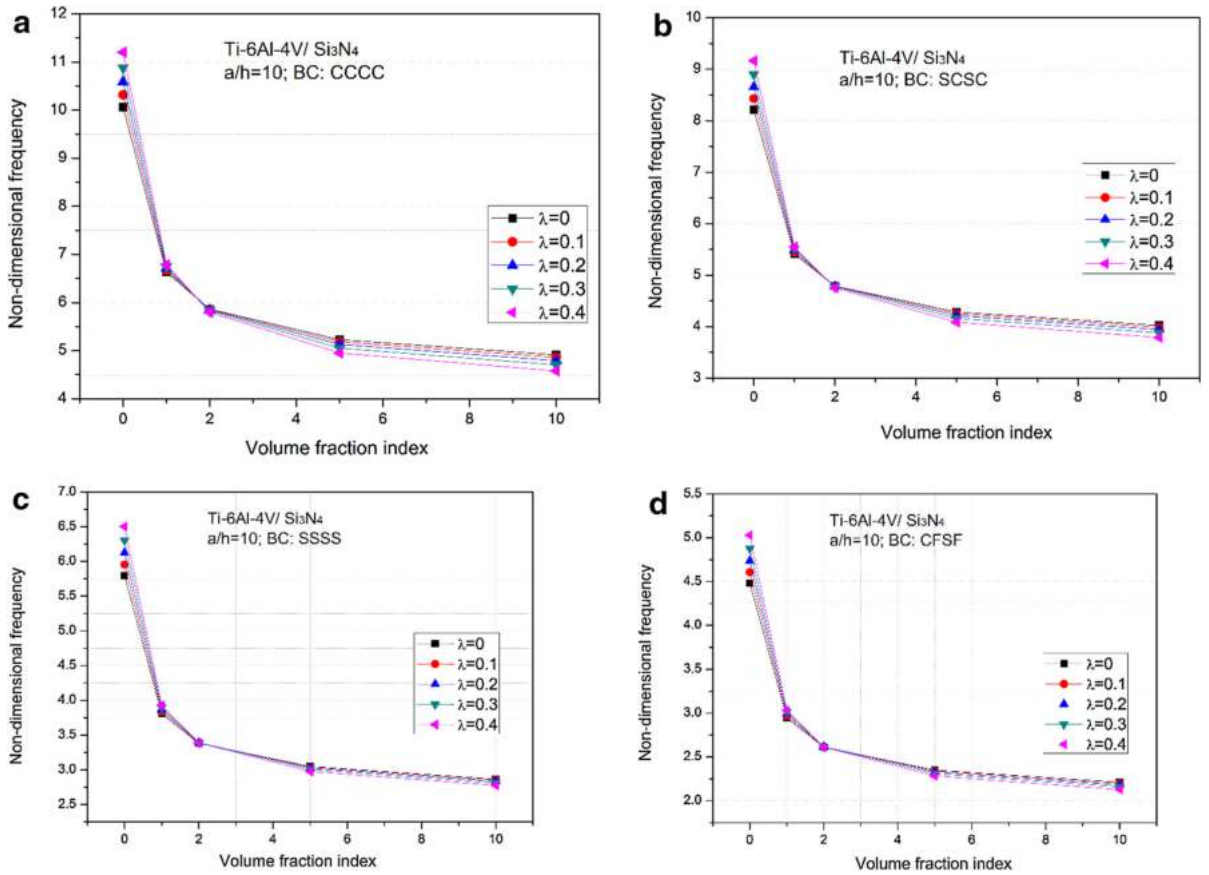

Fig. 7 Non-dimensional frequency versus volume fraction index for different porosity volume fraction (λ)

Tables 4, 5 and 6 show the effect of various side to thickness ratios and volume fraction index on the frequency parameter of SCSC, SSSS, and CFSF FGM plate respectively. This shows the consistent behavior as discussed in the former section. Again, the maximum percentage difference in the results obtained from two different homogenization techniques (Voigt and M–T) is 4.07%. It is notable that the Mori–Tanaka model slightly overpredicts the frequency ratio as compared to Voigt model. In the succeeding sections, only Voigt model is used to compute the effective material properties of FGM plate.

In Fig. 5a, the influence of aspect ratio (*b/a*) and volume fraction index '*n*' on the frequency parameter of fully clamped FGM plate is shown. It is evident from the figure that the frequency parameter decreases with increases in aspect ratio and volume fraction index. Figure 5b–d present the variation of frequency parameter of FGM plate with aspect ratio for SCSC, SSSS, and CFSF boundary conditions respectively. It is observed form the results that for CCCC FGM plate, the frequency parameter decreases up to 33% when aspect ratio increases from 1 to 3, on the other hand, this reduction in the frequency parameter is

approximately 88% for CFSF FGM. Therefore, it can be concluded that the influence of aspect ratio is more on the plate having fewer boundary constraints.

Figure 6a–d represent the effect of porosity on the non-dimensional frequency parameter of CCCC, SCSC, SSSS, and CFSF FGM plate respectively. It is observed that the frequency increases as the porosity volume fraction (λ) increase for all the boundary conditions considered herewith. It is perceived that the range of percentage increment in frequency parameter is approximately 0.5–1.5% for $a/h = 5$, whereas this value is increased to nearly 3.8% for $a/h = 100$. Hence, it is concluded that the thin plate is more sensitive to porosity as a comparison to the thick plate.

In Fig. 7a–d, the influence of porosity on the frequency parameter is demonstrated with the variation of volume fraction index for various boundary constraints. From the obtained results, it is noticed that the when the FGM plate is fully ceramic ($n = 0$), frequency parameter increases as the porosity volume fraction. But as the metal constituent increases ('n' increases from 1 to 10) in the FGM plate, frequency parameter decreases as the porosity volume fraction increases. It is apparent that the maximum change in

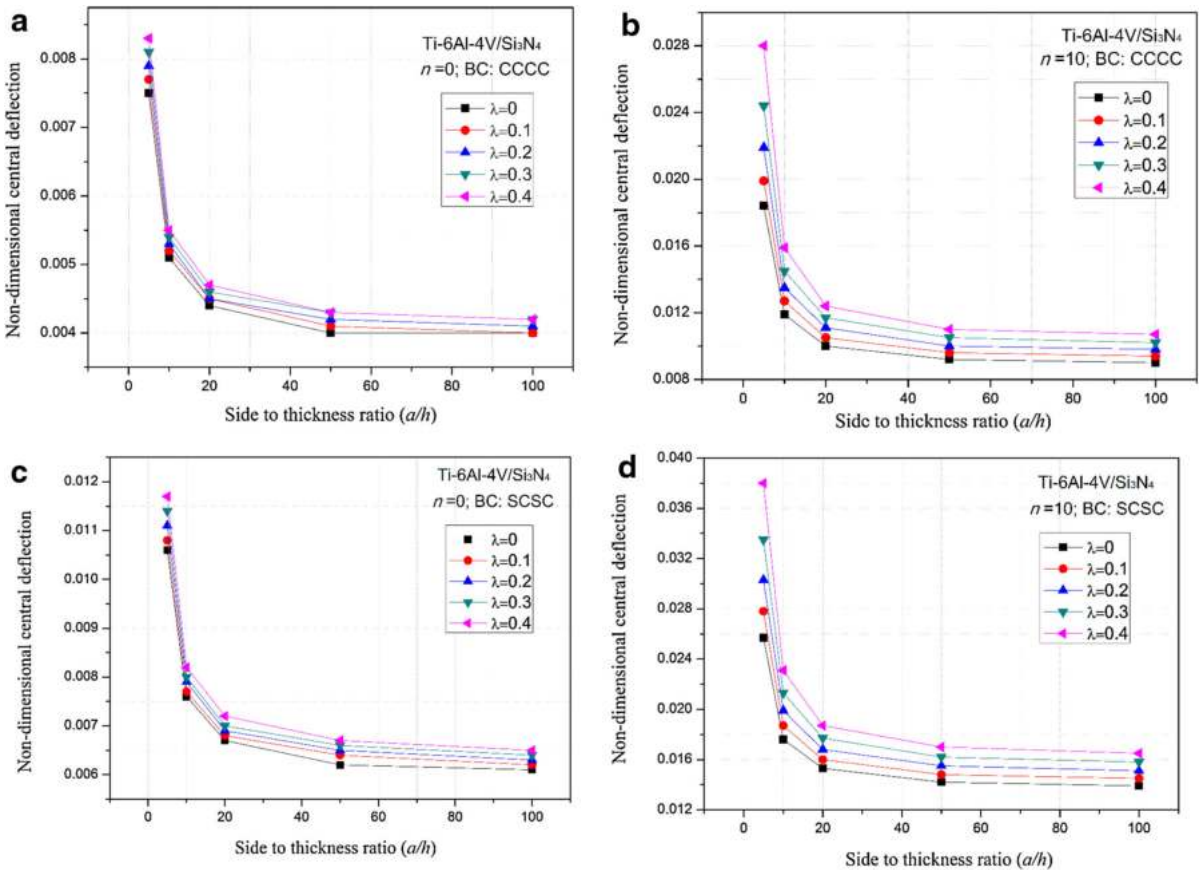

Fig. 8 Variation of central deflection with side to thickness ration and porosity volume fraction index (λ) for FGM plate ($n = 1$ and 10)

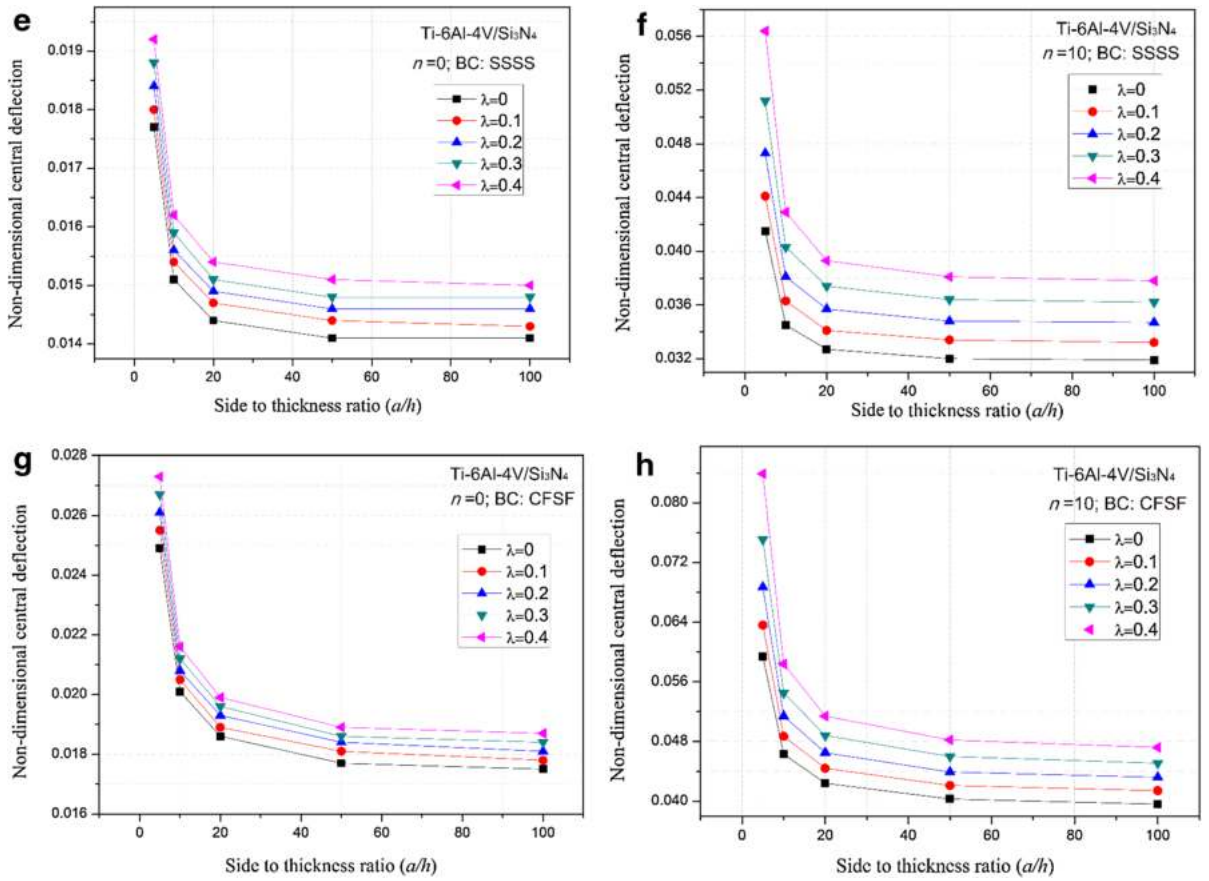

Fig. 8 continued

the frequency is approximately 11% due to porosity when 'n' is 0 but this value is nearly 6% of the higher value of 'n'.

4.2.2 *Flexural response*

In this section, the flexural response is performed for the FGM plate made of Ti–6Al–4V/Si_3N_4 with porosity. The transverse displacement *(w)*, thickness coordinate *(z)* and the pressure *(Q)* applied to the top surface of the plate are presented in nondimensionalized form as

$$\bar{w} = w/h,\ Q = qa^4/E_m h^4\ , \bar{z} = z/h \tag{23}$$

Figure 8a–b depicts the variation of non-dimensional central deflection of (Ti–6Al–4V/Si_3N_4) fully clamped FGM plate with side to thickness ratio and porosity volume fraction for $n = 0$ and 10. It is manifest from the results that the central deflection decreases with increase *a/h* ratio up to a certain limit

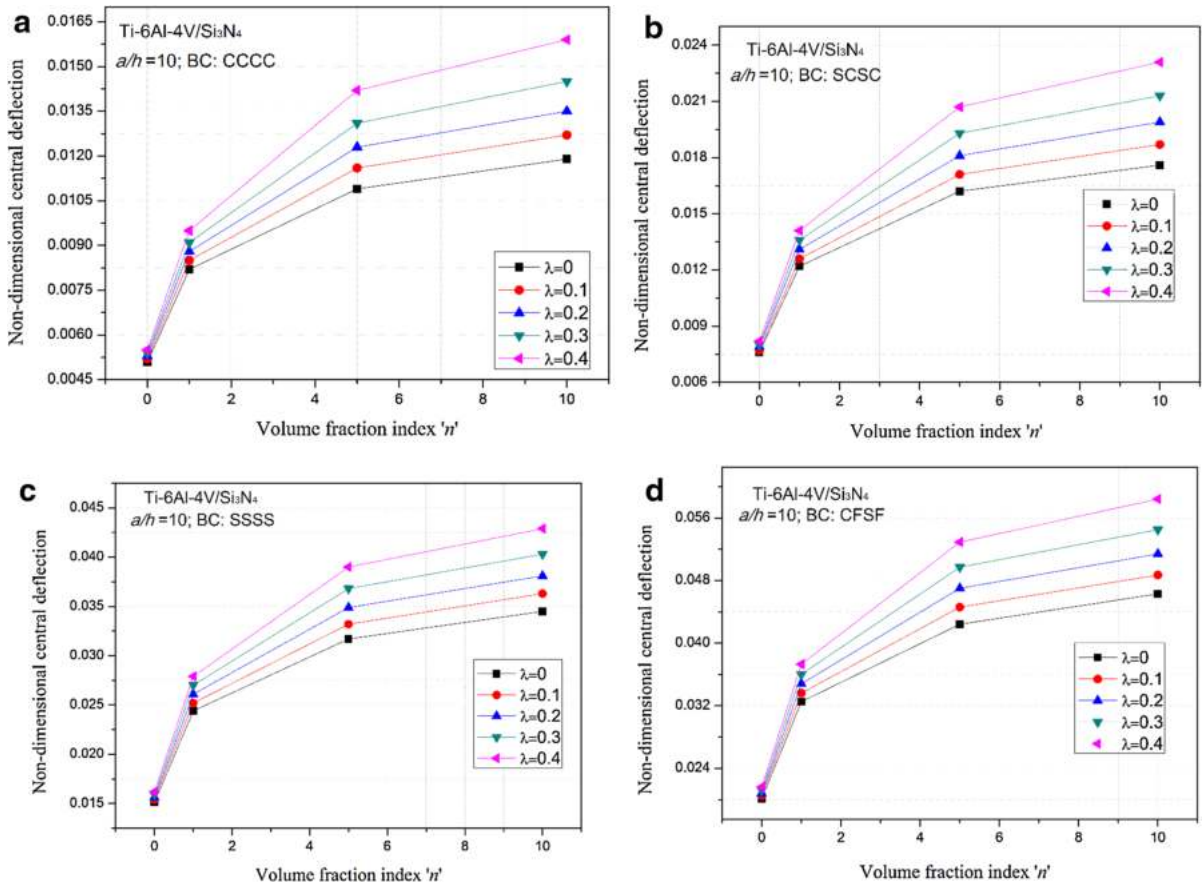

Fig. 9 Variation of central deflection with volume fraction index and porosity volume fraction (λ) for FGM plate

($a/h = 50$) beyond this no substantial change in the deflection occurs. It is also observed that the central deflection increases with porosity volume fraction (λ). In Fig. 8c–h, central deflection is plotted against the side to thickness ratio and porosity volume fraction with $n = 0$ and 10 for SCSC, SSSS, and CFSF boundary conditions respectively. In all the cases, the flexural response reflects the consistent behavior as discussed for Fig. 8a–b.

In Fig. 9a–d, the effect of porosity and volume fraction index on the central deflection of FGM plate is investigated for various boundary conditions. It is observed that the change in central deflection is ranged from 5 to 10% when porosity volume fraction increases from 0 to 0.4 for fully ceramic FGM plate ($n = 0$), whereas this percentage change is reduced to only 18–52% for the higher values of 'n'. Therefore, it is concluded that the flexural response is significantly

influenced by the porosity in the FGM plate having more volume fraction of ceramic.

5 Conclusions

The flexural and vibration response of functionally graded plate with porosity is analyzed using recently developed nonpolynomial higher-order shear and normal deformation theory to ensure its efficiency and applicability. This theory satisfies not only the shear stress-free boundary conditions at the top and bottom surfaces of the plate but also accommodate the thickness stretching effects. The new mathematical model is developed through the reformulation of the rule of mixture to incorporate the porosity phase in the material properties. Finite element formulation has been carried out using C^0 isoparametric element with 72 degrees of freedom per element. Several significant effects of volume fraction of porosity, volume fraction index, geometric configuration, homogenization techniques and boundary conditions on the flexural and vibration characteristics of FGM plate are investigated. The whole analysis concludes with some significant observations that are summarized as follows:

- Porosity volume fraction is an essential parameter in structural component design. The frequency increases as the porosity volume fraction increases.
- The effect of porosity is prominent in metal whereas its effect weakens as ceramic content in the FGM plate increases.
- The effect of porosity is perceptible in thin plates.
- The presence of porosity leads to increase the deflection in all the boundary conditions considered in the present study.
- Significant changes in deflection and frequency observed for $a/h < 50$, but for $a/h > 50$ no notable changes observed in deflection and frequency.

Appendix

Notation and description of various entities associated in mathematical modelling of structural kinematics

a, b, h	Length, width and thickness of the FGM plate	E	Effective Young's modulus
x, y, z	Cartesian coordinate	ρ	Effective mass density
u_o, v_o, w_b	Mid-plane displacements	υ	Poisson's ratio
w	Transverse displacement component	$[\mathbf{M}]$	Mass matrix
κ	Shape parameter	$[\mathbf{K}]$	Stiffness matrix
ε	Linear strain vector	ω	Natural frequency
V_c	Volume fraction of ceramic	$\bar{w}$	Central deflection
V_m	Volume fraction of metal	λ	Porosity volume fraction

$$[\mathcal{N}] = \begin{bmatrix} 1 & 0 & 0 & \Omega_1(z) & 0 & 0 & \Omega_2(z) & 0 \\ 0 & 1 & 0 & 0 & \Omega_1(z) & 0 & 0 & \Omega_2(z) \\ 0 & 0 & 1 & 0 & 0 & 0 & 0 & \Omega_3(z) \end{bmatrix}$$

$$\Omega_1(z) = -z,$$

$$\Omega_2(z) = \psi Sinh^{-1}\left(\frac{\kappa z}{h}\right) - \left(\frac{\kappa\psi}{h}\right),$$

$$\Omega_3(z) = \kappa Cosh^2\left(\frac{\kappa z}{h}\right)$$

$$[\mathbf{M}] = \begin{bmatrix} 1 & 0 & 0 & 0 & 0 & z & 0 & 0 & \Omega_2(z) & 0 & 0 & 0 & 0 & 0 & 0 & 0 \\ 0 & 1 & 0 & 0 & 0 & 0 & z & 0 & 0 & \Omega_2(z) & 0 & 0 & 0 & 0 & 0 & 0 \\ 0 & 0 & 0 & 0 & 0 & 0 & 0 & 0 & 0 & 0 & 0 & 0 & 0 & 0 & 0 & \Omega_3'(z) \\ 0 & 0 & 1 & 0 & 0 & 0 & 0 & 0 & 0 & 0 & 0 & \Omega_3(z) & 0 & \Omega_3'(z) & 0 & 0 \\ 0 & 0 & 0 & 1 & 0 & 0 & 0 & 0 & 0 & 0 & 0 & 0 & \Omega_3(z) & 0 & \Omega_3'(z) & 0 \\ 0 & 0 & 0 & 0 & 1 & 0 & 0 & Z & 0 & 0 & \Omega_2(z) & 0 & 0 & 0 & 0 & 0 \end{bmatrix}$$

References

Alipour, M.M., Shariyat, M., Shaban, M.: A semi-analytical solution for free vibration of variable thickness two-directional-functionally graded plates on elastic foundations. Int. J. Mech. Mater. Des. **6**, 293–304 (2010). doi:10.1007/s10999-010-9134-2

Ameur, M., Tounsi, A., Mechab, I., El Bedia, A.A.: A new trigonometric shear deformation theory for bending analysis of functionally graded plates resting on elastic foundations. KSCE J. Civ. Eng. **15**, 1405–1414 (2011). doi:10.1007/s12205-011-1361-z

Atmane, A.H., Tounsi, A., Bernard, F.: Effect of thickness stretching and porosity on mechanical response of a functionally graded beams resting on elastic foundations. Int. J. Mech. Mater. Des. (2015). doi:10.1007/s10999-015-9318-x

Atmane, H.A., Tounsi, A., Mechab, I., El Bedia, A.A.: Free vibration analysis of functionally graded plates resting on Winkler-Pasternak elastic foundations using a new shear deformation theory. Int. J. Mech. Mater. Des. **6**, 113–121 (2010). doi:10.1007/s10999-010-9110-x

Basset, A.B.: On the extension and flexure of cylindrical and spherical thin elastic shells. Philos. Trans. R. Soc. A Math. Phys. Eng. Sci. **181**, 433–480 (1890). doi:10.1098/rsta.1890.0007

Belabed, Z., Houari, M.S.A., Tounsi, A., Mahmoud, S.R.R., Beg, O.Anwar: An efficient and simple higher order shear and normal deformation theory for functionally graded material (FGM) plates. Compos. Part B Eng. **60**, 274–283 (2014). doi:10.1016/j.compositesb.2013.12.057

Benachour, A., Tahar, H.D., Atmane, H.A., Tounsi, A., Ahmed, M.S.: A four variable refined plate theory for free vibrations of functionally graded plates with arbitrary gradient. Compos. Part B Eng. **42**, 1386–1394 (2011). doi:10.1016/j.compositesb.2011.05.032

Carrera, E., Brischetto, S., Cinefra, M., Soave, M.: Effects of thickness stretching in functionally graded plates and shells. Compos. B Eng. **42**, 123–133 (2011). doi:10.1016/j.compositesb.2010.10.005

Chi, S.H., Chung, Y.L.: Mechanical behavior of functionally graded material plates under transverse load—Part I: analysis. Int. J. Solids Struct. **43**, 3657–3674 (2006). doi:10.1016/j.ijsolstr.2005.04.011

Ebrahimi, F., Zia, M.: Large amplitude nonlinear vibration analysis of functionally graded Timoshenko beams with porosities. Acta Astronaut. **116**, 117–125 (2015). doi:10.1016/j.actaastro.2015.06.014

Ferreira, A.J.M., Batra, R.C., Roque, C.M.C., Qian, L.F.F., Martins, P.A.L.S.: Static analysis of functionally graded plates using third-order shear deformation theory and a meshless method. Compos. Struct. **69**, 449–457 (2005). doi:10.1016/j.compstruct.2004.08.003

Gibson, L.J., Ashby, M.F., Karam, G.N., Wegst, U., Shercliff, H.R.: The mechanical properties of natural materials. II. Microstructures for mechanical efficiency. Proc. R. Soc. A Math. Phys. Eng. Sci. **450**, 141–162 (1995). doi:10.1098/rspa.1995.0076

Grover, N., Singh, B.N., Maiti, D.K.: Analytical and finite element modeling of laminated composite and sandwich plates: an assessment of a new shear deformation theory for free vibration response. Int. J. Mech. Sci. **67**, 89–99 (2013). doi:10.1016/j.ijmecsci.2012.12.010

Gupta, A., Talha, M.: Recent development in modeling and analysis of functionally graded materials and structures. Prog. Aerosp. Sci. **79**, 1–14 (2015). doi:10.1016/j.paerosci.2015.07.001

Gupta, A., Talha, M.: An assessment of a non-polynomial based higher order shear and normal deformation theory for vibration response of gradient plates with initial geometric imperfections. Compos. B **107**, 141–161 (2016). doi:10.1016/j.compositesb.2016.09.071

Gupta, A., Talha, M., Chaudhari, V.K.: Natural frequency of functionally graded plates resting on elastic foundation using finite element method. Procedia Technol. **23**, 163–170 (2016b). doi:10.1016/j.protcy.2016.03.013

Gupta, A., Talha, M., Seemann, W.: Free vibration and flexural response of functionally graded plates resting on Winkler-Pasternak elastic foundations using non-polynomial higher order shear and normal deformation theory. Mech. Adv. Mater. Struct. (2017). doi:10.1080/15376494.2017.1285459

Gupta, A., Talha, M., Singh, B.N.: Vibration characteristics of functionally graded material plate with various boundary constraints using higher order shear deformation theory. Compos. B Eng. **94**, 64–74 (2016a). doi:10.1016/j.compositesb.2016.03.006

Hadji, L., Atmane, H.A., Tounsi, A., Mechab, I., Addabedia, E.A.: Free vibration of functionally graded sandwich plates using four-variable refined plate theory. Appl. Math. Mech. (English Edition) **32**, 925–942 (2011). doi:10.1007/s10483-011-1470-9

Jha, D.K., Kant, T., Singh, R.K.: Free vibration response of functionally graded thick plates with shear and normal deformations effects. Compos. Struct. **96**, 799–823 (2013). doi:10.1016/j.compstruct.2012.09.034

Kant, T., Owen, D.R.J., Zienkiewicz, O.C.: A refined higher-order C o plate bending element. Comput. Struct. **15**, 177–183 (1982)

Karama, M., Afaq, K.S., Mistou, S.: A new theory for laminated composite plates. Proc. Inst. Mech. Eng. Part L: J Mater. Des. Appl. **223**, 53–62 (2009). doi:10.1243/14644207JMDA189

Kashtalyan, M.: Three-dimensional elasticity solution for bending of functionally graded rectangular plates. Eur. J. Mech. A/Solids **23**, 853–864 (2004). doi:10.1016/j.euromechsol.2004.04.002

Kirchhoff GR: Uber das gleichgewicht und die bewegung einer elastischen Scheibe. J Reine Angew Math (Crelle's J) **40**, 51–88 (1850)

Koiter, W.T.: A consistent first approximation in the general theory of thin elastic shells. In Proceedings of First Symposium on the Theory of Thin Elastic Shells. North-Holland, Amsterdam (1959)

Lal, A., Jagtap, K.R., Singh, B.N.: Stochastic nonlinear bending response of functionally graded material plate with random system properties in thermal environment. Int. J. Mech. Mater. Des. **8**, 149–167 (2012). doi:10.1007/s10999-012-9183-9

Levinson, M.: An accurate simple theory of statics and dynamics of elastic plates. Mech. Res. Commun. **7**, 343–350 (1980)

Lo, K.H., Christensen, R.M., Wu, E.M.: A high-order theory of plate deformation—part 2: laminated plates. J. Appl. Mech. **44**, 669 (1977)

Magnucka-Blandzi, E.: Non-linear analysis of dynamic stability of metal foam circular plate. J. Theor. Appl. Mech. **48**, 207–217 (2010)

Mantari, J.L., Guedes Soares, C.: A novel higher-order shear deformation theory with stretching effect for functionally graded plates. Compos. Part B Eng. **45**, 268–281 (2013). doi:10.1016/j.compositesb.2012.05.036

Mantari, J.L.L., Oktem, A.S.S., Guedes Soares, C.: Bending response of functionally graded plates by using a new higher order shear deformation theory. Compos Struct. **94**, 714–723 (2012). doi:10.1016/j.compstruct.2011.09.007

Matsunaga, H.: Stress analysis of functionally graded plates subjected to thermal and mechanical loadings. Compos. Struct. **87**, 344–357 (2009). doi:10.1016/j.compstruct.2008.02.002

Mechab, I., Mechab, B., Benaissa, S., Serier, B., Bachir Bouiadjra, B.: Free vibration analysis of FGM nanoplate with porosities resting on Winkler Pasternak elastic foundations based on two-variable refined plate theories. J. Braz. Soc. Mech. Sci. Eng. (2016). doi:10.1007/s40430-015-0482-6

Mindlin, R.D.: Influence of rotatory inertia and shear on flexural motions of isotropic, elastic plates. ASME J. Appl. Mech. **18**, 31–38 (1951)

Mojdehi, A.R., Darvizeh, A.: Three dimensional static and dynamic analysis of thick functionally graded plates by the meshless local Petrov–Galerkin (MLPG) method. Engineering Analysis with … **35**, 1168–1180 (2011)

Mori, T., Tanaka, K.: Average stress in matrix and average elastic energy of materials with misfitting inclusions. Acta Metall. **21**, 571–574 (1973). doi:10.1016/0001-6160(73)90064-3

Murthy, M. V. V.: An improved transverse shear deformation theory for laminated anisotropic plates. NASA Technical Paper 1903 (1981)

Nguyen, Tk: A higher-order hyperbolic shear deformation plate model for analysis of functionally graded materials. Int. J. Mech. Mater. Des. **11**, 203–219 (2015). doi:10.1007/s10999-014-9260-3

Pandya, B.N., Kant, T.: Finite element analysis of laminated composite plates using a higher-order displacement model. Compos. Sci. Technol. **32**, 137–155 (1988). doi:10.1016/0266-3538(88)90003-6

Prakash, T., Ganapathi, M.: Asymmetric flexural vibration and thermoelastic stability of FGM circular plates using finite element method. Compos. B Eng. **37**, 642–649 (2006). doi:10.1016/j.compositesb.2006.03.005

Qian, L.F., Batra, R.C., Chen, L.M.: Static and dynamic deformations of thick functionally graded elastic plates by using higher-order shear and normal deformable plate theory and meshless local Petrov-Galerkin method. Compos. B Eng. **35**, 685–697 (2004). doi:10.1016/j.compositesb.2004.02.004

Reddy, J.N.: A simple higher-order theory for laminated composite plates. J. Appl. Mech. **51**, 745 (1984). doi:10.1115/1.3167719

Reddy, J.N.: Analysis of functionally graded plates. Int. J. Numer. Meth. Eng. **47**, 663–684 (2000)

Reissner, E.: The effect of transverse shear deformation on the bending of elastic plates. ASME J. Appl. Mech. **12**, 68–77 (1945)

Soldatos, K.P.: A transverse shear deformation theory for homogeneous monoclinic plates. Acta Mech. **94**, 195–220 (1992). doi:10.1007/BF01176650

Talha, M., Singh, B.N.: Static response and free vibration analysis of FGM plates using higher order shear deformation theory. Appl. Math. Model. **34**, 3991–4011 (2010). doi:10.1016/j.apm.2010.03.034

Talha, M., Singh, B.N.: Thermo-mechanical buckling analysis of finite element modeled functionally graded ceramic-metal plates. Int. J. Appl. Mech. **3**, 867–880 (2011a). doi:10.1142/S1758825111001275

Talha, M., Singh, B.N.: Nonlinear mechanical bending of functionally graded material plates under transverse loads with various boundary conditions. Int. J. Model. Simul. Sci. Comput. **2**, 237–258 (2011b). doi:10.1142/S1793962311000451

Tamijani, A.Y., Kapania, R.K.: vibration analysis of curvilinearly-stiffened functionally graded plate using element free Galerkin method. Mech. Adv. Mater. Struct. **19**, 100–108 (2012). doi:10.1080/15376494.2011.572240

Thai, H.T., Choi, D.H.: Efficient higher-order shear deformation theories for bending and free vibration analyses of functionally graded plates. Arch. Appl. Mech. **83**, 1755–1771 (2013). doi:10.1007/s00419-013-0776-z

Thai, H.T., Kim, S.E.: A simple quasi-3D sinusoidal shear deformation theory for functionally graded plates. Compos. Struct. **99**, 172–180 (2013). doi:10.1016/j.compstruct.2012.11.030

Touratier, M.: An efficient standard plate theory. Int. J. Eng. Sci. **29**, 901–916 (1991)

Vaghefi, R., Baradaran, G.H., Koohkan, H.: Three-dimensional static analysis of thick functionally graded plates by using meshless local Petrov-Galerkin (MLPG) method. Eng. Anal. Boundary Elem. **34**, 564–573 (2010). doi:10.1016/j.enganabound.2010.01.005

Wattanasakulpong, N., Ungbhakorn, V.: Linear and nonlinear vibration analysis of elastically restrained ends FGM beams with porosities. Aerosp. Sci. Technol. **32**, 111–120 (2014). doi:10.1016/j.ast.2013.12.002

Wattanasakulpong, N., Prusty, B.G., Kelly, D.W., Hoffman, M: Free vibration analysis of layered functionally graded beams with experimental validation. Mater. Des. (1980–2015) **36** 182–190 (2012). doi:10.1016/j.matdes.2011.10.049

Wu, C.P., Chen, S.J., Chiu, K.H.: Three-dimensional static behavior of functionally graded magneto-electro-elastic plates using the modified Pagano method. Mech. Res. Commun. **37**, 54–60 (2010). doi:10.1016/j.mechrescom.2009.10.003

Xiang, S., Kang, G.: Static analysis of functionally graded plates by the various shear deformation theory. Compos. Struct. **99**, 224–230 (2013). doi:10.1016/j.compstruct.2012.11.021

Yahia, S.A., Atmane, H.A., Houari, M.S.A., Tounsi, A.: Wave propagation in functionally graded plates with porosities using various higher-order shear deformation plate theories. Struct. Eng. Mech. **53**, 1143–1165 (2015). doi:10.12989/sem.2015.53.6.1143

Zenkour, A.M.: A comprehensive analysis of functionally graded sandwich plates: part 2-buckling and free vibration. Int. J. Solids Struct. **42**, 5243–5258 (2005). doi:10.1016/j.ijsolstr.2005.02.016

Zenkour, A.M.: Generalized shear deformation theory for bending analysis of functionally graded plates. Appl. Math. Model. **30**, 67–84 (2006). doi:10.1016/j.apm.2005.03.009

Zhu, P., Liew, K.M.: Free vibration analysis of moderately thick functionally graded plates by local Kriging meshless method. Compos. Struct. **93**, 2925–2944 (2011). doi:10.1016/j.compstruct.2011.05.011

Smart Home Automation using Android Application

Abhishek Saxena[1] Saurabh Saxena[2] Mohit Sharma[3] Ankur Maurya[4] Akshay Kumar[5]
[1,3,4,5]PG Student [2]Assistant Professor
[1,2,3,4,5]Department of Electrical Engineering
[1,2,3,4,5]M.I.T. Moradabad

Abstract— Today is a world of advanced mobile applications which are used exhaustively to save time and energy. These applications ease day-to-day life of a common man. Based on these technologies and applications, we have designed a Home Automation System. In this paper, we propose design and prototype implementation of home automation system that uses Wi-Fi technology and Android operating system. An attractive market for Home Automation System is for busy families and individuals with physical limitations. Users can control electrical appliances in home or office via smart phone. This project aims at providing security and controlling every happening at home or office on your fingers.

Key words: Wi-Fi, Android, Temperatue Sensor, IR Sensors, Microcontroller, Relays, GSM Module, Bluetooth, Stepper Motor

I. INTRODUCTION

The current scenario is such that people have to manually operate various kinds of appliances which at times is not feasible for busy families and individuals with physical limitations. Also there is no effective means of automatic controlling of window curtains, door lock, lighting and temperature in our house according to our requirements.

Home automation refers to providing the capability to control as well as monitor various household activities. Theses may include lighting, heating and air conditioning, security locks on the doors, multimedia, and various appliances. Our system will provide proper notifications to users for such incidences when some unwanted person enters in our house and alert us via sending messages on our mobile phone.

Smart home is a very promising area, which has various benefits such as providing increased comfort, safety and security to people. It is rational use of energy and other resources thus contributing to a significant savings in terms of time and more secure. Such system will be affordable, portable and scalable so that new devices can be easily integrated in to systems. The technology is easy to use and targeted for people without technical background.

II. THEORY

The main objective of this project is to design and implement a cheap and open source home automation system that is capable of controlling and automating most of the house appliances. This application is an easy and manageable web interface for user to run Home Automation System.

In this project we have integrated technologies like Android with Wi-Fi or bluetooth to execute Home Automation System. We designed user Interfaces using Android because Android operating systems are capturing most of the mobile market. It has technical advantages of scalability, flexibility, availability, security and its ease of use for users.

The aim to take Android as platform is because people are familiar as many applications are launched in Android. Android provides interactive graphical user interface which makes an application easy to use for users.

In this application, we used fans, bulbs etc depicted graphically for better understanding of the users. Users can switch ON/OFF any appliances like fan, tube lights etc as per their convenience through mobile application. They can also check the status of appliances even when they are not at home. This application is scalable to add or delete appliances as per user's requirement.

In this application we embedded features like automatic window cutains controlling, automatic door bell, room temperature controlling. One other main feature is to alert user by sending simple text message on user's phone to protect our house from thieves. If an unwanted person enters in our house, our system will sense it and send the signals immediately to server. Server will send message to user mobile application connected with server through Wi-Fi. User can take immediate action on receiving SMS from server.

We have selected Wi-Fi technology to be used in this project because it will keep Home Automation System active and user can interact with server even if user is not present at home.

III. PREVIOUS RESEARCHES

A number of researches have been done on home automation system to make our life more reliable & more comfortable. In starting, only one or two devices were automated by using AVR microcontroller, arduino & zigbee. But number of I/O devices for such controllers were limited to only 2-4 devices so Programmable Logic Controllers (PLC) were used to automate the household equipments because number of I/Os were greater in PLC than such controllers. But price of PLC was very high. Hence it increased the cost of overall system. Also, in starting, these systems were being used only to control the household equipments but now these systems have specialized with extra features like House Security, Automatic door & window, Controlling of equipments using mobile.

Some of the researches on Home automation system are as follows:

1) Smart home automation system using AVR microcontroller by Bulbul Bhaskar and R. Swarnalatha (IJATES Vol. No. 03, Issue No. 02).
2) Remote controlled home automation using android application via wifi connectivity by Prof. Era Johri and Pradnya Bhangale (IJRITCC Vol. No. 03, Issue No. 03).

3) Home automation system using android for mobile phones by Sharon Panth and Mahesh Jivani (IJECSE Vol. 03, No. 01).
4) Home automation using android application and predictive behaviour implementation by Mrs. Latha and Pratik Agarwal (IJET Vol. 01, Issue 03).
5) Home automation and security system using arduino android ADK by P Pavan Kumar and G Tirumala Vasu (IJETER Vol. 03, N0. 06).
6) Home automation using android and Bluetooth by Kanchan, Priyanka Agarwal and Mahesh Vibhute (IJSR Vol.04, Issue 10).

IV. PROPOSED SYSTEM

The Entire project consists of two main phases i.e. Hardware and Software. User has the central control over home appliances by using Android phone application. User commands through Android application whose signal is given to microcontroller via Wi-Fi. Microcontroller has the sever program deployed on it. Server is configured to handle both hardware and software modules.

As per user's command particular appliance is operated (ON/OFF). Server keeps record of log information which is provided to user on demand and temperature readings regularly updated on user's application. In case if an unwanted person enters in our house, it will send notifications to user about it, so necessary actions could be taken and hazards can be avoided. Through Wi-Fi, server and user application is connected. Wi-Fi is chosen to improve system security (by using secure Wi-Fi connection), and to increase system mobility and scalability. In case when no one is present in the room, the appliances will automatically get switched OFF, thus saving electricity.

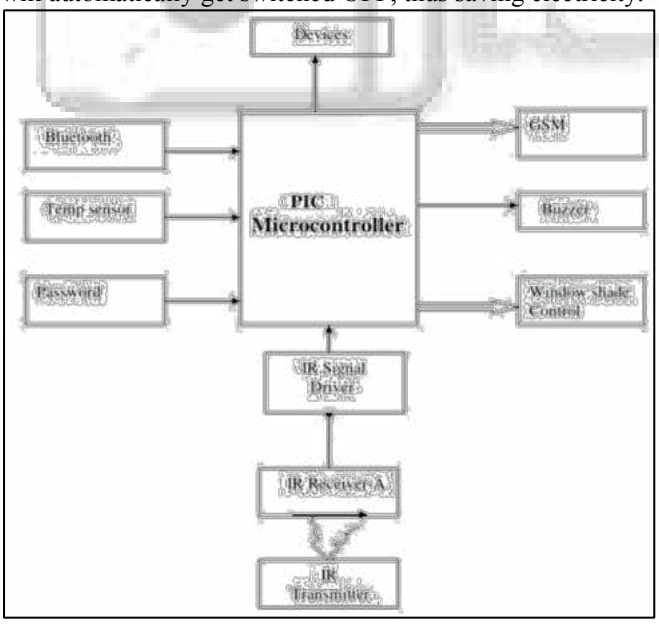

Fig. 1: Block Diagram

A. Hardware Design

The hardware circuit consists of PIC series microcontroller, temperature sensor (LM35), crystal oscilator, Relays and IR sensors. This microcontroller is a 40 pin IC having 8 I/O pins (P X.0-P X.7). The temperature sensor is connected to pin 33, Two Relays to pin 29 and 30, IR sensors to pin 34, Buzzer to pin 29, Bluetooth or WiFi to pin 26 and GSM modem to pin 25.

Switch ON AC power supply of 230V, the Bridge hrectifier converts it into DC. To get a constant output voltage of 5V DC, voltage regulator 7805 is used. Capacitors, (electrolytic or ceramic) and resistors with their specific values are mounted as per the requirements. Crystal Oscillator provides frequency of 11.0592 MHz for microcontroller working. LED's mounted on the circuit indicates whether the circuit is working properly.

B. Software Design

The software design is nothing but designing of graphical user interface on Android application. Using this GUI, user interacts with the system to control devices. For interaction, user initially has to establish connection between Android application and deployed Wi-Fi network. On successful establishment of connection, user can either operate devices (ON/OFF) or acquire log information (energy consumed by each device) about devices. Further, temperature reading will be constantly notified to user via Android application. In case of emergency situations like entry of unwanted person, user will be given immediate notification in the form of simple text message. When IR sensors will detect that no one is present in the room, it will automatically turn OFF appliances, and this information will be sent to Android Application

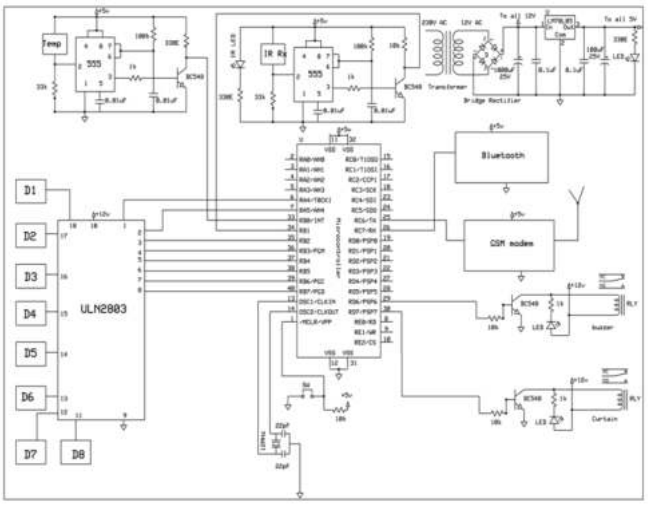

Fig. 2: Circuit Diagram

V. CONCLUSION

This paper proposes a low cost, secure, ubiquitously accessible, remotely controlled solution for home automation which has more features then previous systems and its cost is also low in compare to them. It is more convenient, reliable and energy efficient. The approach discussed in the paper is novel and has achieved the target to control home appliances remotely using the Wi-Fi technology to connect system parts, satisfying user needs and requirements. Looking at the current scenario we have chosen Android platform so that most of the people can get the benefit.

The technology is easy to use and targeted for people without technical background. This technology also provides great assistance to handicapped and aged old people. The proposed system is better from the scalability

and flexibility point of view than the commercially available home automation systems.

REFERENCES

[1] https://www.youtube.com/watch?v=taUrqnSp
[2] http://technav.ieee.org/tag/279/automation
[3] International Journal on Remote controlled home automation using Android application via WiFi connectivity by Prof. Era Johri.
[4] International Journal on Home automation system using android for mobile phone by Sharon Panth.
[5] http://www.sunrom.com/p/rf-serial-data-link-uart-2-4ghz
[6] International Journal on Home automation using Android application & Predictive behaviour implementation by Mrs. Latha A.P.
[7] http://www.ti.com/lit/ds/symlink/lm35.pdf
[8] http://www.tech-faq.com/infrared-sensors.htm

Labyrinth: Volume-7, No.1 January-2016
ISSN 0976-0814; pp. 188-193

The Toughest Decision

- Sugandha Agarwal

Hey! Supriya, "Do you know the news of the day. Authorities decided that a lady named 'Vishakha' will sit in our cabin from today and you know she is a widow, her husband died by sudden heart attack two months back. She is in a doleful condition. It is really woeful. But if she will be in this cabin, I feel it will be a problem for all of us. How can we continue our gleeful discussions in her tragic presence? We don't want to drown in the ocean of melancholy with her as we have our own complexities and hectic schedules. What do you think?" Suddenly Aashima came and whispered all this in Supriya's ear who is her friend and colleague.

"Authorities decided this and it is not in our hands so why to distress our mind unnecessarily. I think it is not going to affect much in future. We will not have much time to gossip as we all have lot of work and projects to finish..." Supriya replied.

Aashima agreed unwillingly and dissatisfaction was clearly visible in her black-brown eyes. She did not say any other word as she observed no interest in Supriya's face and behavior. She went outside to attend her phone call. Supriya again lose herself in the pile of files to complete the pending work. The reason of Supriya's disinterest was in fact her long absence from the office. Actually she was not very much aware what is going on recently in the office where she works as she joined one week back after her maternity leave. Her cynosure was her first baby only. So she almost overheard Aashima's words and continued her work. Aashima also became busy with her project. Soon Supriya find herself that she is not able to concentrate as she was also thinking about that wretched character 'Vishakha' who was sitting on the other side of the cabin near the casement, but clearly visible and audible. She thought to communicate with her as she like to interact with different types of people. Ultimately, she stood from her chair and went on her desk and said:

"Hello! I am Supriya. You are... new joining, I think. Welcome to our office. When did you join here? I think this is not a time of recruitment. What's your designation?" Vishakha was looking quite nervous and her dark-circled eyes seemed engulfed in grief. Supriya felt for a moment that perhaps she asked something wrong. She controlled the situation